The 1st Conference on Laser and Accelerator Neutron Sources and Applications

Held jointly with Optics & Photonics International 2013

Organized by

Institute of Laser Engineering, Osaka University

Co-organized by

The Laser Society of Japan

The IFE Forum (IFE: Inertial Fusion Energy)

The Atomic Energy Society of Japan

In cooperation with

The Japan Society of Plasma Science and Nuclear Fusion Research

April 23 (Tue.) – April 25 (Thu.), 2013

Pacifico Yokohama

Yokohama, Japan

Exhibition	OPTICS & PHOTONICS International Exhibition				
		23. April (Tue)	24. April (Wed)	25. April (Thu)	26. April (Fri)

OPTICS & PHOTONICS International Exhibition

Conferences

ALPS'13
LDC'13
CLSM2013
HEDS2013
LANSA'13
LPCC2013
LANE'13
LIC'13
LEDIA'13
SeTBio'13

Plenary Special Sessions
Opening
Keynote Lecture
Joint Sessions

Reception Party

Exhibition

4

Pacifico Yokohama

Poster Session

OPI Exhibition Hall

D C B A

Inter Continental Yokohama Grand

OPI Congress

Conference Center

Entrance Hall

Registration Desk

221

222

223

224

211 212 213

Tea Room

Secrelarial

315

HEDS 2013 (313, 314)

314

313

SeTBio'13 (311, 312)

312

311

Plenary Session
Joinl Plenary Session A
LIC'13 (302)

302

304

321

Plenary Session
Joinl Plenary Session A
LDC'13 (301)

301

303

316 317 318

Joinl Plenary Session B
ALPS'13 (303)

419

418

Passageway to Convention Hall

CLSM2013 (418)

417

LANE'13 (416, 417)

416

415

LPCC2013 (414, 415)

414

EV (for Equipment)

413

LANSA *13 (413)

412

LEDIA'13 (411, 412)

411

425

421 422 423 424

EV (for Equipment)

512

502

511

Ceiling height 3.0m

Foyer

Ceiling height 2.8m~10m

503

Ceiling height 2.8m~3.0m

Reception (501, 502)

501

Controlling room

Smoking area

Simultaneous Interpreting booth

513 514
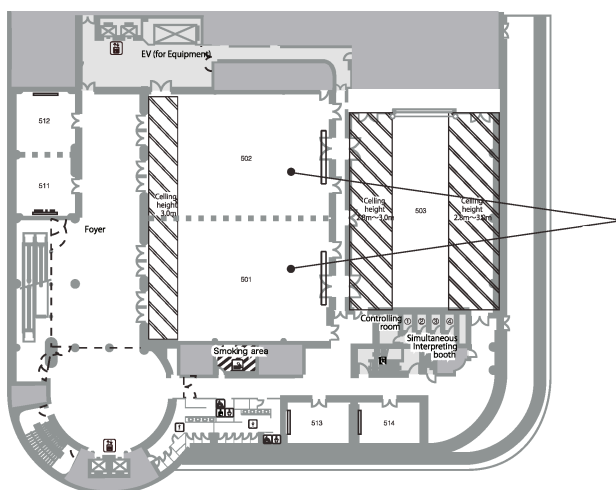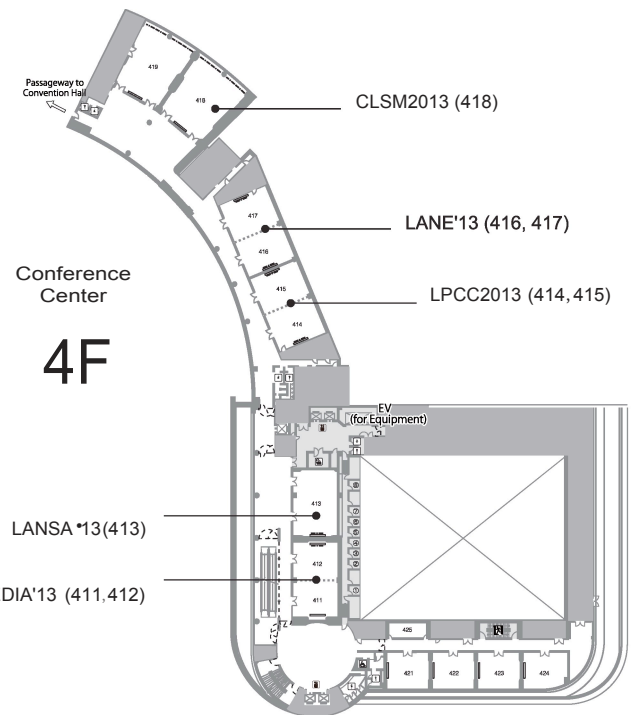
Conference on Laser and Accelerator Neutron Sources and Applications LANSA'13

Tuesday, April 23

Oraginzed by
• The Institute of Laser Engineering, Osaka University
Co-oragnized by
• The IFE Forum (IFE: Inertial Fusion Energy)
• The Laser Society of Japan
• The Atomic Energy Society of Japan
In cooperation with
• The Japan Society of Plasma Science and Nuclear Fusion Research

Hiroshi Azechi
Conference Chair,
Institute of Laser Engineering, Osaka Univ.

Tuesday, April 23

9:30-10:00
Opening Remarks of OPIC'13
Room 301,302

10:00-11:55
Keynote Lectures of OPIC'13
Room 301,302

----- Lunch Break （11:55-13:20） -----

13:20-15:20
Joint Plenary Sessions of OPIC'13
Room 301,302,303

----- Break （15:20-15:40） -----

15:40-15:45
Opening LANSA'13
Room 413

Opening Remarks
15:40   H. Azechi, Institute of Laser Engineering, Osaka University, Osaka, Japan

15:45-18:00
LANSA1 : LANSA Plenary
Room 413

Chair:	H. Nishimura, Institute of Laser Engineering, Osaka University, Osaka, Japan
LANSA1-1	(Plenary) Progress towards ignition on the US National Ignition Facility
15:45	M. Dunne National Ignition facility, Lawrence Livermore National Laboratory, California, U.S.A.
LANSA1-2	(Plenary) RANS present status and future planning for industrial use and transportable compact neutron source
16:30	Y. Otake, A. Taketani, RIKEN, Wako, Japan
LANSA1-3	(Plenary) Basic experiments on accelerator driven subcritical system for transmutation of minor actinide and for innovative neutron source
17:15	M. Misawa, C. Pyeon, T. Yagi , Kyoto university, Kyoto, Japan

-----Conference Reception (18:30-20:30)------

Wednesday, April 24

9:00-12:30
LANSA2: Neutron sources
Room 413

Chair:	M. Roth, Institut for Kernphysik Technische University, Darmstadt, Germany
LANSA2-1	(Invited) Low energy neutron measurements for ignition and capture cross section studies at the National Ignition Facility
9:00	L.A. Bernstein[1], D.L. Bleuel[1], J.A. Caggiano[1] , C. Cerjan[1], R. J. Fortner[1], C. Hagmann[1], R. Hatarik[1], D. Sayre[1], D.H.G.Schneider[1] , W. Stoeffl[1], D. Shaughnessy[1] , K.J. Moody[1] , J. Gostic[1], P.M. Grant[1] , C.B. Yeamans[1], N.P. Zaitseva[1], J.A. Brown[2], N.M. Brickner[2], B.H. Daub[2], P.F. Davis[2], B.L. Goldblum[1], K.A. Van Bibber[2] J. Vujic[2], R.B. Firestone[3], A.M. Hurst[3], A.M. Rogers[3] [1]Lawrence Livermore National Laboratory, California, U. S. A [2]University of California, Berkeley Dept. of Nuclear Engineering, U. S. A. [3]Lawrence Berkeley National Laboratory, U. S. A
LANSA2-2	Fast ignition scheme fusion using high-repetition-rate laser
9:45	Y. Kitagawa[1], Y. Mori[1], O. Komeda[1], R. Hanayama[1], K. Ishii[1], S.Nakayama[1], T. Sekine[2], N. Sato[2], T.Kurita[2], T. Kawashima[2], H. Kan[2], N. Nakamura[3], T. Kondo[3], M. Fujine[3], H. Azuma[4], T. Motohiro[4], T. Hioki[4], M. Kakeno[4], Y. Nishimura[5], A. Sunahara[6], Y. Sentoku[7], E. Miura[8], Y. Arikawa[9], T. Nagai[9], Y. Abe[9], [1]The Graduate School for the Creation of New Photonics Industries, [2]Development Bureau, Hamamatsu Photonics

K.K.
[3] Advanced Material Engineering Div.,
TOYOTA Motor Corporation,
[4] TOYOTA Central Research and Development
Laboratories, Inc.,
[5] Toyota Technical Development Corp.,
[6] Institute for Laser Technology,
[7] Department of Physics, University of Nevada,
[8] National Institute of Advanced Industrial
Science and Technology,
[9] Institute of laser Engineering, Osaka
University,

LANSA2-3   **The advanced neutron diagnostics in the fast ignition experiment by using GEKKO XII and LFEX**

10:15
Y. Arikawa[1], T. Nagai[1], Y. Abe[1], S. Kojima[1],
S. Sakata[1], H. Inoue[1], T. Murata[2],
N. Sarukura[1], M. Nakai[1], H. Shiraga[1],
H. Azechi[1]
[1] Institute of Laser Engineering, Osaka
University,
[2] Kumamoto Univ. Japan

----- Break （10:45-11:00） -----

Chair: L.A. Bernstein, Lawrence Livermore National Laboratory, U. S. A.

LANSA2-4 (Invited) A bright neutron source driven by short pulse lasers

11:00
M. Roth,
Institut for Kernphysik Technische University
Darmstadt, Germany,

LANSA2-5   **High-Energy Neutron Source Generation Using the Omega EP Laser**

11:45
D.P. Higginson[1,2], J.M. McNaney[2],
V. Yu Glebov[3], G.M. Petrov[4], B. Qiao[1],
C. Stoeckl[3], D.C. Swift[2], D.L. Bleuel[2],
J. Cobble[5], J. Davis[4], J.A. Frenje[6],
P.K. Patel[2], G. Tynan[1], and F.N. Beg[1]
[1] University of California-San Diego, U. S. A.
[2] Lawrence Livermore National Laboratory,
U. S. A.
[3] Laboratory for Laser Energetics, University
of Rochester, Rochester, U. S. A
[4] Naval Research Laboratory, Washington,
[5] Los Alamos National Laboratory,
[6] Massachusetts Institute of Technology,

----- Lunch Break （12:30-13:30） -----

13:30-15:00
LANSA3: Poster Session

Exhibition Hall D

LANSAp3-1 The development of the neutron detector for the fast ignition experiment by using LFEX and GEKKO XII facility
T. Nagai, M. Nakai, Y. Arikawa, Y. Abe,
S. Kojima, S. Sakata, H. Inoue, S. Fujioka,
H. Shiraga, N. Sarukura, T. Norimatsu, and
H. Azechi,
Institute of Laser Engineering, Osaka
University, Osaka, Japan

LANSAp3-2   **Development of multichannel TOF neutron spectrometer for the fast ignition experiment**
Y. Abe, H. Hosoda, Y. Arikawa, T. Nagai,

S. Kojima, S. Sakata, H. Inoue, Y. Iwasa,
K. Iwano, M. Nakai, T. Norimatsu, and
H. Azechi
Institute of Laser Engineering, Osaka
University, Osaka, Japan

LANSAp3-3   **The neutron imaging diagnostics and unfolding technique for fast ignition experiment**
H. Inoue[1], Y.Arikawa[1], S. Nozaki[2], S. Fujioka[1],
T.Nagai[1], S. Kojima[1], Y. Abe[1], S.Sakata[1],
M. Nakai[1], H. Shiraga[1], and H.Azechi[1],
[1] Institute of Laser Engineering, Osaka
[2] Okinawa National College of Technology

LANSAp3-4   **Generation of directed energetic neutron beams using short pulse lasers**
G. M. Petrov[1], D. P. Higginson[2], J. Davis[1],
Tz. B. Petrova[1], C. McGuffey[2], B. Qiao[2],
and F. N. Beg[2]
[1] Naval Research Laboratory, Plasma Physics
Division, U.S.A.
[2] Mechanical and Aerospace Engineering,
University of California-San Diego, U.S.A.

LANSAp3-5   **Simplified neutron detector for angular distribution measurement of p-Li neutron source**
M. Sakai, S. Tamaki, I. Murata
Graduate School of Engineering,
Osaka University, Osaka, Japan

LANSAp3-6 Development of compton X-ray spectrometer for the fast ignition experiment
S. Kojima[1], Y. Arikawa[1], T. Nagai[1], Y. Abe[1],
S. Sakata[1], H. Inoue[1], T. Namimoto[1],
M. Nakai[1], H. Shiraga[1], H. Azechi[1],
M. Asakawa[2], T. Ozaki[3], R. Kato[4]
[1] Institute of Laser Engineering, Osaka
University, Osaka, Japan
[2] Kansai University, Osaka, Japan
[3] National Institute for Fusion Science, Japan
[4] The Institute of Science and Industrial
Research, Osaka University, Osaka, Japan

LANSAp3-7 Development of the high energy bremsstrahlung X-ray spectrometer by using (γ,n)reaction
S.Sakata[1], Y.Arikawa[1], S.Kojima[1], Y.Abe[1],
T.Nagai[1], H.Inoue[1], R.Kato[2], M.Nakai[1],
H.Siraga[1], H.Azechi[1]
[1] Institute of Laser Engineering, Osaka
University, Osaka, Japan
[2] Institute of Science and Industrial Research,
Osaka University, Osaka, Japan

LANSAp3-8 Study on nuclear transmutation of nuclear waste by 14MeV neutrons
T. Kitada, A. Umemura, K. Takahashi
Osaka University, Graduate School of
Engineering, Division of Sustainable Energy
and Environmental Engineering, Osaka, Japan

LANSAp3-9 Method of beam steering with FWM in ICF -Compensation of PC beam direction and generation with scattered beam from a foam target-
N. Kameyama, H. Yoshida,
Gifu University, Gifu, Japan

LANSAp3-10 Generation of monoenergetic deuterons by tailored intense laser pulses for high fluence energetic neutron production
S. M. Weng[1], M. Murakami[1], J. W. Wang[1,4],

M. Chen [2], Z. M. Sheng [2], N. Tasoko [1],
P. Mulser [3], W. Yu [4]

[1] *Institute of Laser Engineering, Osaka University, Osaka, Japan*

[2] *Key Laboratory for Laser Plasmas and Department of Physics, Shanghai Jiaotong University, China*

[3] *Theoretical Quantum Electronics (TQE), Technische Universität Darmstadt, German,*

[4] *Shanghai Institute of Optics and Fine Mechanics, Chinese Academy of Sciences, China*

LANSAp3-11 The ESS-BILBAO Project
F. Sordo, The ESS-BILBAO Team Edificio Cosimet Paseo Landabarri nº 2, 1ª Planta. Leioa, Spain

----- Break （15:00-15:15）-----

15:15-17:00
LANSA4: Applications

Room 413

Chair: M. Murakami, Institute of Laser Engineering, Osaka University

LANSA4-1 **(Invited) Studies on accelerator-driven system in JAEA**

15:15 *Toshinobu Sasa and Hiroyuki Oigawa J-PARC Center, Japan Atomic Energy Agency, Japan*

LANSA4-2 **Nuclear reaction analysis of the Li-ion battery electrodes by proton and neutron beams**

16:00 *K.Mima [1], Raquel Gonzalez Arrabal [2], K.Fujita [1], Miguel Panizo Laiz [2] Y.Orikasa [3], Y.Uchimoto [3], A.Yamazaki [4], T.Kamiya [4], H.Sawada [5], C.Okuda [5], Y.Ukyo [5], S.Nakai [1], S.Sakabe [6], H.Nishimura [7], T.Saito [8], T.Yanagawa [9], H.Sakagami [9], J. Manuel Perlado [2] and Y.Kato [1]*

[1] *The Graduate School for the Creation of New Photonics Industries*
[2] *Institute of Fusion Nuclear, UPM*
[3] *Graduate School of Human and Environmental Studies, Kyoto University*
[4] *Takasaki Advanced Radiation Research Institute, Japan Atomic Energy Agency*
[5] *Toyota Central R&D Labs.,*
[6] *Institute for Chemistry, Kyoto University*
[7] *Institute of Laser Engineering, Osaka University*
[8] *Battery Research Div., Toyota Motor*
[9] *National Institue of Fusion Science, Japan*

LANSA4-3 **Development of high-average-power short-pulse laser system for the isotope-specific nondestructive assay using laser-Compton γ-rays**

16:15 *M. Mori, A. Kosuge, H. Okada, H. Kiriyama, Y. Ochi,, M. Tanaka, and K. Nagashima, Advanced laser development group, Quantum Beam Science Directorate, Japan Atomic Energy Agency, Kizu, Japan*

Thursday, April 25

9:00-12:15
LANSA5: Neutron sources

Room 413

Chair: I. Murata, Osaka University, Osaka, Japan,

LANSA5-1 **(Invited) A planning effort for severe fusion neutron source generation in Korea and fusion-fission hybrid transmutation reactor R&D**

9:00 *Jung-Hoon Han [1], G.S. Lee [2], Y.S. Hwang [1], B.G. Hong [3] , Yong-Su Na [1], Han-Gyu Joo [1], Hyung-Jin Shim [1], and K-DEMO team*
[1] *CARFRE, Seoul National University, 599 Gwanak-ro, Gwanak-gu, Seoul, Korea, tel.*
[2] *National Fusion Research Institute, Korea,*
[3] *Jeon-Buk National University, Korea,*

LANSA5-2 **Transformation of the beam intensity distribution and formation of a uniform ion beam by means of nonlinear focusing**

9:45 *Y. Yuri, T. Yuyama, T. Ishizaka, I. Ishibori, and S. Okumura, Takasaki Advanced Radiation Research Institute, Japan Atomic Energy Agency*

LANSA5-3 **Generation of high-quality proton beams with nanotube accelerator**

10:15 *M. Murakami [1] M. Tanaka [2] [1] Institute of Laser Engineering, Osaka University, Osaka, Japan [2] Department of Engineering, Chubu University, Japan*

----- Break （10:15-10:30）-----

Chair: M. Nakai, Institute of Laser Engineering, Osaka University, Osaka, Japan,

LANSA5-4 **(Invited) Compact accelerator driven neutron sources and their applications**

10:30 *M. Furusaka and H. Sato Faculty of Engineering, Hokkaido University, Hokkaido, Japan*

LANSA5-5 **Development of X-band 30 MeV Linac neutron source at decommissioned experimental reactor "Yayoi" for Fukushima nuclear accident analysis**

11:15 *M. Uesaka [1], K. Dobashi [1], T. Fujiwara [1], K. Tagi [1], H. Harda [2] [1] Nuclear Professional School, University of Tokyo, Tokyo, Japan [2] Japan Atomic Energy Agency, Japan*

----- Lunch Break （11:45-13:30）-----

13:30-15:45
LANSA 6: Neutron diagnostics

Room 413

Chair: D.P. Higginson, University of California-San Diego, U.S.A

LANSA6-1 **(Invited) Low-energy neutron spectrometer for boron neutron capture therapy**

13:30 *I. Murata and T. Obata, Division of Electrical, Electronic and Information Engineering, Graduate School of*

Engineering, Osaka University, Osaka, Japan,

LANSA6-2 **A new neutron time-of-flight detector to measure the MeV neutron spectrum at the National Ignition Facility**

14:15 *R. Hatarik[1], J. A. Caggiano[1], V. Glebov[2], J. McNaney[1], C. Stoeckl[2], and D. H. G. Schneider[1]*
[1]*Lawrence Livermore National Laboratory, California, U. S. A.*
[2]*Laboratory for Laser Energetics, University of Rochester, U. S. A.*

LANSA6-3 **High-performance neutron imaging with microns scale resolution using LiF crystal detector**

14:45 *A. Faenov[1,2], M. Matsubayashi[3], T. Pikuz[1,2], Y. Fukuda[1], M. Kando[1], R. Yasuda[3], H. Iikura[3], T. Nojima[3], T. Sakai[3], M. Shiozawa[4], Y. Kato[5]*
[1]*Quantum Beam Science Directorate, Japan Atomic Energy Agency, Japan*
[2]*High Temperatures, Russian Academy of Sciences, Russia,*
[3]*Quantum Beam Science Directorate, Japan Atomic Energy Agency, Kizu, Japan*
[4]*Nippon SOKEN, Japan*
[5]*The Graduate School for the Creation of New Photonics Industries, Hamamatsu, Japan*

LANSA6-4 **Nuclear emulsion technique for fast neutron measurement using automatic track analysis system**

15:15 *H. Tomita[1], H. Minato[1], Y. Sakai[1], K. Morishima[2], K. Ishihara[1], M Isobe[3], J. Kawarabayashi[1], T. Naka[2], T. Asada[2], T. Nakano[2], M. Nakamura[2], T Iguchi[1], K. Ogawa[3], K. Ochiai[4]*
[1]*Graduate School of Engineering, Nagoya University*
[2]*Graduate School of Science, Nagoya University,*
[3]*National Institute for Fusion Science,*
[4]*Fusion Research and Development Directorate, Japan Atomic Energy Agency*

----- **Break** （15:45-16:00）-----

16:00-17:15
LANSA 7: Neutron sources

Room 413

Chair: K. Mima, *The Graduate School for the Creation of New Photonics Industries, Hamamatsu, Japan*

LANSA7-1 **Efficient and stable neutron generation by Coulomb explosion of solid nanoparticles using DPSSL-pumped high-repetition-rate 20-TW laser**

16:00 *N. Satoh, T Watari, K Matsukado, T Sekine, Y. Takeuchi, Y Hatano, R. Yoshimura, K. Nishihara, M. Takagi, and T. Kawashima, Hamamatsu Photonics, K. K*

LANSA7-2 **High yield neutron production via laser accelerated deuteron ion beam**

16:30 *F.Aymond, D. Kelley, J.T. Morrison, M. Storm, M. McMahon, K.U. Akli, E. Chowdhury, R.L. Daskalova, D. Schumacher, R. R. Freeman, The Ohio State University, SCARLET,*

Laser Facility, U. S. A.

LANSA7-3 **Monte-Carlo simulations for neutron production of laser driven D(d,n) and ^{7}Li(d,xn) reactions using MCUNED**

17:00 *J. Alvarez[1], P.Sauvan[2], J. Perlado[1], J. Sanz[2]*
[1] *Instituto de Fusión Nuclear, Universidad Politécnica de Madrid, José Gutierrez Abascal, Madrid, Spain*
[2]*Departamento de Ingeniería Energética, Universidad de Educación a Distancia, Madrid, Spain*

17:30-17:40

Closing Remarks

17:30 *K. Mima, The Graduate School for the Creation of New Photonics Industries, Hamamatsu, Japan*

Oral presentations

Conference on Laser and Accelerator Neutron Sources and Applications(LANSA'13), Yokohama, Japan, Apr. 23 - Apr. 25, 2013

Progress towards ignition on the US National Ignition Facility

Mike Dunne
Director for Laser Fusion Energy,
Lawrence Livermore National Laboratory,
7000 East Avenue Livermore, CA 94550,

The National Ignition Facility (NIF), the world's largest and most energetic laser system, is now operational at Lawrence Livermore National Laboratory. The NIF's 192 beams are capable of delivering over 1.8-megajoule, 500-terawatt, ultraviolet laser light, over 60 times more energy than any previous laser system. The NIF can create temperatures of more than 100 million degrees and pressures more than 100 billion times Earth's atmospheric pressure. These conditions, exceeding those at the center of the sun, have never before been created in the laboratory. This facility is designed to compress fusion targets to the conditions required for thermonuclear burn, liberating more energy than is required to initiate the fusion reaction. The system flexibility allows multiple target designs to be fielded, offering substantial scope for optimization of a robust target design.

RANS present status and future planning for industrial use and transportable compact neutron source

Yoshie Otake, Atsushi Taketani,
[1] RIKEN, 2-1 Hirosawa, Wako, Saitama , Japan

We have just constructed the compact neutron source using proton linac with 7MeV, named RANS (RIKEN Accelerator-driven compact neutron source) and have thermal and fast neutron beam in RIKEN Wako campus now. Two types of the detector can be used for the thermal neutron experiment, one is the combination of scintillator and CCD camera for the 2D imaging or 3D, CT, imaging experiment, and another is with RPMT for the TOF imaging experiment. The large area detector for the fast neutron whose energy is in the range of MeV is now developing. We introduce the combination of the plastic scintillator and the MPPC. We are planning to develop new transportable non-destructive inspection system including compact neutron source and diagnostic software for the large scale structures such as bridges. Neutron imaging data taken in RIKEN, and the detection signal of fast neutron will be shown and discussed.

Basic Experiments on Accelerator Driven Subcritical System for Transmutation of Minor Actinide and for Innovative Neutron Source

Tsuyoshi Misawa, Cheolho Pyeon and Takahiro Yagi

Kyoto University Research Reactor Institute, Kumatori, Osaka 590-0494, Japan

Phone:+81-72-451-2376, Fax: +81-72-451-2603, Email:misa@rri.kyoto-u.ac.jp

Abstract: *An accelerator driven subcritical system (ADS) is a new hybrid system combined with subcritical reactor and an accelerator. It has attracted worldwide attention for transmuting minor actinides due to its superior safety characteristics. A basic research on ADS was started using KUCA and FFAG proton accelerator at KURRI for developing ADS for transmutation or for an innovative neutron source which can be utilized like a present research reactor.*

1. Introduction

An accelerator driven subcritical system (ADS) is a new hybrid system combined with nuclear fuel and an accelerator which can inject neutrons into a reactor. Because a core in ADS is operated in subcritical state and its steady state can be achieved by injected neutrons from an accelerator, energetic reactivity accidents hardly occur at ADS and its operation can be terminated by simply stopping the accelerator operation without using control rods. It has attracted worldwide attention in recent years for transmuting nuclear wastes such as minor actinides and long-lived fission products due to its superior safety characteristics and potential for burning nuclear wastes because of using high energy neutrons. At Kyoto University Research Reactor Institute (KURRI), a new project for research on ADS has been performed using a multi-core type research reactor, Kyoto University Critical Assembly (KUCA) whose maximum power is 100 W, combined with a Cockcroft-Walton type accelerator to produce 14 MeV neutrons by D-T reactions or an up to date FFAG (Fixed Field Alternating Gradient) accelerator shown in Fig. 1 to produce proton beam with 100 to 150 MeV. The purposes of ADS basic research in KURRI are to develop a new system for transmutation of minor actinides or for an innovative neutron source which can be utilized like a present research reactor.

2. Basic experiment at KUCA

In 2009, the world's first experiments on ADS with KUCA and the FFAG proton accelerator shown in Fig. 2 were successfully started by producing high energy neutrons generated by bombarding a tungsten target [1]. These ADS experiments at KUCA include various kind of reactor physics measurements; reaction rate measurement by using activation foils, neutron spectrum measurement by neutron activation method or liquid scintillator technique, subcriticality measurement, neutron noise analysis, reactor dynamics measurements caused by perturbation and so on to investigate basic characteristics of ADS. Since one of the features of KUCA is that it is easy to change the core configuration or fuel composition for altering neutron energy spectrum,

those ADS experiments have been carried out at various cores. These experimental data were also analyzed by Monte Carlo code, such as MCNPX, or other deterministic calculation codes to investigate various reactor physics parameters in ADS.

For example, subcriticality measurement in real time at ADS is an important research subject in ADS development to assure safety operation under subcritical state, and neutron noise analysis method is thought to be one of appropriate methods for this purpose because of its accuracy and reliability. The ADS system, neutron counts are fluctuated not only by the effect of chain reaction that is observed in a critical reactor, but also by the periodic operation of external neutron source from the accelerator. Including these effects, new formulation based on the variance-to-mean ratio method (Feynman-alpha method) and new noise data acquisition system were developed, which have been adopted in KUCA experiments [2]. Through the experiments, it was found that subcriticality of the system that was obtained from the prompt neutron decay constant (alpha value) can be observed in a real time by analyzing neutron noise data acquired during operation of ADS.

Note that since the usage of thorium fuel in ADS to produce ^{233}U has been one of attractive purposes for ADS operation, KUCA core loaded with thorium metal fuel were also used for ADS research and various static and kinetic parameters including thorium reaction rate has been measured.
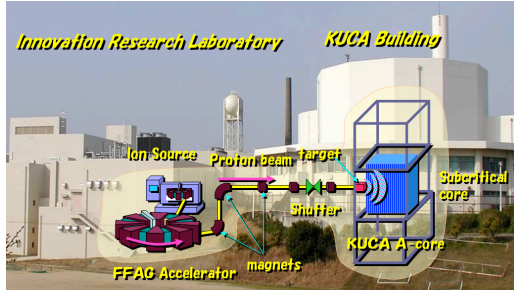

Fig. 1. FFAG proton accelerator

Fig. 2. KUCA and FFAG complex for ADS research at KURRI

3. ADS neutron source

A research reactor such as KUR (Kyoto University Reactor, whose thermal power is 5 MW) has been widely used as a stady state strong neutron source for reserch activities such as neutron activation analysis, neutron diffraction analysis, neutron radiography, production of radioisotopes and so on. Recently, safety demand for nuclear reactor operation has become more severe, which is also applied even to research reactors whose thermal power level is much less than conventional power reactors, then construction of new research reactors becomes difficult especially in Japan because of the Fukushima NPP accident. On the other hand, the advantage of ADS is its safety operation characteristics and ability to produce various energy neutrons, and it can be used as an intense neutron source like a reserch reactor.

Figure 3 shows an example of designed ADS for neutron source. It uses pin type UO_2 fuels like a power reactor and light water as moderator material. Proton beams are injected horizontally from outside into the core and are bombarded into beryllium target located at the center of the core to produce high energy neutrons. The performance of ADS such as thermal power and neutron intensity largely depends on power of proton beam, namely, the performance of accelerator, and in this design, it is assumed to use a compact cyclotron accelerator (30 MeV proton beam in 2 mA) for BNCT cancer therapy which has been recently deveoped and available at KURRI. This neutron source system has several neutron irradiation holes at inner region of the core to insert irradiation materials from outside by using such as a pneumatic system. Thermal neutron flux distibution is shown in Fig.4, and it is found that neutron flux shows maxmium value at the irradiation holes. In this design, thermal neutron power is approximately 30 kW and the peak value of thermal neutron flux at irradiation hole is about 1.2×10^{12} (n/sec/cm^2), which is comparable to the value in KUR at 400 kW operation. This fact indicates that the perfomance of the present ADS neutron source, namely the intensity of thermal neutron flux, is comparable to a low power research reactor and the amount of spent fuel produced by its operation is less than 10% compared with conventional reactor operation with same thermal flux level. Reserchers who use the neutron irradiation holes at KUR require much higher thermal neutron intensity for neutron source, however, since this is a preliminary design of new ADS, more improved results will be expected through detailed investigation, for example, arrangement of fuel pins or irradiation holes, and improvement of the performance of acclerator.

Fig. 3. Example of ADS for neutron source
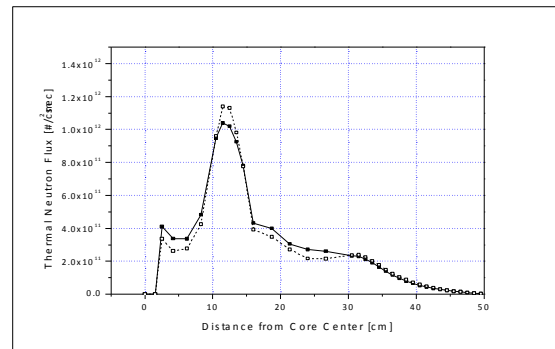
Fig. 4. Thermal neutron flux distribution

4. Conclusions

The basic experimental research on ADS has just been started using KUCA, and other worldwide ADS research project will be followed from now. We will continue the project on ADS research for development of the future nuclear system for transmutation of minor actinides or for an innovative intense neutron source.

References

[1] C. H. Pyeon, T. Misawa, et al., "First Injection of Spallation Neutrons Generated by High-Energy Protons into the Kyoto University Critical Assembly," J. Nucl. Sci. Technol., 46, 1091 (2009).

[2] Y. Kitamura, et al. "Application of Variance-to-mean Technique to Subcriticality Monitoring for Accelerator-Driven Subcritical Reactor," Int. J. Nucl. Energy Sci. and Technol., 2, 266 (2006).

Low Energy Neutron measurements for Ignition and Capture Cross Section Studies at the National Ignition Facility

L.A. Bernstein[1], D.L. Bleuel[1], J.A. Caggiano[1] , C. Cerjan[1], R. J. Fortner[1], C. Hagmann[1], R. Hatarik[1], D. Sayre [1], D.H.G. Schneider[1] , W. Stoeffl[1], D. Shaughnessy[1] , K.J. Moody[1] , J. Gostic[1] , P.M. Grant[1] , C.B. Yeamans[1], N.P. Zaitseva [1], J.A. Brown[2], N.M. Brickner[2], B.H. Daub[2] , P.F. Davis[2], B.L. Goldblum[1] , K.A. Van Bibber[2] J. Vujic[2], R.B. Firestone[3], A.M. Hurst[3], A.M. Rogers[3]

[1] Lawrence Livermore National Laboratory, 7000 East Avenue, Livermore CA USA, (925)-858-3531, bernstein2@llnl.gov
[2] University of California – Berkeley Dept. of Nuclear Engineering
[3] Lawrence Berkeley National Laboratory, 1 Cyclotron Rd, Berkeley CA USA

Abstract: *DT fuel loaded capsules at the National Ignition Facility (NIF) regularly produce sub-MeV "thermal" neutrons that can provide insight into implosion dynamics and open the possibility of measuring spectrum-averaged (n,γ) cross sections using ICF plasmas. In this paper we describe the development of a NIF-based Low Energy Neutron Spectrometer (LENS).*

1. Introduction

The National Ignition Facility (NIF) at LLNL has succeeded in achieving unprecedentedly high fuel areal density (ρR_{fuel}) values in excess of 1 g/cm^2 [1]. While the primary goal of this effort has been to trap the α-particle energy from the D+T reaction in order to achieve thermonuclear ignition, a fortuitous scientific side-effect is that a significant fraction of the 14 MeV neutrons from the D+T reaction scatter until they "thermalize" to the *keV* energies of the fuel itself. The number and spectral distribution of these thermal neutrons are excellent probes of the temperature and plasma confinement time of the cold fuel and potentially provide a window into the cold fuel entropy for the first time. In addition to their value as a plasma diagnostic, these neutrons are also ideally suited to studies of the neutron capture reactions that are responsible for the formation of the elements heavier than iron [2].

However, no capability currently exists at the NIF to measure neutrons with E_n < 140 keV. We have therefore undertaken an effort to build a *Low-Energy Neutron Spectrometer* (LENS) to measure downscattered neutrons down to *eV* energies. This development effort utilizes the intense, thick-target deuteron break-up neutron source at the Lawrence Berkeley National Laboratory (LBNL) 88-Inch Cyclotron to test novel neutron scintillator materials in a highly-segmented geometry designed to maximize signal bandwidth while minimizing ambient background arising from capture of scattered neutrons.

2. Low Energy Neutrons at NIF

An indirectly driven cryogenic NIF hohlraum+capsule is well suited to the production of low-energy neutrons. The NIF laser causes an explosive compression of a DT-loaded plastic capsule from an initial radius of 1 mm to a final value on the order of 30-40 μm. This compression forms a "cold" fuel layer with $\rho R_{fuel} \geq 1$ g/cm^2 and a temperature about 100 eV (>10^6 K) which causes 3-7% of the 14.1 MeV neutrons produced in the T(D,n)α reactions to scatter to energies between 10-12 MeV. The downscattered ratio (DSR) of the number of 10-12 MeV neutrons divided by the number of 13-15 MeV primary neutrons is the main diagnostic used to determine peak ρR_{fuel}. The capsule assembly remains

Figure 1: HYDRA neutron spectrum simulations for a typical NIF cryogenic shot (blue line) and a Maxwell-Boltzmann distribution for kT=850 eV (red line).

confined for several hundreds of ps allowing 10^{-2}-10^{-3} of the neutrons to scatter multiple times down to energies that reflect the time-averaged temperature of the capsule constituents. Figure 1 shows a hydrodynamic simulation of a NIF shot in neutrons per MeV as a function of energy from the HYDRA code package. The simulation shows a low-energy "bump" corresponding to partially- and/or fully-thermalized neutrons which is well fit using a Maxwell-Boltzmann distribution with a temperature of 850 eV (red line).

Experimental evidence for the existence of these low-energy neutrons comes from the observation of ^{198}Au arising from the neutron capture on the
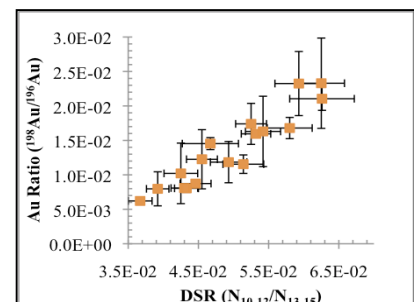

Figure 2: Ratio of ^{198}Au/^{196}Au for all NIF shots where SRC was fielded from Jan.-Sept. 2012 vs. the downscattered ratio (DSR) from NIF NTOF detectors.

$\approx$100 mg of ^{197}Au in the hohlraum surrounding the NIF capsule. Low-energy neutrons are particularly effective at producing neutron capture products due to the increase in the neutron capture cross section with decreasing neutron energy. Figure 2 shows a plot of the ^{198}Au/^{196}Au ratio for hohlraum debris collected using the Solid Radchem (SRC) diagnostic at NIF vs. DSR for shots that took place between November 2011 and August 2012. The monotonic correlation in this plot suggests that the same mechanism, neutron scattering, is responsible for the generation of both 10-12 MeV and low-energy neutrons.

3. LENS design features

A LENS situated on one of the 20 m nToF lines at NIF would share many characteristics with the 960 channel LANSA (Large Neutron Scintillator Array) spectrometer designed by Cable et al. for use at the Nova laser [3]. However, a NIF-based LENS would measure the energy of incoming neutrons in current mode for neutrons with energies greater than a critical energy E_{crit} and then "cross-over" to individual pulse mode for lower neutron energies, functioning in a manner similar to LANSA. For energies below E_{crit}, LENS could be absolutely calibrated using a non-ICF neutron source in a manner similar to the existing NIF nToF system for energies above E_{crit} [4].

Individual LENS elements will contain materials with enhanced low-energy neutron response, such as the Li-doped glass employed at the GEKKO laser facility [5] or a commercially available Boron-loaded scintillator such as BC-454 from Saint-Gobain [6]. In addition to these materials we are exploring the use of a new class of Lithium-doped plastics being developed at LLNL by the group led by Dr. N. Zaitseva [7]. Each LENS element will be small enough to ensure that background from the Compton scatter of ambient neutron capture γ-rays could be removed through the use of a pulse-height threshold. Estimates using MCNP for the photon flux in the 20 m neutron alcove at NIF indicate that a 256-channel LENS comprised of 5 mm x 5 mm right cylindrical elements would accomplish these goals.

Figure 3 shows the ratio of the number of neutrons per μs on a single LENS element 20 m from the center of the NIF chamber for HYDRA simulations of capsules with confinement times of 800, 1200 and 5000 ps
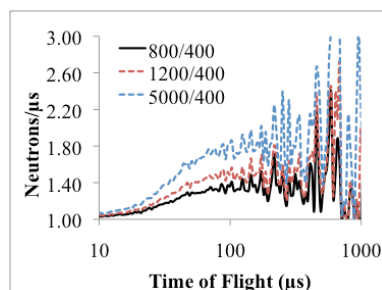

Figure 3: Simulations of the ratio of neutrons/μs for a LENS element for plasma confinement times of 800, 1200 & 5000 ps compared to 400 ps from HYDRA.

relative to one with a confinement time of 400 ps. The difference in these curves for t>2 μs shows the ability of a LENS for determining plasma confinement times. In addition, the overall hit rate for a single LENS element never exceeds 1 event/10 ns indicating that pulse mode operation could potentially be possible for all neutron energies at these modest yields.

The large number of LENS elements is ideally suited to the multi-anode photomultiplier tube (PMT) and digital electronic technologies. Leading candidates include the 64-channel HAMAMATSU H8500 PMT [8] and the CAEN V1740 64 channel VME digitizing units [9].

4. Conclusions

Design work has commenced for a highly segmented Low Energy Neutron Spectrometer (LENS) for use at NIF. LENS will provide unique insight into the dynamics of the plasma and enable ICF-based neutron capture cross section measurements. The LENS development and testing work is taking place using thick-target deuteron break-up and Li(p,n) neutron sources at the LBNL 88-Inch Cyclotron.

References

1. A. Mackinnon *et al.,* Phys. Rev. Lett. **108**, 215005 (2012).

2. M.R. Busso, G.J. Wasserburg, R. Gallino, Annu. Rev. Astron. Astrophys.. 37:239–309 (1999).

3. M.B. Nelson and M.D. Cable, Rev. Sci. Instrum. **63**, 4874 (1992); doi: 10.1063/1.1143536.

4. R. Hatarik, L.A. Bernstein, M.L. Carman, D.H.G. Schneider, N.P. Zaitseva, and M. Wiedeking, Rev. Sci. Instrum. Vol. **83** #10 085292RSI (2012).

5. Y. Arikawa *et al.,* Pr3+-doped fluoro-oxide lithium glass as scintillator for nuclear fusion diagnostics, Rev. Sci. Instrum. 2009 Nov;80(11):113504.

6. http://www.detectors.saint-gobain.com/../Product../BC454-Data-Sheets.pdf

7. N. Zaitseva, I. Pawelczak, M. Faust, P. Martinez, A. Glenn, L. Carman, N. Bowden, S. Payne, "Pulse Pulse Chape Discrimination with Li-containing organic scintillators" to be submitted to Nucl. Instrum. Meth. (2012).

8. http://209.73.52.252/assets/pdf/parts_H/H8500C_H8500D_TPMH1308E01.pdf

9. http://www.caen.it/csite/CaenProd.jsp?idmod=591&parent=11

Fast Ignition Scheme Fusion Using High-Repetition-Rate Laser

Y. Kitagawa[1]*, Y. Mori[1], O. Komeda[1], R. Hanayama[1], K. Ishii[1], S.Nakayama[1], T. Sekine[2], N. Sato[2], T. Kurita[2], T. Kawashima[2], H. Kan[2], N. Nakamura[3], T. Kondo[3], M. Fujine[3], H. Azuma[4],T. Motohiro[4], T. Hioki[4], M. Kakeno[4],Y. Nishimura[5], A. Sunahara[6], Y. Sentoku[7], E. Miura[8],Y. Arikawa[9],T. Nagai[9], Y. Abe[9],

[1]*The Graduate School for the Creation of New Photonics Industries,*
1955-1 Kurematsu-cho, Nishi-ku, Hamamatsu, Shizuoka 431-1202 Japan,
[2]*Development Bureau, Hamamatsu Photonics K.K. 1820, Kurematsu-cho, Nishi-ku, Hamamatsu 431-1202 Japan,*
[3]*Advanced Material Engineering Div., TOYOTA Motor Corporation, 1200, Mishuku, Susono, Shizuoka 410-1193 Japan,*
[4]*TOYOTA Central Research and Development Laboratories, Inc., 41-1Yokomichi, Nagakute, Aichi 480-1192 Japan,*
[5]*Toyota Technical Development Corp., 1-21 Imae, Hanamoto-cho, Toyota, Aichi 470-0334 Japan,*
[6]*Institute for Laser Technology, 1-8-4 Utsubo-honmachi, Nishi-ku, Osaka 550-0004 Japan,*
[7]*Department of Physics, University of Nevada, Reno 1664 N VIRGINIA ST Reno, NV 89557,*
[8]*National Institute of Advanced Industrial Science and Technology, 1-1-1 Umezono, Tsukuba, Ibaraki 305-8568 Japan,*
[9]*Institute of laser Engineering, Osaka University, 2-6 Yamadaoka, Suita, Osaka 565 Japan*

A high-repetition-rate LD-laser pumped laser HAMA is used to the fusion research. The fast-ignition scheme fusion emitted X-ray radiations and neutrons. Also the Laser for Fast Ignition Experiment (LFEX), directly heats a preimploded core, enhancing DD neutron yields by a factor of 1000 (5×10^8 neutrons), the best ever obtained in fast-ignition scheme. The results indicate that fast-ignition scheme is an effective path toward core heating and easier than the self-ignition scheme. The mini reactor CANDY is planed.

Introduction: Roadmap to the power plant

A lot of works are necessary to realize the power plant[1]. One key issue is the development of a high-repetition-rate, high-efficiency laser with output energies of the order of kilojoules or greater. Another is fuel fabrication and high-repetition fuel injection. In addition, power plant technology, such as an innovative wall materials, will need to be developed.

FIG. 1. Neutron yield versus laser energy: 0th (0.1∼ 1kJ laser), 1st (1∼ 100 kJ) and 2nd phase (100 kJ∼ 10 MJ laser).

We divide the roadmap for achieving a fusion plant into three phases. The zeroth phase involves developing 1-kJ drivers to engineering tests and to produce neutrons. No fuel compression is considered. The first phase is to develop a breakeven machine that uses a 100-kJ driver. Here the fuel is compressed to 100× the solid density or more. The second phase is to demonstrate a commercial reactor. The fuel may be compressed to around 500×.

Figure 1 plots the expected neutron yield and fusion gain versus the input laser energy. The input laser energy is divided 50% to implosion and 50% to fast-heating. The zeroth phase does not provide any fuel compression, but a fuel heating. 100 × compression is considered for the 2nd phase and $100 \sim 500\times$ for the 3rd. The zeroth phase output will be an unified mini-reactor CANDY, a concept of kJ fast-ignition scheme unified machine, as shown in Figure 3. In the second phase, 1.8 MJ laser energy yields the thermal power gain of 200, when the deuterium-tritium (DT) bullet fuel is compressed to 500×the solid density each 0.1 second.

We have developed a laser-diode- (LD-)pumped laser system HAMA with a repetition rate of 10 Hz. This repetition rate is high enough for this stage. We are currently in the zeroth phase.

Fast ignition scheme fusion using double foil illuminated by high-repetition-rate laser

The fast-ignitor scheme in inertial confinement fusion is that at the maximum compression timing, the imploded core is irradiated with a laser pulse in a few tens of a picosecond, which is much shorter than the hydrodynamic disassembly time of the irradiated spot. Such a short-pulse laser generates hot electrons and ions at the cutoff region, which penetrate into the core and form a hot spot. From the spot, the α burning wave spreads over the core.

Here, as reported partially in [2] using a simple implosion scheme, we show that the hot electrons deposit
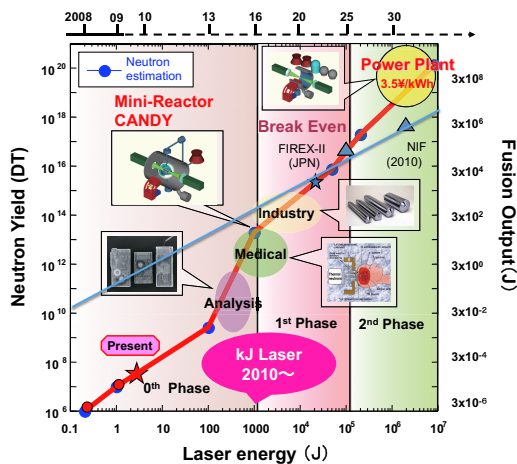
energy to the peripheral plasma before reaching the ablation surface and also they reach the core and deposit some energy in it to emit x-ray radiations. Based on the neutron yields observed in the experiment the core is supposedly heated up to a few hundred electronvolts of temperature as long as the core stagnates.

A pair of off-axial 7.6-cm-diameter dielectric-coated mirror (OAP) counter-focused the beams, such that Long pulse beam-1 and Short pulse beam-1 are focused from the right-hand direction of the target and Long pulse beam-2 and Short pulse beam-2 approach from the left-hand side. The lasers used here are divided from HAMA. The target consists of two parallel 2-mm square plain foils. The foil is made of CD and is 11 μm thick, supported with 100-μm-thick stainless steel. The separation (gap) between the foils is 100 μm. Figure 2 plotted X-ray
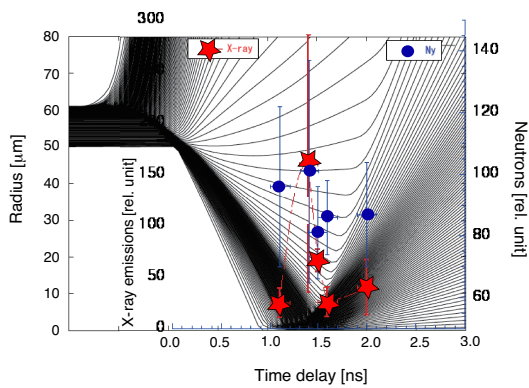

FIG. 2. Diamond : X-ray core-emissions versus the heating beam delay on radius-time diagram. Dot : DD thermal neutron time of flight signal from a plastic scintillator[2].

core-emissions and DD thermal neutron yield versus the heating beam delay, showing that the imploded cold core is heated by the heating beam to emit X-ray radiations, which is similar to the PW laser results[3]. At 1.4 ns, the neutron yield was around 1000. Since the simulation suggests the core density is compressed to 2×the solid CD density of 1.1 g/cm^3 at least, then the deuteron density will be $n_D = 9 \times 10^{22}$ cm^{-3}. The core temperature will be 300 eV.

The result that the heating pulse effectively transport its energy to the core plasma, is promising for promoting the laser fusion scheme.

Thousand times enhanced neutron yields from a fast-ignition scheme LFEX laser at Osaka

The ultra-intense laser LFEX at ILE heated the preimploded core of a deuterated polystyrene shell target, resulting in 5×10^8 DD neutrons. This value is signifi-

cantly higher than the yields obtained from the previous fast-ignition experiments. In the absence of LFEX laser ignition, the core yielded less than 10^6 neutrons; in particular, we achieved an enhancement in the yields by a factor of 1000 by the LFEX beam. LFEX increased the core temperature by a factor of more than two, i.e., from 0.8 keV to 2 keV. Here the polar implosion has an advantage of being able to quickly ignite the core as the ignition laser is capable of reaching closer to the core than a spherical implosion. Our results demonstrated an easier path of ignition and burning by producing a hot spot by means of hot electrons and fast ions.

kJ system CANDY

Our study established that the fast-ignition scheme is a promising fusion path.

Figure 3 shows an unified mini-reactor CANDY, a concept of kJ fast-ignition scheme unified machine at the he zeroth phase output. Cryogenic DT fuel pellets are injected at 10 Hz. Two counter beams for implosion and following two counter beams for core heating are coaxially illuminated. A liquid-metal blanket surrounding the reaction area absorbs the emissions and neutrons. The liquid metal circuit includes a heat converting system and a tritium recovering system. Although CANDY may generate a gain less than 1 %, but is a near future mile stone on the roadmap to the power plant.
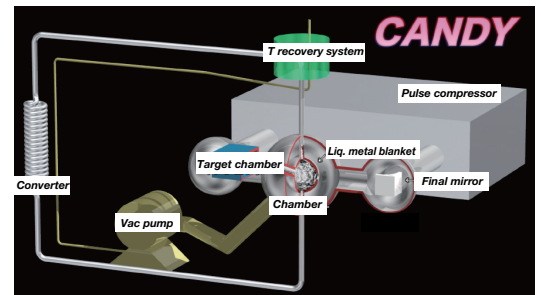
FIG. 3. The Mini-Reactor CANDY, a concept of kJ fast-ignition scheme unified machine.

[1] Hogan W. J. 1995 *Energy from Inertial Fusion, Ch. 3. IFE Power Plant Design Principles* (edited by Hogan W. J. IAEA, Vienna, Austria)
[2] Kitagawa Y. *et al.* 2012 "Fusion Using Fast Heating of a Compactly Imploded CD Core" *Phys. Rev. Lett.* **108**, 155001
[3] Kitagawa Y. *et al.* 2005 "Petawatt laser heating of uniformly imploded CD shell target" *Phys. Rev. E* **71**, 016403-1-5

The advanced neutron diagnostics in the fast ignition experiment by using GEKKO XII and LFEX

Yasunobu Arikawa [1], Takahiro Nagai[1], Yuki Abe[1], Sadaoki Kojima[1], Shohei Sakata[1], Hiroaki Inoue[1], Takahiro Murata[2],
Nobuhiko Sarukura[1], Mitsuo Nakai[1], Hiroyuki Shiraga[1], Hiroshi Azechi[1]
1)   Institute of Laser Engineering, Osaka University, 2-6 Yamadaoka, Suita, Osaka, Japan, Tel: +81-6-6879-8775 ,
Email : arikawa-y@ile.osaka-u.ac.jp
2) Kumamoto University

Abstract: *The progress of the neutron diagnostics in the fast ignition experimental project in Institute of Laser Engineering, Osaka University was presented. The oxygen quenching and Benzophenon quenching are applied in the liquid scintillator which is developed for the primary neutron spectroscopy. On the other hand Pr-doped ^6Li fluorophosphates glass scintillator was developed and the down scattered neutron diagnostics was demonstrated.*

1. Introduction

In the inertial confinement fusion research neutron diagnostics is one of the most essential for evaluating ion temperature or areal density. Especially in the fast ignition experiment, the neutron diagnostics has a critical issue of the harsh background caused by strong x-ray pulse generated by fast heating laser. In this regard, very rapid response scintillator is indispensable. The liquid scintillator with the oxygen is attractive method to supress the slow decay component called afterglow [1,2], however even more faster response has been needed in the fast ignition experiment in the GEKKO XII and LFEX facility. On the other hand the down scattered neutron diagnostics is another challenging subject. The down scattered neutron signal must be discriminated via time of flight (TOF) from much stronger primary neutron which arrives earlier than down scattered neutron. The ^6Li glass scintillator based detector was developed for this aim [3], and implemented into the GEKKO XII-LFEX experiment. In this paper the liquid scintillation based TOF detector and the ^6Li glass based multi-channel single hit detector are presented.

2. Liquid scintillation detector for the fast ignition experiment

The liquid scintillator which had been originally reported in the paper [1] was modified in our research [2]. The detailed information about the scintillator or the detector will be presented separately in this conference. The dye was chosen "BBQ" having emission peaked around 380 nm because which can quenched with Benzophenon with absorption peak of 380 nm. The figure 1 shows the comparisons of the decay curve and table 1 shows the fall time (90 %- 10%) and light output against mass fraction of the Benzophenon.

The liquid scintillator has been implemented into the fast ignition experiment by using GEKKO XII and LFEX laser facility. The multi channel liquid scintillation detector construct with 7 channels was developing with the unquenched and 1 wt% Benzophenon quenched liquid scintillator.
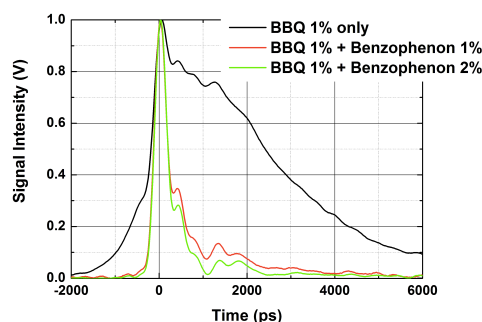
Figure 1 The comparison of the decay curve of the Benzophenon quenched BBQ liquid scintillator

	Fall time (90%-10%)	Light output
unquenched	5400 ps	100%
1%	875 ps	6%
2%	625 ps	4%

Table 1 The summary of the fall time and light output

Figure 2 shows the example of the signals observed in the fast ignition experiment. The Figure 2.(a) shows the signal with the conventional plastic scintillator based detector. Figure 2 (b) shows the newly developed liquid scintillators coupled with the gated photomultiplier tube (PMT). Among 7 signals, Channel 1 which used unquenched liquid scintillator and Channel 6 which uses 1 weight % quenched are highlighted. The excellent performance was clearly shown in this experiment. By using these advanced detectors the deuterium-deuterium (DD) neutron yield around 10^6 was successfully measured.

3. 256-channel ^6Li scintillation neutron spectrometer

The fast responding ^6Li fluorophosphates glass scintillator named APLF80+3Pr or APLF80+3Ce have been developed in our previous work [3, 4]. Furthermore APLF80+3Pr glass has been manufactured to pixel scintillator array and a multi channel single hit detector for down scattered neutron diagnostics. The scintillator array has been coupled with a multi anode PMT and 256-channels of anode signal were connected into 500-

(a)

(b)

Figure 2 (a) The typical signal of the plastic scintillator BC422Q and (b) multi channel liquid neutron scintillator in the fast ignition shot. Among the 7 channels the channel 1 with unquenched BBQ liquid and channel 6 with 1-w% Benzophenon quenched BBO liquid are high lighted.
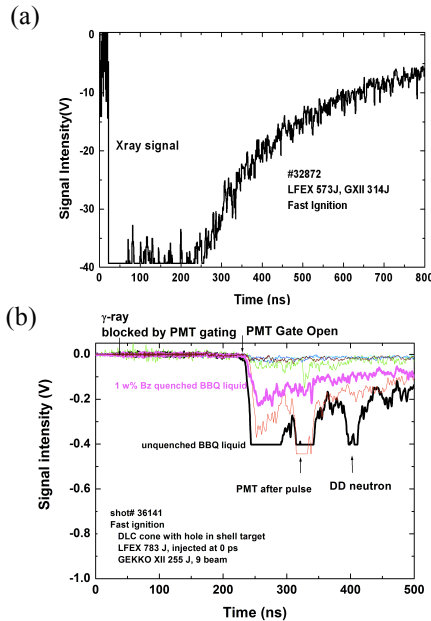
ps Time to Digital Convertor (TDC) [5]. The implosion experiment for demonstrating down scattered neutron detection was conducted in GEKKO XII. CD (deuterated- polystylen) with the diameter of 500 μm and the thickness of 7 μm was imploded with the 12 beams of the GEKKO XII with the average laser energy of 279 J. The down-scattered detector was set at 20 cm from target with a x-ray shield made by 2-cm lead. The primary neutron yield observed by plastic scintillator to be 3.2×10^5. Figure 3 (a) is the photograph of the detector and (b) shows observed down scattered neutron signal. 15 counts of the primary at 10 ns and a down scattered neutron signal at 38 ns are seen. The signals 50 at and around 80 ns are confirmed as γ-ray via (n,γ) reaction at target chamber and scattered neutron from target chamber, respectively. Fuel areal density (ρR) was estimated from the ratio of primary neutron and down scattered neutron to be 0.7 ± 0.7g/cm^2. Although only a count of down-scattered neutron was obtained thus the estimated value of ρR has a 100% error, the detection of the down-scattered neutron from DD fusion with low neutron yield was successfully demonstrated. This system will be completed with installing a 256-channel, 3 GHz/ 1.25 GPPS, 10-bit digitizer array shown in Fig 3(a) in right. After completion of the digitizer, down-scattered neutron will be observed in upcoming implosion experiment or fast ignition experiment. This detector has potential to apply to various experiment of laser induced neutron generation such as nuclear synthesis experiment [5] proposed in national ignition facility.

(a)

(b)
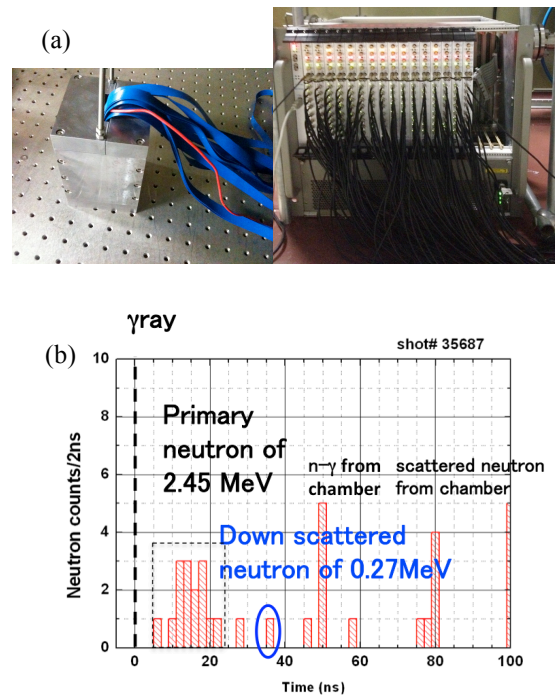
Figure 3 (a) The photograph of the 256-channel down scattered neutron detector (left) and 256-channel of digitizer and (b) the signal of the down scattered neutron observed in the implosion experiment by

7. Conclusions

The progress of the neutron diagnostics in the fast ignition experiment in the Institute of Laser Engineering, Osaka University was presented. The oxygen quenching and Benzophenon quenching is applied in the liquid scintillator which is developed for the primary neutron spectroscopy. On the other hand Pr-doped ^{6}Li fluorophosphates glass scintillator was developed and the down scattered neutron diagnostics was demonstrated.

Acknowledgement

References

[1] C. Stoeckl, Rev. Sci. Instrum. 81, 10D302 (2010).
[2] T. Nagai, et.al., J. Appl. Phys. 50, 080208 (2011)
[3] Y.Arikawa, et. al., Rev. Sci. Instrum. 80, 113504 (2009)
[4] Y.Arikawa, et.al., Rev Sci. Instrum. 81, 106105 (2010)
[5] M.R. Busso, et.al., Rev. Astron. Astrophys.. 37:239–309 (1999).

Conference on Laser and Accelerator Neutron Sources and Applications(LANSA'13), Yokohama, Japan, Apr. 23 - Apr. 25, 2013

A bright neutron source driven by short pulse lasers

M. Roth[1,2], D. Jung[2], K. Falk[2], N. Guler[2], O. Deppert[1], M. Devlin[2], A. Favalli[2], J. Fernandez[2], D. Gautier[2], M. Geissel[3], R. Haight[2], C. E. Hamilton[2], B. M. Hegelich[2], R. P. Johnson[2], F. Merrill[2], G. Schaumann[1], K. Schoenberg[2], M. Schollmeier[3], T. Shimada[2], T. Taddeucci[2], J. L. Tybo[2], F. Wagner[1], S. A. Wender[2], C. H. Wilde[2], G. A. Wurden[2]

[1]*Institut für Kernphysik, Technische Universität Darmstadt, Schloßgartenstrasse 9, D-64289 Darmstadt, Germany*

[2]*Los Alamos National Laboratory, Los Alamos, NM 87545, USA*

[3]*Sandia National Laboratories, Albuquerque, NM 87185, USA*

Neutrons are a unique tool to alter and diagnose material properties and excite nuclear reactions with a large field of applications. It has been stated over the last years, that there is a growing need for intense, pulsed neutron sources, either fast or moderated neutrons for the scientific community. Accelerator based spallation sources provide unprecedented neutron fluxes, but could be complemented by novel sources with higher peak brightness that are more compact. Lasers offer the prospect of generating a very compact neutron source of high peak brightness that could be linked to other facilities more easily.

We present experimental results on the first short pulse laser driven neutron source powerful enough for applications in radiography. For the first time an acceleration mechanism (BOA) based on the concept of relativistic transparency has been used to generate neutrons. This mechanism not only provides much higher particle energies, but also accelerated the entire target volume, thereby circumventing the need for complicated target treatment and no longer limited to protons as an intense ion source. As a consequence we have demonstrated a new record in laser-neutron production, not only in numbers, but also in energy and directionality based on an intense deuteron beam. This enabled the use in imaging applications with high temporal resolution as the neutron beam has a pulse duration of less than a nanosecond.

The beam contained, for the first time, neutrons with energies in excess of 80 MeV and showed pronounced directionality, which makes then extremely useful for a variety of applications. Using short pulse lasers we have been able to get a radiograph of an unknown object using the hard x-rays of the laser matter interaction and neutrons of different energies. This allows also for determining the material composition of an object. The data thereby match the simulation data for our test samples.

The results also address a larger community as it paves the way to use short pulse lasers as a neutron source. They can open up neutron research to a broad academic community including material science, biology, medicine and high energy density physics as laser systems become more easily available to universities and therefore can complement large scale facilities like reactors or particle accelerators. We believe that this has the potential to increase the user community for neutron research largely.

Memo

High-Energy Neutron Source Generation Using the Omega EP Laser

D.P. Higginson[1,2)], J.M. McNaney[2)], V. Yu Glebov[3)], G.M. Petrov[4)], C. Stoeckl[3)], D.C. Swift[2)], D.L. Bleuel[2)], J. Cobble[5)], J. Davis[4)],
J.A. Frenje[6)], P.K. Patel[2)], G. Tynan[1)], and F.N. Beg[1)]
[1)] University of California-San Diego, La Jolla, CA, [2)] Lawrence Livermore National Laboratory, Livermore, CA,
[3)] Laboratory for Laser Energetics, University of Rochester, Rochester, NY, [4)] Naval Research Laboratory, Washington, DC,
[5)] Los Alamos National Laboratory, Los Alamos, CA, [6)] Massachusetts Institute of Technology, Cambridge, MA

Abstract: The generation of high-energy (> 10 MeV) neutrons is assessed experimentally on the Omega EP laser. An angle-depenent neutron yield of 3×10^9 n/sr over the entire energy range, as well as a yield of 10^8 n/sr neutrons above 12 MeV is reported.

1. Introduction

The generation of high-energy neutrons is of great interest to a number of applications including fusion energy, material damage studies, homeland security, non-destructive material detection and temperature measurement in opaque materials. The new technique [1] for laser-generated neutrons is demonstrated experimentally on the Omega EP laser. Using multiple diagnostic techniques, the neutron generation is quantitatively assessed in terms of neutron energy and total yield. A common method of neutron generation with lasers is to use a dual-target setup, where ions are accelerated by the laser from a thin foil into a secondary converter target where they undergo nuclear reactions to create protons [2, 3]. This method can be used to create high-energy neutrons by accelerating deuterons from the primary foil into a low-Z material [1], since such reactions are exothermic with Q-values exceeding 15 MeV. This has been shown experimentally to produce neutrons above 18 MeV on the Titan laser [4] and up to 150 MeV on the Trident laser [5].

2. Experimental Setup and Ion Generation
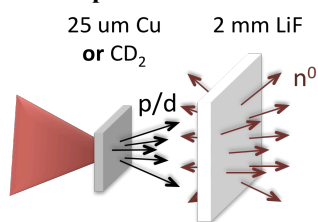

25 um Cu or CD₂   2 mm LiF

Fig. 1. Experimental setup for neutron generation using the Omega EP laser.

The setup of the Omega EP experiment is shown in Fig. 1, where the laser is shown incident on a primary foil of either Cu or CD_2 to accelerated protons and/or deuterons, respectively, into a 2 mm LiF converter. The Omega EP laser contained about 1 kJ of laser energy in a 10 ps pulse to achieve a laser intensity of 10^{19} W/cm^2. The ion spectra were recorded (with the LiF converter removed) using both a Thomson Parabola and absolute number and spectra of the protons was obtained using Radiochromic Film stacks.

These indicated that the protons obtained maximum energies around 50 MeV, with slope temperatures around 7 MeV and conversion efficiencies around 4.5%. We note here that when using a CD2 target, that similar proton acceleration was still observed.

3. Neutron Yields

To capture the neutron yields for broad range neutrons below 10 MeV two methods were used. First, CR-39 pieces were placed at multiple angles within the target chamber during every shot. CR-39 is a plastic that is damaged by neutrons through knock-on collisions that create holes that can be counted in the material after etching with a strong base. Secondly, Ni slabs were placed at multiple angles. The reaction ^{58}Ni(n,p)^{58}Co has a fairly high cross-section and is sensitive to neutrons above 2 MeV, as plotted in Figure 2. The total neutron yield was calculated by observing gamma yield using highly-shielded low-background gamma spectrometers at LLNL, which was required due to the long 71 day half-life.
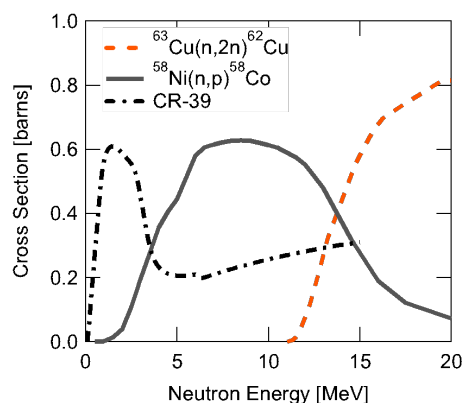

Fig. 2. Plot of the cross-section of various nuclear reactions used for neutron detection. Note that the CR-39 sensitivity is normalized.

The yields for the different geometries are plotted in Figure 3. One can see that the CD2 setup produces a larger number of neutrons, especially in the forward direction. The neutron yields for all setups are higher in the forward

direction due to the momentum of the incident particles. The maximum yields of lower-energy neutrons in the forward direction are found to be around 3×10^9 n/sr. This is a substantial increase over the Titan laser results [4]. However, this is 3 times lower than results produced on the Trident laser with 12x less laser energy [5]. Such a result highlights the necessity to increase laser contrast to improve ion acceleration.
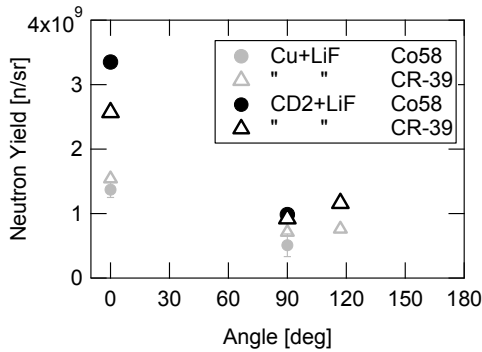

Fig. 3. Yield of low energy neutrons as a function of angle for both Cu and CD_2 setups.

To determine the absolute number of high-energy neutrons, a pieces of Cu were placed within the chamber at 90° from the target normal. The $^{63}Cu(n,2n)^{62}Cu$ reaction has a cross-section than begins at 12 MeV and thus is only sensitive to high-neutrons. However, the reaction $^{63}Cu(\gamma,n)^{62}Cu$ will also activate the target, and therefore we took shots with no LiF converted to get the background signal to subtract. The ^{62}Cu isotope decays through the β^+ channel, so coincidence counters were used on site to record the activity levels. The high-energy neutron yields are shown in Figure 4, where a maximum of 10^8 n/sr neutrons above 12 MeV is observed. Also, as expected the Cu foil setup does not produce high-energy neutrons, as all reactions of protons in LiF are endothermic.
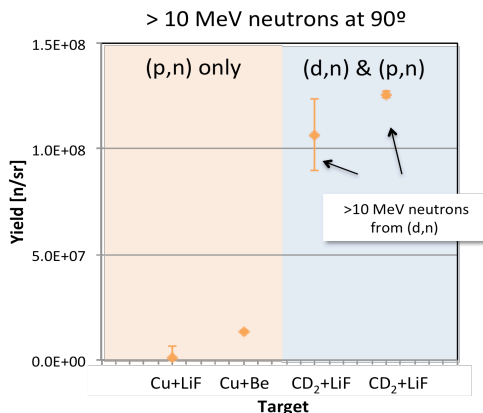
Fig. 4. Yield of high-energy neutrons as a function for shots using the Cu and CD_2 setups.

Additionally, a neutron time-of-flight detector was deployed at Omega using gated PMTs attached to fast scintillators [6]. This diagnostic showed neutron energies in excess of 15 MeV as shown in Figure 5.
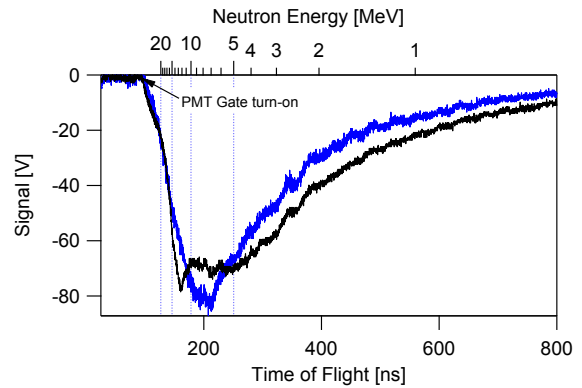
Fig. 5. Neutron signal traces using a gated time-of-flight detector.

7. Conclusions

We have demonstrated the production of high-energy neutrons on the Omega EP laser and obtained yields of 3×10^9 n/sr and 10^8 n/sr for low and high energy neutrons, respectively.

Acknowledgement

References

[1] J. Davis *et al*., "Neutron production from ^{7}Li(d,xn) nuclear fusion reactions driven by high-intensity laser–target interactions", Plasma Phys. Control. Fusion **52**, 045015 (2010)

[2] K. L. Lancaster, *et al*., "Characterization of ^{7}Li(p,n)^{7}Be neutron yields from laser produced ion beams for fast neutron radiography", Phys. Plasmas **11**, 3404 (2004)

[3] D. P. Higginson, *et al.*, "Laser generated neutron source for neutron resonance spectroscopy", Phys. Plasmas **17**, 100701 (2010)

[4] D. P. Higginson, *et al*., "Production of neutrons up to 18 MeV in high-intensity, short-pulse laser matter interactions", Phys. Plasmas **18**, 100703 (2011)

[5] M. Roth, *et al*., "Bright Laser-Driven Neutron Source Based on the Relativistic Transparency of Solids", Phys. Rev. Lett. **110**, 044802 (2013)

[6] C. Stoeckl, *et al*., "A gated liquid-scintillator-based neutron detector for fast-ignitor experiments and down-scattered neutron measurements", Rev Sci. Instrum. **81**, 10D302 (2010)

Conference on Laser and Accelerator Neutron Sources and Applications(LANSA'13), Yokohama, Japan, Apr. 23 - Apr. 25, 2013

Studies on Accelerator-driven System in JAEA

Toshinobu Sasa and Hiroyuki Oigawa

J-PARC Center, Japan Atomic Energy Agency, Tokai, Ibaraki, 319-1195, JAPAN, Tel. +81-29-282-6948, Fax. +81-29-282-5671,
sasa.toshinobu@jaea.go.jp

Abstract: After Fukushima accident, reduction of radioactive wastes got much attention. To realize it, Partitioning-Transmutation technology is noted at the national fuel cycle policy. To perform basic studies, Japan Atomic Energy Agency has promoted to construct the Transmutation Experimental Facility and performed design within the framework J-PARC project.

1. Introduction

Due to the Great East Japan Earthquake and ensuing tsunami, Fukushima-Daiichi Nuclear Power Plant have been seriously damaged and many nearby residents are still forced to be evacuated. The cabinet of Japan decided to reduce the dependency to nuclear power generation. The Science Council of Japan suggests prioritizing research and developments (R&Ds) to reduce the radiological burden of high level wastes (HLW).

Japan Atomic Energy Agency (JAEA) precedes R&Ds to reduce the radiological hazard of HLWs by Partitioning and Transmutation (P-T) technology[1]. Within the framework of the J-PARC project, JAEA also promoted to construct the Transmutation Experimental Facility (TEF) to study the minor actinide (MA) transmutation by both fast reactors and accelerator driven systems (ADS)[2]. TEF locates at the end of LINAC, which is also important components to be developed for future ADS, and share the proton beam with other experimental facilities in J-PARC. R&Ds for important technologies required to build the facilities are also performed, such as requirement of MA bearing fuel into the critical assembly, spallation product removal method especially for the polonium, and so on. The objectives and construction schedule of the facilities, the latest design concept, and key technologies to construct TEF are described.

2. Description of JAEA Proposed ADS

JAEA's reference design of ADS[2] is a tank-type subcritical reactor, where lead-bismuth eutectic (LBE) alloy is used as both the primary coolant and the spallation target, as shown in Fig. 1. The spallation target region locates at a central part of the core. In the target region, LBE is flowing from the core bottom along to the dedicated wrapper tube and flow guide. About 1.5 GeV-30 MW proton beam is supplied from the accelerator to operate the ADS.

A tank-type system is adopted to take advantage to eliminate the necessity of heavy primary piping. All primary components, including two primary pumps and four steam generators are set up in the reactor vessel. The heat generated in the target and the core is removed by forced convection of the primary LBE, and transferred through the steam generators to a secondary water/steam system for power conversion. The inlet and outlet coolant temperatures were set to 300 and 407 ℃, respectively, to prevent material corrosion by LBE.
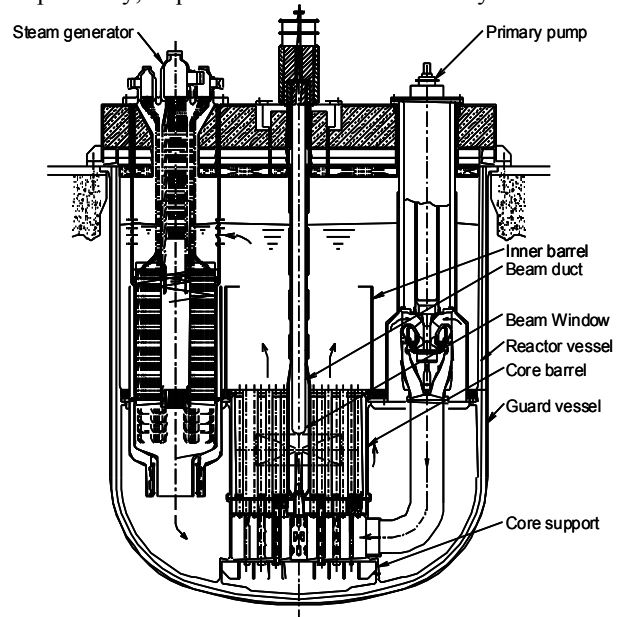
Fig. 1 ADS for transmutation of MA proposed by JAEA

Nitride fuel, which is suitable for reprocessing for ADS, is selected. To minimize the burnup reactivity change and the power peaking, the fuel region is divided into several zones with the different fuel composition. About 2,500 kg of MA is loaded in the core and 10% of them can be transmuted annually. The maximum k_{eff} during whole burnup cycles was set to 0.97. The burnup swing in whole cycles is about 3 % Δk/k.

3. Outline of Transmutation Experimental Facility

As shown in Fig.2, TEF consists of two individual buildings; ADS Target Test Facility (TEF-T)[3] and Transmutation Physics Experimental Facility (TEF-P)[4].

Two buildings are connected by beam transport line with low power beam extraction mechanism using laser beam. TEF-T is planned as a material irradiation facility which can accept a maximum 400 MeV-250 kW proton beam into LBE spallation target. It also has an availability to use various purposes such as measurement of the reaction cross sections of MA and structural materials, medical isotope production and so on. TEF-P is a facility with critical assembly to study neutronics

and controllability of ADS. Using these two facilities, basic physical properties of subcritical system and engineering tests of spallation target will be studied. R&Ds for several important technologies required to build the facilities are also performed, such as laser charge exchange technique to extract very low power beam for reactor physics experiments, remote handling method to load MA bearing fuel into the critical assembly, spallation product removal method especially for the polonium, and so on.

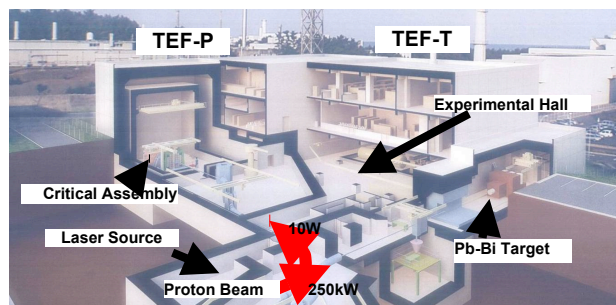Fig. 2 Transmutation Experimental Facility

3.1 R&Ds for TEF-T

The main purpose of TEF-T is to obtain the data to evaluate the actual lifetime of beam window. TEF-T mainly consists of a spallation target, a cooling circuit, and hot cells to handle the spent target and irradiation test pieces. A proton beam current density of 20 μA/cm^2, which is almost same as future ADS design, was adopted as a reference. The irradiation performance of reference case was evaluated around 8 DPA/yr by 400MeV-250kW beam irradiation. Further optimization of the target design to increase DPA is underway.

When LBE is irradiated by high-energy proton or neutrons, polonium isotopes will be accumulated and it should be carefully controlled. The removal method of polonium was studied for the design of exhaust circuit of TEF-T. An equilibrium vaporization test of polonium from liquid Pb-Bi was performed and equilibrium vaporization characteristics were measured by transpiration method with LBE which was irradiated at the JAEA/JMTR[5]. It was shown that at the low temperature around 450 ºC, which considered as a standard operational condition of TEF-T and future ADS, most accumulated polonium were remained in LBE as a chemical compound with Pb or Bi which is much hard to evaporate than elemental polonium.

Another experiment to recover evaporated polonium in exhaust circuit was performed[6]. LBE samples were irradiated at the JAEA/JRR-4 and were heated in special vacuum vessel up to 690 ºC. By adopting multi-layered filter, which consists of two different finenesses stainless steel mesh, escaped polonium can be decreased to 1/400.

3.2 R&Ds for TEF-P

The present accuracy of nuclear data is not sufficient for ADS design. To improve the accuracy of the nuclear data especially for MA, both the differential experiments and the integral experiments are necessary, while the integral experiments on MA are more difficult than those on the major actinides. One of the main purposes of TEF-P is to perform integral experiments using MA.

TEF-P is designed referring to existing Fast Critical Assembly (FCA) in JAEA/Tokai to keep consistency of previous huge experimental data. The effectiveness of MA-loaded experiments with certain amount of MA was discussed[15,25]. In the procedure, imaginary experimental data using TEF-P are assumed to estimate the reduction of the errors in the effective cross sections. The data by TEF-P was assumed to be equal to the calculation result, and experimental error taken from the past experiments in FCA. By using certain amount of MA, which is about order of kg, typical improvement was observed.

4. Conclusions

JAEA has been promoting various R&Ds on ADS. As for the basic experimental studies necessary for future ADS construction, plan to build Transmutation Experimental Facility has been proposed. The design optimization of TEF-T to improve irradiation performance, R&D for polonium management was carried out. The effectiveness of TEF-P experiments using certain amount of MA was assessed quantitatively.

References

[1] T.Sasa, et al., "Research and development on accelerator-driven transmutation system at JAERI", Nuclear Engineering and Design 230, 209-222 (2004).

[2] K.Tsujimoto, et al., "Feasibility of Lead-Bismuth-Cooled Accelerator-Driven System for Minor-Actinide Transmutation" ,Nucl. Tech., 161, 315-328 (2008).

[3] T.Sasa, et al., "Conceptual Study of Transmutation Experimental Facility (2) Study on ADS Target Test Facility" (in Japanese), JAERI-Tech 2005-021 (2005).

[4] H.Oigawa, et al., "Conceptual Design of Transmutation Experimental Facility", Proc. Global2001, Paris, France (CD-ROM, 2001).

[5] S.Ohno, et al., "Equilibrium Evaporation Behavior of Polonium and Its Homologue Tellurium in Liquid Lead-Bismuth Eutectic", Journal of Nuclear Science and Technology, 43:11, 1359-1369 (2006).

[6] T.Obara, Y.Yamazawa, T.Sasa "Polonium decontamination performance of stainless steel mesh filter for lead alloy-cooled reactors", Progress in Nuclear Energy, 53, 1056-1060 (2011).

[7] T.Sugawara et al., "Analytical Validation of Uncertainty in Reactor Physics Parameters for Nuclear Transmutation System," J. Nucl. Sci. Technol. 47(6), 521-530 (2010).

Nuclear Reaction Analysis of the Li-ion Battery Electrodes by Proton and Neutron Beams

K.Mima[1], Raquel Gonzalez Arrabal[2], K.Fujita[1], Miguel Panizo Laiz[2] Y.Orikasa[3], Y.Uchimoto[3], A.Yamazaki[4], T.Kamiya[4], H.Sawada[5], C.Okuda[5], Y.Ukyo[5], S.Nakai[1], S.Sakabe[6], H.Nishimura[7], T.Saito[8], T.Yanagawa[9], H.Sakagami[9], J. Manuel Perlado[2] and Y.Kato[1]

[1] The Graduate School for the Creation of New Photonics Industries
[2] Institute of Fusion Nuclear, UPM
[3] Graduate School of Human and Environmental Studies, Kyoto University
[4] Takasaki Advanced Radiation Research Institute, Japan Atomic Energy Agency
[5] Toyota Central R&D Labs.,
[6] Institute for Chemistry, Kyoto University
[7] Institute of Laser Engineering, Osaka University
[8] Battery Research Div., Toyota Motor Corp.
[9] National Institute for Fusion Science

New diagnostic methods for the Li depth distribution have been proposed and demonstrated for the Li-ion battery. The Nuclear Reaction Analysis (NRA) by ion and neutron beams was applied. The POP experiments by an accelerator proton beam were carried out for the Li-ion battery electrode analysis. The POP experiments results and the applicability of laser produced ion and neutron beam for the NRA will be presented.

1. Introduction

The long life, high capacity and safety have been the issues for developing high performance Li-ion battery. Form this point of views, it is required to control the Li depth distribution of the electrodes during charge and discharge. It is not easy to diagnose the depth distribution of Li-ions in the electrode, since they are embedded in the metal layers. The promising methods are the Nuclear Reaction Analysis (NRA) and/or the Particle Induced Gamma Emission (PIGE) by using ion and neutron beams. The schematic view of this diagnostic system is illustrated in Fig.1. There are several nuclear reactions which can be used for diagnosing the Li depth distribution. One attractive way is the neutron induced nuclear reactions[1]

PIGE/PIXE

Ref.[1],[2]

X-ray detector
Gamma detector
Neutron beam
Ion beam generator
γ -ray
X-ray
^{4}He
neutron
^{4}He
: nuclear
: electron
Particle detector

- **PIXE (Particle Induced X-ray Emission): K_α-line --->** **Heavy element diagnostics : Co(p, p'X) , Ni(p, p'X),Fe(p,p'X)**
- **PIGE (Particle Induced γ-ray Emission):** **Light element : ^{7}Li(p, p'γ) ^{7}Li (Eγ=0.478 MeV)**
- **NRA (Nuclear Reaction Analysis): ^{7}Li(p,α) ^{4}He (E$_{he}$ =16MeV)** , **^{6}Li(n,t)^{4}He (4.78MeV)**
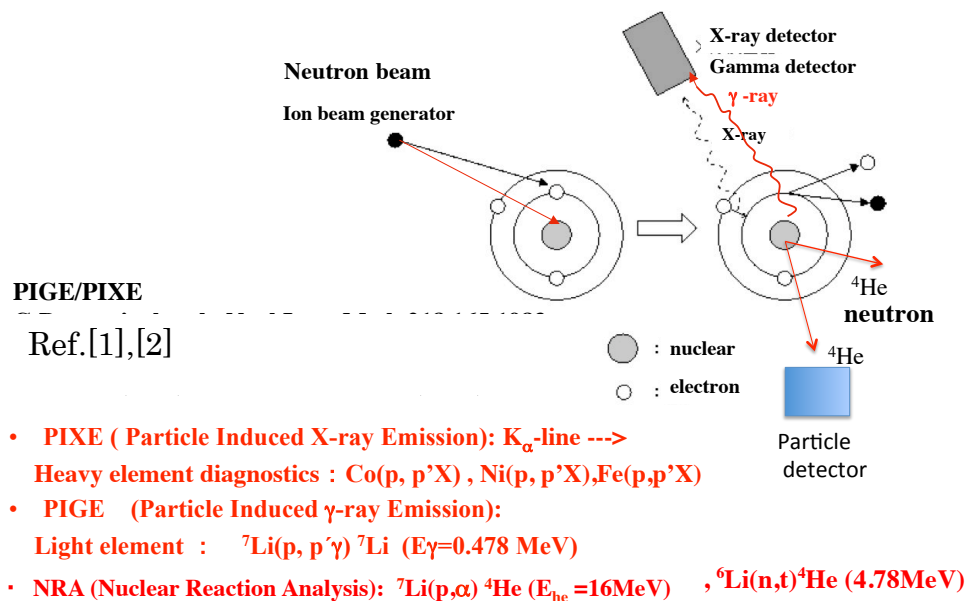
Fig.1 Schematic view of NRA, PIGE, and PIXE

2. PIG experiments of Li-ion battery positive electrodes

The elemental distribution of as-received (non-charged) and charged Li-ion battery positive electrodes containing $Li_xNi_{0.8}Co_{0.15}Al_{0.05}O_2$ ($0.75 \leq x \leq 1.0$) micro-particles as active material is characterized by combining μ-PIXE and μ-PIGE techniques at TIARA, JAEA[4]. PIGE measurements evidence that the Li distribution is inhomogeneous (existence of Li-rich and Li-depleted regions) in as-received electrodes corresponding with the distribution of secondary particles but it is homogeneous within the studied individual secondary micro-particles. The dependence of the Li distribution on electrode thickness and on charging conditions is characterized by measuring the Li distribution maps in specifically fabricated cross-sectional samples. These data show that decreasing the electrode thickness down to 35 μm and charging the batteries at slow rate give rise to more homogeneous Li depth profiles.

3. POP experiments for applying NRA to Li-ion battery characterization by accelerator driven proton beams

For applying the NRA to Li-ion battery electrodes, we irradiated a 3 MeV proton beam to an electrode of $LiFePO_4$ on a Al substrate which was charged with high rate (30C). Then, the alpha particle spectra were measured at TIARA, JAEA, Japan and the Sevilla University, Spain [5].
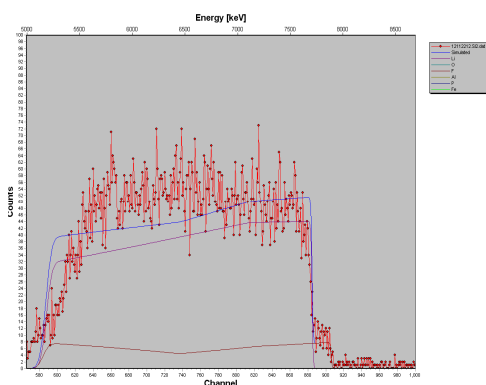

Fig.2 ^{4}He energy spectrum in 3MeV proton irradiation on a $LiFePO_4$ sample. The related nuclear reactions are $^7Li(p,\alpha)^4He$, and $^{19}F(p,\alpha)^{16}O$

The figure 2 [5] shows an example of the alpha particle spectrum of the positive electrode. By the experiments, we got a confidence to determine the Li-ion depth profile from the spectrum. The solid dotted red, broken red, and blue curves in Fig.2 are for the Li-P, F-P reactions, and total neutron yield respectively in a simulation by SIMNRA. Here, the Li concentration was assumed uniform for the 20 μm thick sample after high rate charge. The experiment result indicate that the Li concentration is higher near the Al layer surface.

5. Application of laser produced neutron to Nuclear Reaction Analysis

Low energy neutrons could be produced by the $^7Li(p,\gamma n)^7Be$ reaction. This reaction has a threshold at 1.9MeV and the resonance peak at 2.3MeV. When the 2.3 MeV proton beam irradiates Li metal, the neutrons are directed forward and the energy is about 0.5MeV ~ 0.4MeV. Such neutrons have a very high nuclear reaction cross section which is greater than 1.0 barn as shown in Fig.3. The well known reaction: $^6Li(n,t)^4He$ (4.8MeV) will produce T and the energy spectrum of T will provide the depth distribution of the sample.
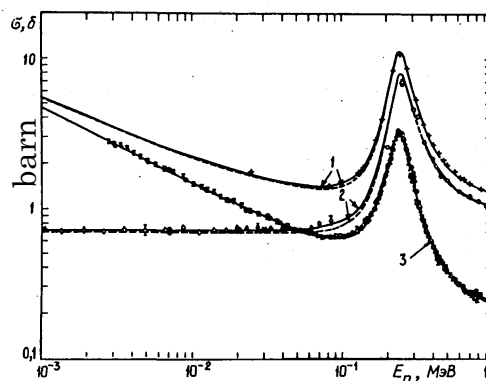
Fig.3 Cross-sections in the neutron energy from 0.001MeV-1.0MeV. 1:total, 2:elastic scattering, 3: $^6Li(n,t)^4He$ reaction.

Reference
1. T. Tadic, M. Jaksic, Z. Medunic, E. Quartarone and P. Mustarelli, Nucl. Instr. and Meth. in Phys. Res. B **181** (2001) 404-407.
2. G.Deconninck, etal.,NIM, 218(1983)165
3. M.Mateus, etal., NIMB,266(2008)1490
4.K.Mima, etal., NIMB 290(2012)79
5. Raquel Gonzalez Arrabal, etal (to be submitted to NIMB, 201

Development of high-average-power short-pulse laser system for the isotope-specific nondestructive assay using laser-Compton γ-rays

Michiaki MORI, Atsushi KOSUGE, Hajime OKADA, Hiromitsu KIRIYAMA
Yoshihiro OCHI, Momoko TANAKA, and Keisuke NAGASHIMA

Advanced laser development group,
Quantum Beam Science Directorate, Japan Atomic Energy Agency

Umemidai 8-1, Kizugawa, Kyoto 619-0215 JAPAN
Phone +81-774-71-3379
FAX +81-774-71-3379
e-mail: mori.michiaki@jaea.go.jp

Abstract: *A high-average-power (100 W class) high-repetition-rate (80 MHz) laser system for laser-Compton γ-ray source has been developed. 80 MHz repetition rate is synchronized to repetition rate of electron bunch from compact electron recovery linac (cERL). In addition, a photon storage cavity (i.e. enhancement cavity) which provides boosted photons at the interaction point has also been developed. These equipments are necessary to generate ultra-high brilliance γ-ray photons .*

1. Introduction

By using nuclear resonance fluorescence (NRF), specific isotopes can be analyzed precisely[1-5]. For such application, low energy spread γ-rays are required. Compton scattering include inverse Compton scattering is an inelastic scattering of a photon by a free charged particle, usually electron. It results in change in energy of the photon, called the Compton effect. The Laser-Compton Scattering (LCS) γ-rays have good features: energy tunable, quasi-monochromatic, and beam like spatial distribution. Consider a LCS γ-ray source system at the head-on collision configuration with a 350 MeV electron beam ($\gamma_e \sim 680$) and a wavelength of 1 μm laser beam ($\hbar\omega_0 \sim 1.2$ eV), that gives an up-shifted photon energy of $\hbar\omega_r \sim 4\gamma_e^2 \hbar\omega_0 \sim 2$ MeV, which value is favourable for non-destructive inspection by using NRF (see in Fig.1).

In particular, by small value of the scattering cross-section of the electron and photon (i.e. Thomson scattering cross-section: $\sigma_0 = 6.7 \times 10^{-25}$ cm^{-2}), it is necessary for supplying ultra-high brilliant γ-rays to generate not only large current electron beam but also intense laser beam[4,5]. Especially, high-average-power short pulse laser system and photon storaging system would be key equipments to generate such intense laser field.

We have been developing high average power (~ 100 W class) and high repetition rate(~ 80 MHz) short pulse ($\sim$ps) laser system in parallel with development of laser storage cavity (i.e. enhancement cavity) for nondestructive detection of isotopes by using NRF.

2. High power laser system

Fig.2 shows a block diagram of 100 W class short pulse laser system (Yb-fiber based laser). In the present status of laser development, 20 W average power with the pulse duration of 0.3 ps and 78 MHz repetition rate is achieved after the pulse compression with main-amp stage.
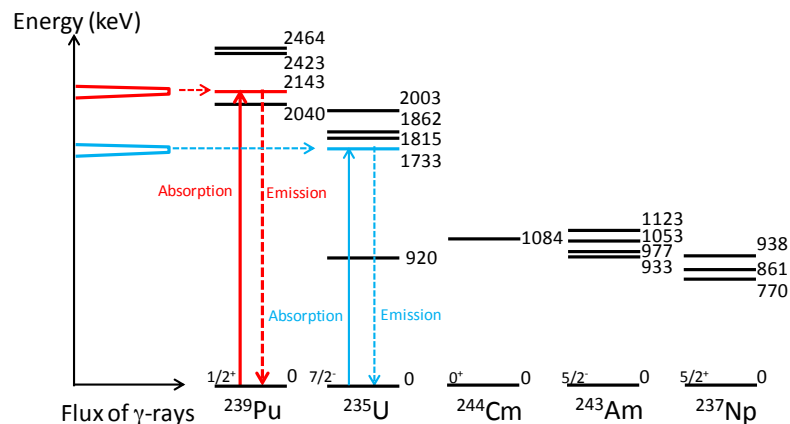

Fig.1 Schematic view of the nondestructive assay system based on nuclear resonance fluorescence with laser Compton scattering gamma-ray source.
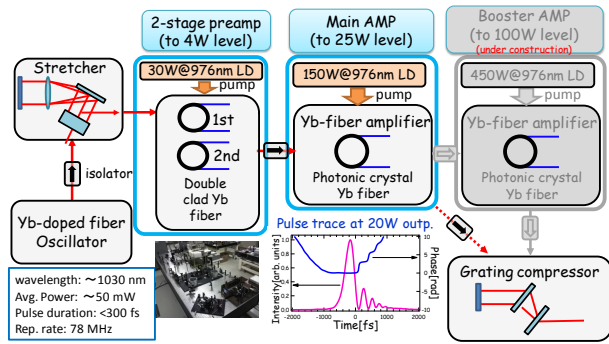
Fig. 2 Block diagram of high average power laser system. Temporal pulse trace of laser beam is inset.

In particular, synchronization between laser beam and electron bunch is necessary. A commercial-based 1-chip frequency synthesizer integral circuit (IC) for the radio communication is consisted a controller logic, a low noise digital phase frequency detector (PFD), a precision charge pump, a programmable divider. It provides high quality and stable radio communication. We tried to develop synchronization system based on 1-chip frequency synthesizer IC (see in Fig.3). Less than 1ps timing jitter is achieved by dual loop phase-locked-loop (PLL) configuration. This value is low enough to synchronize between short pulse laser beam and picosecond electron bunch.
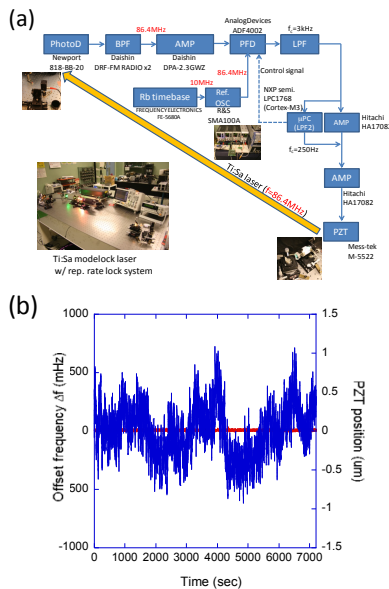

Fig. 3 (a) Block diagram of synchronization module. (b) Offset frequency of the laser repetition rate ($\sim$80MHz).

In addition, low-loss optical configuration for photon storaging has been demonstrated. At this experiment, polarization dependence of constructive and destructive interference inside the cavity was used to detect difference of the cavity length between laser oscillator (Ti:Sa mode-lock laser (test laser)) and enhancement cavity. In order to generate such dependence, 3-mirror image inverter was used. The advantage of this method from another error detection techniques is not only higher photon storaging but also controllability of stored

laser beam polarization via electrically switching of cavity lock.
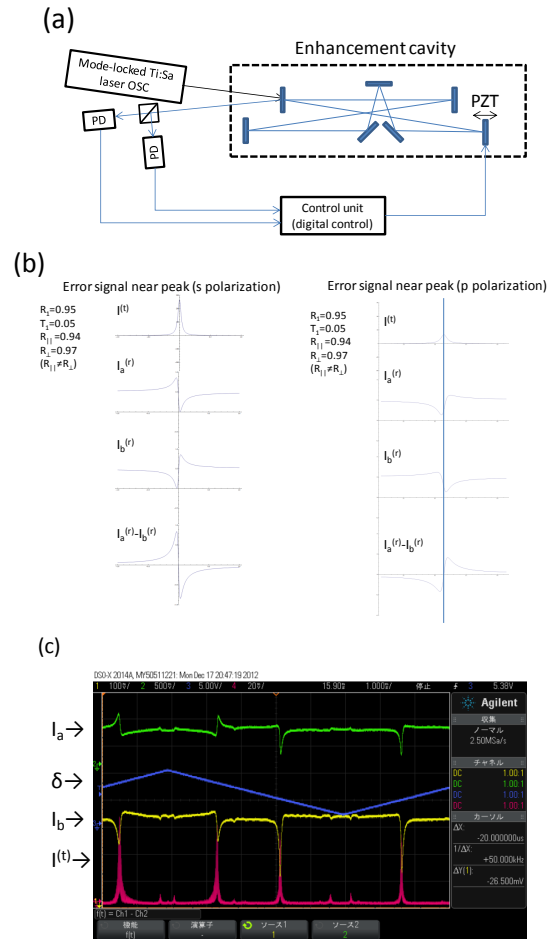
Fig. 4 (a) Schematic view of the experimental setup for enhancement cavity test. (b) Simulated stored laser beam and detected error signal as a function of cavity error. (c) Observed stored laser and error signal as a function of cavity error δ.

Acknowledgement

References

[1] W. Bertozzi, R.J. Ledoux, Nucl. Instr. and Meth. B 241 820 (2005).

[2] J. Pruet, D.P. McNabb, C.A. Hagmann, F.V. Hartemann, C.P.J. Barty, J. Appl. Phys. 99 123102 (2006).

[3] C.A. Hagmann, J.M. Hall, M.S. Johnson, D.P. McNabb, J.H. Kelley, C. Huibregtse, E. Kwan, G. Rusev, A.P. Tonchev, J. Appl. Phys. 106 0849801 (2009).

[4] R. Hajima, T. Hayakawa, N. Kikuzawa, and E. Minehara, J. Nucl. Sci. Technol. 45 441 (2008).

[5] T. Hayakawa, N. Kikuzawa, R. Hajima, T. Shizuma, N. Nishimori, M. Fujiwara, and M. Seya, Nucl. Instr. Meth. A 621 695 (2010).

Conference on Laser and Accelerator Neutron Sources and Applications(LANSA'13), Yokohama, Japan, Apr. 23 - Apr. 25, 2013

A planning effort for severe fusion neutron source generation in Korea and fusion-fission hybrid transmutation reactor R&D

Jung-Hoon Han[1], G.S. Lee[2],) Y.S. Hwang [1], B.G. Hong[3], Yong-Su Na[1], Han-Gyu Joo[1], Hyung-Jin Shim[1], and K-DEMO team
[1] CARFRE, Seoul National University, 599 Gwanak-ro, Gwanak-gu, Seoul, Korea, tel. 82-2-880-7213, fax 82-70-8255-6459
junghoonhan@snu.ac.kr, [2] National Fusion Research Institute [3] Jeon-Buk National University

Abstract: *After successful construction of KSTAR superconducting tokaamk and participation to ITER Korean national fusion programme is planning for K-DEMO baseline R&D for the beyond ITER period. After completion of K-DEMO baseline R&D design and construction R&D would start. Reflecting fusion energy development programme and foreseen nuclear energy prospective fusion-fission hybrid transmutation R&D is in progress as an academy sector base programme organized by CARFRE, Seoul National University*

1. Introduction

In December 1995, the KSTAR (Korea Superconducting Tokamak Advanced Research) project started as the first major step forward to a full-scale fusion energy research and development program in Korea. By adopting ITER relevant technologies such as Nb3Sn superconducting magnets in full-scale, succeeded in developing a new generation of steady-state fusion research facility. After the successful construction of KSTAR, Korea joined the ITER project to fulfill the second milestone of fusion energy realization path. As ITER construction is in progress there are on-going push forward activities for "Beyond ITER period" among ITER Member States for fast realization of fusion energy with a practical demonstration of fusion electricity generation on power plant scale, a Demonstration Fusion Power Plant (DEMO), to mitigate the growing global Climate Change damage. Reflecting DEMO preparation activity among ITER Member States and as a response to the request for "Future Energy Vision" from our society after Fukushima accident, in Korea, a Korean DEMO (K-DEMO) design and R&D planning activity, was initiated in 2012. The aim is to launch a new national program for DEMO relevant R&D activities starting from the year 2014 to bridge technical gaps that exist between ITER plasma and nuclear regime and that of DEMO.

2. Severe neutron source K-DEMO planning

K-DEMO[1] would be implemented in two phased process. The first stage will develop components for the second stage, and the second stage is aimed for to produce fusion electricity. In design and specifications, K-DEMO in the final stage should be few steps away from a commercial plant in terms of technology and performance. Conceptual study of K-DEMO and the implementation plan for core technology R&D based on a gap study with priority are under planning.

2.1 DEMO Baseline Technology Development Program

To cultivate DEMO related R&D activities DEMO Baseline Technology Development Program is under planning. It consists of four subprograms, which are burning plasma physics and technology, supporting technology, material technology, fusion power plant technology. Under these four subprograms eight specific programs are determined and listed in Table 1.

Table 1. Baseline technology development program

Burning plasma physics and technology	Plasma physics and simulation
	Divertor and Blanket
Supporting Technology	Superconductor
	Heating, Current Drive, Diagnostics, Fueling
Material Technology	Structure material
	Plasma facing components and material
Power Plant Technology	RAMI
	Licensing

This baseline R&D program would last for eight years and would be converted to DEMO design activities which are under the framework of Korean National Fusion Energy Development Plan and backed by the "Korean Fusion Energy Development Promotion Law".

2.2 Baseline technology R&D implementation plan
Most of eight R&D activities would be carried with research facilities allocated to Korean university environments which would interact with national and international research organization in fusion and closely related disciplines. This setting would spread most updated fusion R&D activities to most of engineering and science areas of academic sectors in Korea. And it would strengthen a close communication among science and technology R&D activities for fusion energy development.

2.3 K-DEMO design study
After eight years DEMO relevant baseline R&D along with K-DEMO conceptual study K-DEMO design activity will start as described in Korean Fusion Energy

Development Plan roadmap. K-DEMO design baseline would be adopted from ITER by following conservative engineering approach yet adopting any newly developed technology which would shorten the development path and reduce development cost. During the design study and design process ITER engineering experiences and featured experimental results would be an essential ingredients along with the results from already operating steady state capable tokamak such as EAST, KSTAR, and upcoming newly installed facility JT60-SA. After several years of design activity construction for phase I K-DEMO would start around year 2035.

3. Fusion-Fission hybrid transmutation reactor R&D

CARFRE (Center for Advance Research in Fusion Reactor Engineering) in Seoul National University (SNU), established in 2008 and supported by Korean government, has been carrying out its given mission of R&D in fusion reactor engineering. Under on-going international and national activities for a preparation of substantial fusion neutron sources, DEMO, recently, two more missions are added, one is functioning as a center piece of the next step Korean DEMO technology R&D planning and the other is conducting fusion-fission transmutation reactor R&D in Korea as a major mission to propel in a close collaboration with SNU Nuclear Engineering department.

3.1 Research Motivation
In Korea twenty three nuclear power plants are in operation and four of them is PHWR and nineteen are PWR. Korea does not have any reprocessing facility for the spent nuclear fuel (SNF). SNFs are now stored at the nuclear power plant storage in a compacted form to extend its storing capacity, but within ten years it might reach the limitation. Under this circumstance and reflecting Korean geopolitical situation among three possible feature of fusion-fission hybrid, i.e., fissile fuel breeding, power generation, and nuclear waste transmutation the most demanded choice is deep burn of SNF. Along with this Korean nuclear situation, from fusion side, ITER project has been launched since 2007 and also BA for DEMO activity are also launched as international activity and nationally K-DEMO activity would start in a near time scale. Therefore it is a proper time to discuss about FFH-transmutation reactor and its possible R&D path in the near future.

3.2 Possible figures for FFH transmutation reactor
From engineering point of view and knowledge base piled from the experiences from ITER, KSTAR, and other relevant tokamak the most possible FFH concept is based on large tokamak[2, 3]. With possible low fusion gain Q of 1-3 from ITER like tokamak and sustained plasma, either long pulse or steady-state operation modes, which are now developing for ITER operation "ITER like FFH" with FFH blanket would be a doable concept with existing or near term future technologies. Besides "ITER like FFH" another concept based on spherical tokamak is also being developed at CARFRE, which is operating spherical tokamak VEST(Versatile Experiment Spherical Torus)[4] .

3.2 Implementation for FFH-transmutation reactor (TR)
FFH-TR design process could be implemented when K-DEMO phase I is completed. By this time most of technology development and operation study would be in matured or being verified stages and necessary licensing process is in progress. With strong international collaboration in terms of partnership and agreement FFH-TR serve as an 'incinerator' for the piled SNF from centuries' long operation of nuclear power plant , which is a necessary instrument for maintaining economy for substantial period of time with high efficiency electricity generation without generating much climate pollutant to the atmosphere.

4. Conclusions
FFH-TR could be a necessary option to clear up SNF with substantial fusion neutron sources, which is foreseen to be developed within a sizable period with existing or near term to be developed technologies with strong international collaboration among the countries, which are operating nuclear power plants to maintain their economies and also developing fusion energy for the future.

References
[1] G. S. Lee, Keeman Kim, Y. S. Hwang, J. H. Han, H. C. Kim, K. H. Im, G. H. Neilson, T. Brown, P. Titus, and C. Kessel " Korean fusion road map: K-DEMO design and R&D Plan," *submitted to 25th Symposium on Fusion Engineering* (2013).
[2] I. Murata, Y. Yamamoto, S. Shido, K. Kondo, A. Takahashi, E. Ichimura, and K. Ochiai "Fusion-driven hybrid system with ITER model," Fusion Engineering and Design, Vol.75-79, 871-875 (2005).
[3] Jung-Hoon Han, et al, "A conceptual study for a feasible fusion energy utilization plant", Fusin Science and Technology, Vol.56, Number 2, 930-934 (2009).
[4] Y.H. An, K.J. Chung, B.K. Jung, C. Sung, H.Y. Lee, Y.S. Na, T.S. Hahm and Y.S. Hwang "Design and Construction of Versatile Experiment Spherical Torus at SNU," *53rd Annual Meeting of the APS Division of Plasma Physic, Salt LakeCity* (2011).

Transformation of the Beam Intensity Distribution and Formation of a Uniform Ion Beam by Means of Nonlinear Focusing

Yosuke Yuri, Takahiro Yuyama, Tomohisa Ishizaka, Ikuo Ishibori, and Susumu Okumura

Takasaki Advanced Radiation Research Institute, Japan Atomic Energy Agency,

1233 Watanuki-machi, Takasaki, Gunma 370-1292

Abstract: *Target heating is a critical problem in neutron production using a high-intensity beam. We, therefore, study nonlinear beam focusing using multipole magnets for tailoring the transverse beam intensity distribution. The distribution transformation by the nonlinear force is theoretically described. A large-area uniform ion beam is experimentally formed using octupole magnets.*

1. Introduction

Large-area uniform irradiation is a basic accelerator technique for bringing about a homogeneous irradiation effect on a sample. In accelerator-based neutron facilities, uniform irradiation is required in order to avoid thermal stress or damage of a target vessel. A high-intensity driver beam is usually defocused by quadrupole magnets or scanned by ac dipole magnets on the target, depending on an irradiation condition. However, these are not always sufficient for the reduction of local target heating.

As another method, the use of the nonlinear force from multipole magnets is feasible. With this *nonlinear focusing method*, the tail of the Gaussian transverse intensity distribution can be folded into the inside through the nonlinear focusing force produced by multipole magnets (mainly, octupole magnets) and thus the intensity distribution can be made uniform on the target [1, 2]. Actually, the beam transformation by means of nonlinear focusing has been already realized in several facilities [3-5] and designed for future high-power neutron facilities [6, 7]. For extensive understanding of the nonlinear focusing method, we have been studying the transformation of the beam intensity distribution by means of nonlinear focusing theoretically as well as experimentally [2, 5].

In this presentation, the transformation of the transverse intensity distribution is explored more in detail when the beam is focused by an octupole magnet in a beam transport line. In order to see how the beam distribution is transformed by the multipole force, the beam envelope on the target is analytically derived as a function of the multipole strength from the second-order moments. To verify the theoretical consideration, a particle tracking simulation is performed. The present result is helpful for the design and experiment of the beam irradiation using multipole magnets. Furthermore, an experiment with ion beams is carried out at the azimuthally-varying-field (AVF) cyclotron in Japan Atomic Energy Agency (JAEA). We experimentally demonstrate that a uniform beam can be formed using octupole magnets.

2. Beam dynamics theory

Assume that a charged particle travels along the linear beam transport line composed of quadrupole and multipole magnets. We here consider only one transverse direction of motion in order to eliminate the complexity of the analysis. According to Ref. [2], the on-target spatial distribution ρ_t of the beam focused by a multipole magnet can be determined analytically. It is given, using the initial distribution ρ_0 at the multipole magnet (number of poles: $2n$, integrated strength: K_{2n}) as follows:

$$\rho_t = \rho_0 \left/ \left[\sqrt{\frac{\beta_t}{\beta_0}} \cos\phi - \sqrt{\beta_0\beta_t}\sin\phi \frac{K_{2n}}{(n-2)!} x_0^{n-2} \right] \right., \quad (1)$$

where β_0 and β_t are, respectively, the beta functions at the multipole magnet and at the target, ϕ is the betatron phase advance from the multipole magnet to the target, and x_0 is the particle's coordinate at the multipole magnet.

We here consider the root-mean-square (rms) radius of the on-target beam. It can be described using the second-order moments:

$$\left\langle \left(x_t - \langle x_t \rangle\right)^2 \right\rangle = \int \left(x_t - \langle x_t \rangle\right)^2 \rho_t dx_t, \quad (2)$$

where x_t is the particle's coordinate at the target. The moment can be analytically integrated by incorporating Eq. (1) and assuming the initial Gaussian distribution, $\rho_0 = 1 \left/ \sqrt{2\pi\varepsilon\beta_0} \right. \mathrm{Exp}\left[-x_0^2 \left/ (2\varepsilon\beta_0)\right.\right]$, with the rms emittance ε of the beam. We thus have the rms beam radius σ, which is the square root of the second-order moment. For the octupole-focusing ($n=4$) case,

$$\sigma = \sqrt{\varepsilon\beta_t} \sqrt{1 - \varepsilon\beta_0^2 K_8 \tan\phi + \frac{5}{12}\left(\varepsilon\beta_0^2 K_8 \tan\phi\right)^2} \left|\cos\phi\right|. \quad (3)$$

The beam size can be reduced by an octupole magnet with a proper field polarity. As the octupole strength is increased, the Gaussian tail is folded into the inside, then the central region is made uniform, and finally the beam size is minimized for $K_{OCT}L_{OCT} = 6 \left/ \left(5\varepsilon\beta_0^2 \tan\phi\right)\right.$.

Similarly, the rms beam size can be obtained for any order of multipole focusing. The beam centroid, which can be obtained from the first-order moment, is always zero as long as the order n of the multipole magnet is even and the initial beam is on-axis.

3. Numerical simulation

Single-particle tracking simulations were performed to confirm the analytical result in the previous section. We

considered an actual lattice layout of the beam transport system equipped with octupole magnets at the JAEA AVF cyclotron. Only the horizontal degree of freedom of the beam motion was considered in the present simulation so that numerical results can be compared with the analytical results. As an initial condition of the beam, a beam whose distribution is Gaussian and horizontal rms emittance is 10π mm mrad is assumed.

Figure 1 shows the on-target spatial distributions of the beams focused with several different octupole strengths. With a proper polarity of the magnet, the tail of the Gaussian beam is folded, and thus the resultant distribution has a steep edge. An almost uniform distribution can be formed at a certain octupole strength. The dependence of the rms beam size on the octupole strength agreed with the theoretical prediction Eq. (3).

4. Experiment

The transformation of the intensity distribution was experimentally investigated using 10-MeV proton beams from the JAEA AVF cyclotron.

A uniform beam was formed in the following procedure: The beam extracted from the cyclotron, which often had an asymmetric intensity distribution, was firstly smoothed to a Gaussian-like transverse distribution through multiple Coulomb scattering of a thin foil. Then, the Gaussian-like beam was focused by octupole magnets. In order to form a large-area uniform beam efficiently, a dedicated beam optics that suppressed the betatron coupling induced by octupole magnets was utilized [5].

The on-target intensity distribution of the beam is shown in Fig. 2 where a flat-top uniform distribution is formed. The rms uniformity of the flat-top region was 5%. The peripheral high-intensity peak can be adjusted by the octupole strength, and even flattened by removing the tail of the Gaussian-like beam in a specific location upstream [5] or by additionally focusing a dodecapole magnet [2].

5. Conclusion

We explored the effect of octupole focusing on the transverse beam intensity distribution through theoretical analysis, numerical simulations and experiments. The changes in the rms size of the beam were analytically

shown. The validity of the theoretical consideration was tested through single-particle tracking simulations. In the experimental study at the JAEA AVF cyclotron, a two-dimensional uniform beam was formed using octupole magnets. Such an ion beam with a specific transverse distribution tailored by the nonlinear focusing force has been already employed for the beam application in space science [8] and will be a useful tool also for neutron production.

References

[1] P. F. Meads, Jr., "A Nonlinear Lens System to Smooth the Intensity Distribution of a Gaussian Beam," IEEE Trans. Nucl. Sci. **30**, 2838 (1983).

[2] Y. Yuri, N. Miyawaki, T. Kamiya, W. Yokota, K. Arakawa, and M. Fukuda, "Uniformization of the Transverse Beam Profile by Means of Nonlinear Focusing Method," Phys. Rev. ST Accel. Beams **10**, 104001 (2007).

[3] N. Tsoupas, L. Ahrens, S. Bellavia, R. Bonati, K. A. Brown, I-Hung Chiang, C. J. Gardner, D. Gassner, S. Jao,W.W. Mackay, I. Marneris, W. Meng, D. Phillips, P. Pile, R. Prigl, A. Rusek, L. Snydstrup, and K. Zeno, "Uniform beam distributions at the target of the NASA Space Radiation Laboratory's beam line," Phys. Rev. ST Accel. Beams **10**, 024701 (2007).

[4] A. Bogdanov, V. Anferov, M. Ball, D. V. Baxter, V. P. Derenchuk, A. V. Klyachko, T. Rinckel, and K. Solberg, "Uniform Beam Intensity Redistribution in the LENS Nonlinear Transport Line," Proc. 2007 Particle Accelerator Conference, Albuquerque, USA, 2007, p. 1748.

[5] Y. Yuri, T. Ishizaka, T. Yuyama, I. Ishibori, S. Okumura and K. Yoshida, "Formation of a Large-Area Uniform Ion Beam Using Multipole Magnets in the TIARA Cyclotron," Nucl. Instrum. Methods Phys. Res. A **642**, 10 (2011).

[6] P. A. P. Nghiem, N. Chauvin, M. Comunian, O. Delferriere, R. Duperrier, A. Mosnier, C. Oliver, and D. Uriot, "The IFMIF-EVEDA challenges in beam dynamics and their treatment," Nucl. Instrum. Methods Phys. Res. A **654**, 63 (2011).

[7] K. Thomsen, F. Heinrich, M. Butzek, J. Wolters, F. Sordo, and A. I. S. Holm, "Some technical issues for a cannelloni spallation-target at high power," Nucl. Instrum. Methods Phys. Res. A **682**, 42 (2012).

[8] M. Imaizumi, Y. Yuri, P. R. Bolton, S. Sato, and T. Ohshima, "Innovative technologies on proton irradiation ground tests for space solar cells," Proc. 38th IEEE Photovoltaic Specialist Conference, Austin, USA, 2012 p. 2831.
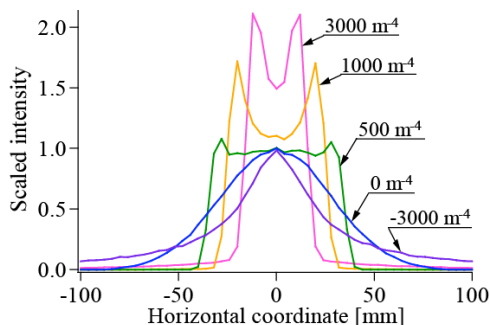
Fig. 1. On-target real-space distributions of the beam focused by an octupole magnet with several different strengths.
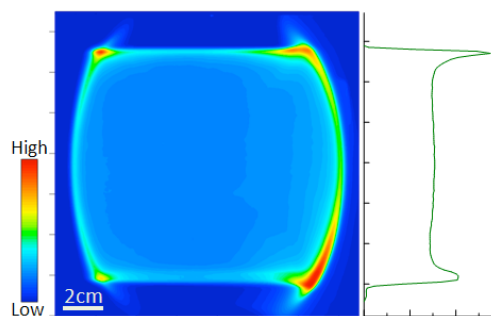

Fig. 2. Spatial intensity distribution of the proton beam focused by octupole magnets. It was obtained using a radiochromic film.

Generation of High-Quality Proton Beams with Nanotube Accelerator

M. Murakami[1] and M. Tanaka [2]

[1] Institute of Laser Engineering, Osaka University, 2-6 Yamada-oka, Suita, Osaka 565-0871, Japan
Phone: +81-6-6879-8743; Fax: +81-6-6879-8743; Email : murakami-m@ile.osaka-u.ac.jp
[2] Department of Engineering, Chubu University, Aichi 487-8501, Japan

Abstract: *A novel ion acceleration scheme is proposed: Carbon nano-tubes containing low-Z materials are irradiated by an ultrashort intense laser. Due to the resultant electrostatic field, the nanotube and embedded materials play the roles of the barrel and bullets of a gun, respectively, to produce highly collimated and quasimonoenergetic ion beams.*

1. Introduction

Ion acceleration driven by ultraintense ultrashort laser pulses has been intensively studied in the past decade because a number of future applications are expected. For practical use of the accelerated ions, it is crucial to produce high-quality beams that are monoenergetic and collimated. We here propose a novel ion acceleration scheme using carbon nanotubes (CNTs), in which embedded fragments of low-Z materials are irradiated by an ultrashort intense laser to eject substantial numbers of electrons. Due to the resultant unique electrostatic field, the nanotube and embedded materials play the roles of the barrel and bullets of a gun, respectively, to produce highly collimated and quasimonoenergetic ion beams.
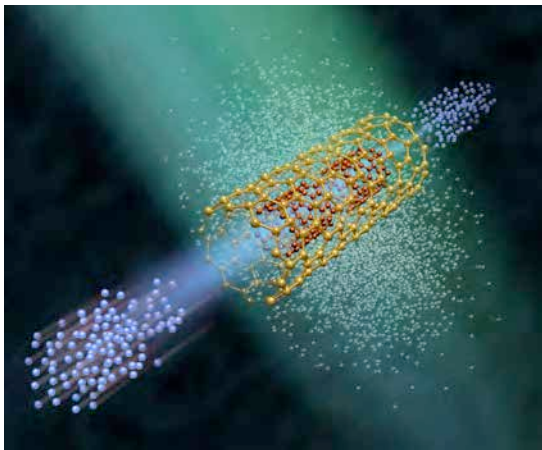
Fig. 1. Schematic view of a nanotube accelerator.

2. The nanotube accelerator

Figure 1 shows the schematic view of a nanotube accelerator. The double nested nanotubes are irradiated by an ultrashort intense laser pulse. The outer carbon nanotube is chemically adsorbed with heavy atoms such as gold, while the inner nanotube is made of light materials such as hydrogen and carbon to form the projectiles. Upon laser irradiation, electrons inside the nanotubes are ejected within a few laser cycles (comprising the small white particles around the nanotubes). The remaining nanotubes composed of positive ions generate a unique electrostatic Coulomb field so that the inner ions are accelerated along the axis symmetrically toward both ends of the outer nanotube. As a result, a pair of quasimonoenergetic collimated ion beams are obtained.
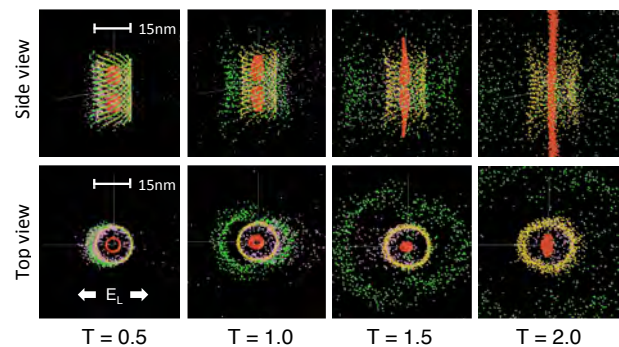

Fig. 2. Three dimensional N-body simulation result.

3. N-body simulation

We have performed *N*-body charged particle simulations, in which all of the particle-to-particle Coulomb forces are computed exactly. The relativistic version of the Newtonian equations of motion are used, similar to molecular dynamics simulations of microwave heating of salty water and ice. Moreover, our simulation includes the Lennard-Jones attractive potentials for pairs of like atoms, and repulsive potentials for other species as a core exclusion to avoid numerical divergences. Such *N*-body simulations are the most suitable numerical approach for treating parametric domains in which the plasma scale becomes significantly shorter than the Debye length.

Figure 2 shows snapshots of the nanotube accelerator dynamics at sequential times, obtained in the *N*-body simulations in a side view (upper row) and top view (lower row). The outer nanotube is of 30 nm in length and 15 nm in diameter, with gold atoms (yellow) chemically adsorbed onto the carbon atoms (green). Inside the nanotube, two cylindrical bullet nanotubes made of hydrogen (red) are embedded. Sinusoidal laser light is applied with intensity $I_L = 10^{18}$ W cm^{-2}. During

the first laser cycle, ionized electrons (white) are ejected by the laser field. Simultaneously the saddle-shaped Coulomb field forms to squeeze and accelerate the projectile ions along the *z*-axis.

At *t* = 0, sinusoidal laser light is incident on the nanotube from a radial direction perpendicular to the axis. The linearly polarized electric field is $E_L = E_0 \sin(2\pi T)$ for $T > 0$, where $T = t/t_0$ is the time normalized to the laser period $t_0 = 2.7$ fs for a titanium-sapphire laser at a wavelength of $\lambda_L = 0.8$ mm. In Fig. 2, the field amplitude is $E_0 = 3 \times 10^{12}$ V m^{-1}, corresponding to a laser intensity of $I_L = 10^{18}$ W cm^{-2}. At such an intensity, the gold atoms are photoionized to a state of about $Z_{Au} = 20$, while the carbon and hydrogen atoms are fully ionized to $Z_C = 6$ and $Z_H = 1$, respectively. If the laser is irradiated from one side, the present scheme has an applicable upper limit ($I_L \sim 10^{20}$ W cm^{-2}) to keep high collimation performance, over which the ions are also accelerated by ponderamotive force along the same direction of the incident laser. The maximum ion energy is expected to increase with the system size and laser intensity according to the principles of a Coulomb explosion [1-3].

4. Energy spectrum

Figure 3 shows temporal evolution of the proton energy spectrum in the axial (solid curves) and radial (dashed curve at $T = 5$) directions. Corresponding two-dimensional dynamics has been shown in Fig. 2. Quasimonoenergetic protons with an energy of $E_{max} = 1.5$ MeV are produced at $T = 5$. If the hydrogen atoms are replaced by carbon atoms, the maximum ion energy increases to 10 MeV for the same target structure. The maximum energy can also be increased by enlarging the target size.

A good measure of the collimation is E_z/E_r, where E_z and E_r denote the average kinetic energies of the projectile ions in the axial and radial directions, respectively. In Fig. 3, $E_z \sim 1.4$ MeV and $E_r \sim 0.017$ MeV for the final stage of acceleration at $T = 5$, so that $E_z/E_r \sim 85$, which indicates a strikingly high degree of collimation. Finally, the energy coupling efficiency h_c is an important index of the ion beam generation from an engineering point of view. It is defined as the ratio of the integrated kinetic energy of the projectile ions to the absorbed laser energy. In the present work, the values of h_c are of the order of 1% or less. By optimizing the design of the nanotube structure and laser parameters, h_c is expected to increase to several percent.
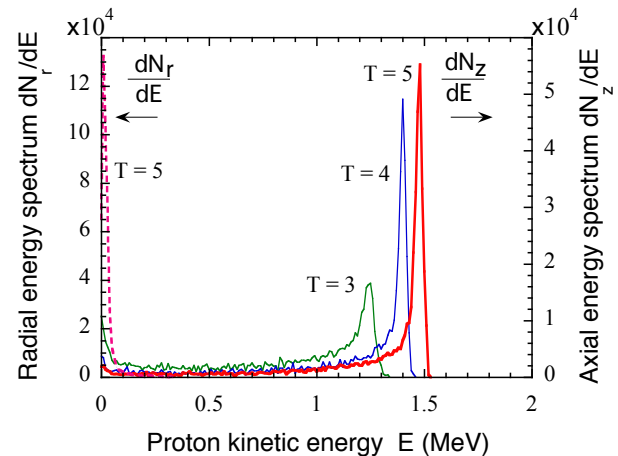

Fig. 3. Temporal evolution of energy spectrum.

5. Summary

We have proposed an ion acceleration scheme using structured nanotubes, that operate under irradiance of ultrashort ultraintense laser pulses, to produce high-quality ion beams. Detailed three-dimensional particle simulation has demonstrated the generation of quasimonoenergetic highly-collimated 1.5-MeV proton beams. The present concept leads to a view of CNTs different from an existing one, that until now had only been considered to be solid-state devices. It has been demonstrated that spacial control in nano-scale fabrication is as crucial as temporal control in femto-scale laser operation. For further practical studies of the present scheme, it will be crucial that multiple nanotubes are uniformly produced in size and uniformly arranged in direction.

References
[1] K. Nishihara, H. Amitani, M. Murakami, S.V. Bulanov, and T.Zh. Esirkepov, "High energy ions generated by laser driven Coulomb explosion of cluster" Nucl. Instrum. Methods Phys. Res. A **464**, 98 (2001).

[2] M. Murakami and K. Mima, "Efficient generation of quasimonoenergetic ions by Coulomb explosions of optimized nanostructured clusters", Phys. Plasmas **16**, 103108 (2009).

[3] B. Ramakrishna, M. Murakami, M. Borghesi, L. Ehrentraut, P.V. Nickles, M. Schnurer, S. Steinke, J. Psikal, V. Tikhonchuk, and S. Ter-Avetisyan, "Laser-driven quasimonoenergetic proton burst from water spray target", Phys. Plasmas **17**, 083113 (2010).

Compact Accelerator Driven Neutron Sources and Their Applications

Michihiro Furusaka and Hirotaka Sato

Faculty of Engineering, Hokkaido University, Kita-13 Nishi-8, Kita-ku, Sapporo, Hokkaido 060-8628, Japan

Tel./Fax: +81-11-706-6677; E-mail: furusaka@eng.hokudai.ac.jp

Abstract: *Several compact accelerator driven neutron sources (CANS) are available now; the electron linac driven pulsed cold neutron source at Hokkaido University (HUNS) is a typical example. We conducted demonstration experiments such as small angle neutron scattering, energy resolved neutron imaging and even a soft error experiment for real network equipment.*

1. Laboratory based compact accelerator driven neutron source

Neutron is a powerful tool, but usually we need either a research reactor or a large accelerator based neutron source, and sometimes it is not so easy to get access to one of these facilities. Compact accelerator driven neutron sources (CANS) could fill the niche of the lack of laboratory X-ray source equivalent neutron source. LENS at Indiana University in the USA is one of such sources, based on a proton linac of 13 MeV and aiming at eventual goal of a few tens of kW source. CPHS of Tsinghua University in China is a similar one under construction and coming online soon.

We are proposing "Laboratory neutron source", that is affordable to university and other laboratory people, easy to maintain, yet we can conduct real experiments. In Japan, several such CANSs have been built quite recently; one at Kyoto University, KUANS, and the other at RIKEN, RANS. They are based on proton linac of 3 to 7 MeV; 0.1 mA; about 0.3 to 0.7 kW at around 50 Hz repetition rate.

At Hokkaido University, we have a compact electron linac driven neutron source, HUNS, of which maximum power is about 1 kW when the parameters of 35 MeV-30 μA, 50 Hz are selected. The performance of it is almost equivalent to those of the above sources and it is a good test bench of such "laboratory neutron source". HUNS has a coupled solid methane moderator at around 17 K. "Coupled" means without a shielding layer in between the moderator and the reflector around it to reduce the pulse-width. With this cold neutron source, we can conduct reasonable neutron experiments, as follows.

2. Development of small and intermediate-angle neutron scattering instruments

At a compact neutron source, we need a different approach to optimize instruments. In case of small-angle neutron scattering (SANS) instrument, we relax angular resolution to get higher intensity. It is called intermediate-angle neutron scattering instrument, iANS. With about 14 mm diameter sample at about 5 m, we put 16 of 1/2 inch diameter 600 mm effective length helium-3 gas filled linear position sensitive detectors (LPSD) about 450 mm downstream of the sample position.

We have also conducted SANS experiment in steel samples with and without nanoscopic precipitates.

With 5 hours of measurement, we can see the difference at the relatively large Q range as shown in Fig. 1, although it is a preliminary analysis.
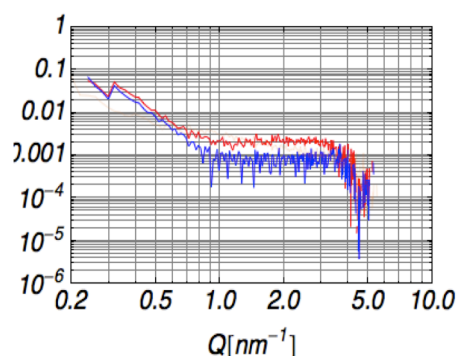

Fig. 1. Steel samples with (upper curve) and without (lower curve) nanoscopic precipitates.

3. Development of new imaging techniques using pulsed neutrons

Energy resolved neutron-imaging method using the time-of-flight (TOF) technique is expected as a new material analysis tool. This method can non-destructively visualize physical and chemical information in a bulk material over large area with high spatial resolution. For example, crystallographic and metallographic information can be evaluated quantitatively by the Bragg edge transmission spectroscopy [1]. By the resonance absorption spectroscopy [2], element, nuclide, lattice vibration and temperature can be deduced and by the wavelength-dependent polarization analysis of polarized neutrons [3], information of magnetic field strength and the direction of it would be obtained. Therefore, at HUNS, we are developing these techniques, performing application experiments, and carrying out the test experiments of new TOF imaging detectors [4,5].

Table 1 shows a performance comparison between pulsed neutron imaging facilities at J-PARC and HUNS, in terms of the flux for measurement time, the wavelength resolution for precision of visualized values, the field of view for visualized area and the divergence for spatial resolution. The HUNS pulsed neutron imaging facility does not have so good performances.

Table 1. Performance comparison between pulsed neutron imaging facilities at J-PARC and HUNS.

	Flux (n/cm²/s)	Wavelength resolution (%)	Field of view (cm×cm)	Divergence (mrad)
J-PARC MLF BL10	4.8×10^7	0.33	10×10	$\pm0.5 \sim \pm7$
HUNS cold BL	8.6×10^3	2.7	10×10	±17

However, under such experimental condition, we have successfully developed new techniques. For example, Fig. 2 shows the first quantitative evaluation results of crystallographic texture and microstructure obtained by the Bragg edge transmission imaging. These were firstly achieved at HUNS in the world. The birth of this new unique technology has given a big impact toward research fields of not only the neutron imaging but also the materials science.

Thus, a compact accelerator based neutron experimental facility also can sufficiently carry out various experiments on research, development and application. This is because the research activity at such facility can be based on unique ideas and we can perform many trial experiments to check new ideas.
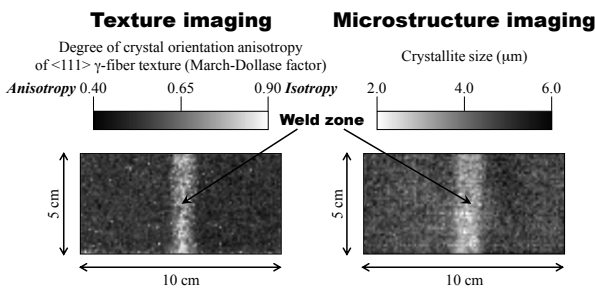
Fig. 2. The first quantitative evaluation results of crystallographic texture and crystallite size obtained by the Bragg edge transmission imaging, firstly achieved at HUNS in the world.

4. Soft-error experiments of telecommunication devices

Recently, telecommunications carriers are concerned about failures caused by the soft-error. The soft-error is a temporary error that occurs in semiconductor devices. The error is sometimes caused by nuclear reactions of neutrons generated by cosmic rays in the atmosphere. Therefore, we conducted some soft-error experiments on telecommunication devices using Hokkaido University linac for the verifications of i) soft-error tolerance of network telecommunication devices, ii) fault detection process and switching process of network route when soft-error is caused, and iii) the effect of measures for soft-errors.

In order to efficiently measure the number of network device, three telecommunication devices were irradiated at the same time; three neutron beamlines connecting to one fast neutron source were available during this experiment. Fig. 3 shows a result of the Monte-Carlo simulation of the neutron energy spectrum at the irradiation position.
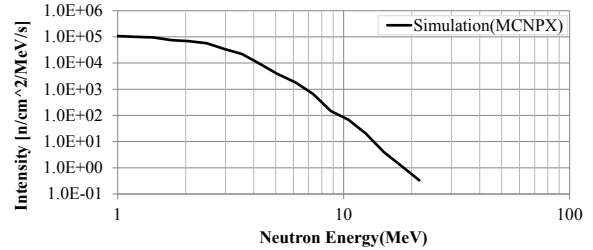

Fig. 3. Source neutron energy spectrum obtained by simulation calculation for the soft-error experiments.

Compared to the mean soft-error interval calculated from failure rate of the actual field and the experimental condition, the mean soft-error interval of the experiment was 1.6 times longer. In addition, we also found that failure rates in the field and the experimental correspond to each telecommunication device. Furthermore, we have confirmed that the number of soft-errors reduced to 1/5 after the measures for soft-errors. Thus, we found that the soft-error experiments can be well carried out with compact accelerator based neutron sources, and various useful data can be obtained very efficiently through the experiment. Therefore, we expect that we can improve the reliability of telecommunication devices by an incorporating-level compact accelerator on the development process in the future.

References

[1] H. Sato, T. Kamiyama and Y. Kiyanagi, "A Rietveld-Type Analysis Code for Pulsed Neutron Bragg-Edge Transmission Imaging and Quantitative Evaluation of Texture and Microstructure of a Welded α-Iron Plate", Mater. Trans. **52**, 1294-1302 (2011).

[2] H. Sato, T. Kamiyama and Y. Kiyanagi, "Pulsed neutron imaging using resonance transmission spectroscopy", Nucl. Instrum. Methods A **605**, 36-39 (2009).

[3] T. Negishi, T. Shinohara, H. Sato, H. Hasemi, T. Kamiyama and Y. Kiyanaigi, "Preliminary experiment of magnetic imaging using polarized pulsed neutrons at HUNS", Physics Procedia (to be published).

[4] H. Sato, O. Takada, S. Satoh, T. Kamiyama and Y. Kiyanagi, "Development of material evaluation method by using a pulsed neutron transmission with pixel type detectors", Nucl. Instrum. Methods A **623**, 597-599 (2010).

[5] S. Uno, T. Uchida, M. Sekimoto, T. Murakami, K. Miyama, M. Shoji, E. Nakano, T. Koike, K. Morita, H. Sato, T. Kamiyama and Y. Kiyanagi, "Two-dimensional Neutron Detector with GEM and its Applications", Physics Procedia **26**, 142-152 (2012).

Development of X-band 30 MeV Linac Neutron Source at Decommissioned Experimental Reactor "Yayoi" for Fukushima Nuclear Accident Analysis

Mitsuru Uesaka[1], Katsuhiro Dobashi[1], Takeshi Fujiwara[1], Kazuhiro Tagi[1], Hideo Harda[2]
[1] Nuclear Professional School, University of Tokyo, 2-22 Shirakata-shirane, Tokai, Naka, Ibaraki, Japan
[2] Japan Atomic Energy Agency, 4-49 Muramatsu, Tokai, Naka, Ibaraki, Japan

Abstract: Just after the decommission of the experiment reactor "Yayoi" of University of Tokyo, the X-band (11.424GHz) electron linac is allocated into its core space as a neutron source for the nuclear analysis for the Fukushima nuclear plant accident in 2014. We should now accumulate more precise nuclear data of U, Pu, TRU and MA especially in epithermal (0.1-10 eV) neutrons. First we plan to perform the TOF (Time Of Flight) transmission measurement of the total cross sections of the nuclei for 0.1-10 eV neutrons.

1. Introduction

We plan to use our X-band electron linac (11.424GHz, 30 MeV) as a neutron source[1,2] for the nuclear analysis for the Fukushima nuclear plant accident. Originally we developed the linac for Compton scattering X-ray source. Quantitative material analysis and forensics will start several years later after the safe settlement of the accident is established. For the purpose, we should now accumulate more precise nuclear data of U, Pu, TRU and MA especially in epithermal (0.1-10 eV) neutrons. Therefore, we have decided to suspend the Compton scattering X-ray experiment and allocate the linac to the core of the experimental nuclear reactor "Yayoi" (see Fig.1) which is now under the decommission procedure. Yayoi is the experimental fast neutron reactor (<1 MeV neutron, 2 kW, 10^{11} neutrons/ cm^2 /s) , which is now under decommission. Due to the compactness of the X-band linac, it can be installed into the fuel core space. Therefore, we can reuse the whole structure of the reactor and neutron beam-lines. It is becoming more important to maintain the activity as a neutron source facility recently.

2. 30 MeV X-band (11.424GHz) electron linac

It is basically designed and operated as a Compton scattering monochromatic X-ray source. The X-band linac (see Fig.2) consists of the 3 MeV thermionic RF gun, solenoid magnet for focusing, α magnet as an energy filter, 700 mm accelerating tube and other components. 50 MW 1 μs X-band klystron and 500 kV modulator are used. ~10^4 micro-bunches of 20 pC and 1 ps(rms) forms 200 mA for 1 μs and 10 μA in average at 50 Hz. The macro-pulse length can be tuned down to 100 ns. The 3 MeV thermionic RF gun, solenoid magnet and α magnet are adopted for low emittance beam with the radius of 0.1 mm (rms) at the collision point with our YAG laser. However, not low emittance but high average current is crucial as a neutron source. Therefore, the low energy part is replaced with 20 keV thermionic gun and 3 MeV traveling wave buncher to get ~0.5 kW beam output.

Fig.2 30 MeV X-band (11.424GHz) electron linac

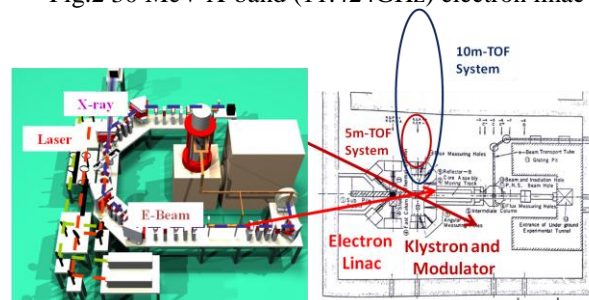Fig.1 Fast Neutron Experimental Reactor "Yayoi" of University of Tokyo

Fig.3 Allocation of the linac to Yayoi area

Schematic drawing of shipping and allocation of the linac to the Yayoi area is shown in Fig.3. The linac itself is set in the core space of the reactor and the klystron and modulator are put aside the shielding structure.

3. Design of TOF Line and Detector for Fukushima Nuclear Accident Analysis

We should prepare more precise nuclear data of U, Pu and related nuclei for the quantitative material analysis and forensics of melted fuel and structural materials. Neutron active method is most promising for the purpose. First we plan to perform the TOF transmission measurement of the total cross sections of the nuclei for 0.1-10 eV neutrons (see Fig.4). Uncertainty of the data of Pu in this region contains ~5% while less than 1% for thermal and epithermal neutrons.
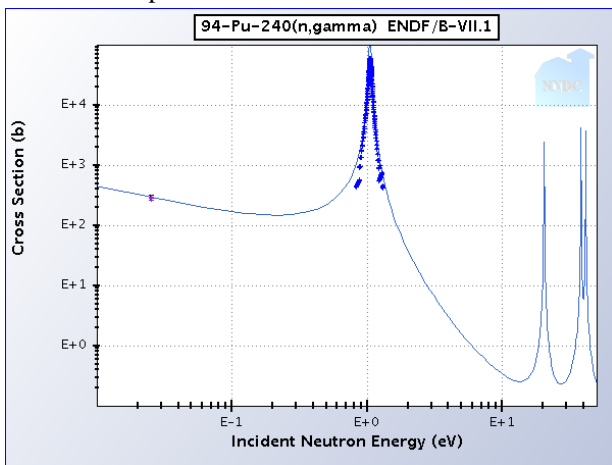
Fig.4 (n ,γ) cross section of 94-Pu-240 for 0.1-10 eV neutron

Optimization of the design of a neutron target (Ta, W, depleted U) and moderator, TOF line and neutron detector (Ce:LiCAF) of high sensitivity and fast response is underway. One example of the time-energy relation of neutron obtained by J-PARC is shown in Fig.5. 0.1 – 10 eV energy range corresponds to ms time delay at TOF. In order to get this range and resolution at a TOF line of less than 10 m, the pulse length of electron and neutron should be around 100 ns. Electron energy, macro-pulse length, power and neutron yield are ~30 MeV, 100 ns – 1 micros, <0.5 kW and <10^{12} n/s, respectively. The moderator to achieve the above neutron yield and pulse length is now under design.
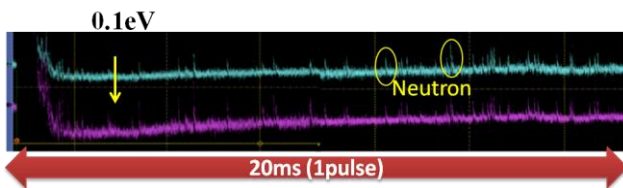

Fig.5 Example of the time – energy relation of neutron obtained by J-PARC.

Since the neutron yield for 100 ns short pulse is rather limited, we have to design highly sensitive detector. For the purpose, we adopt Ce:LiCAF as a scintilator. We are developing its detector system. One example of the signals for neutrons from Cf-252 and γ−rays from Co-60 are shown in Fig.6. Moreover, we plan to form a large detection area to enhance the signal intensity. Finally, we expect to realize ~10 times more signal-to-noise ratio compared to a conventional BF_6 detector.

Installation, commissioning and measurement starts in 2014. Detailed design and way how to contribute to the analysis of the Fukushima nuclear plant accident will be presented
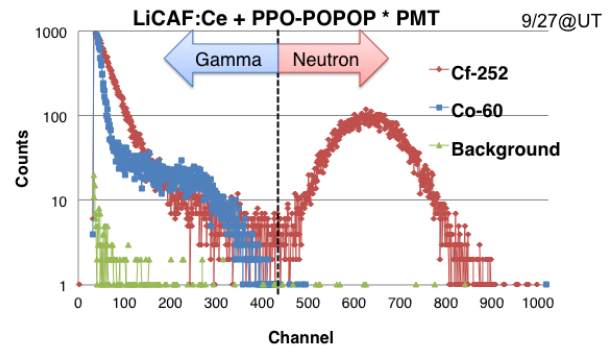

Fig.6 Signals from for neutrons from Cf-252 and γ−rays from Co-60

4. Summary and Subjects

We are going to compose the X-band linac based neutron source at the decommissioned experimental reactor "Yayoi" area and start the nuclear data acquisition for Fukushima nuclear accident analysis. Furthermore, 60 kW 30 MeV S-band linac is also designed for the on-site neutron active method analysis in Fukushima in future.
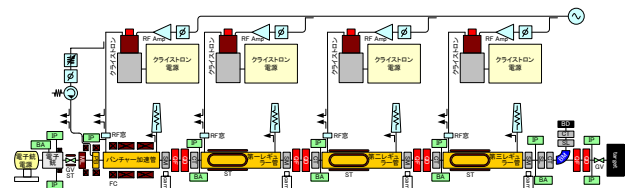

Fig.7 Layout of 60 kW 30 MeV S-band linac for On-site Neutron Active Method Analysis in Fukushima

References

[1] M.S. de Jong, *"PRODUCING MEDICAL ISOTOPES USING X-RAYS"*, THXA01, Proc. of IPAC2012(New Orleans)

[2] H. Kobayashi, T. Kurihara, H. Matsumoto, M. Yoshioka, H. Kumada, A. Matsumura, H. Sakurai, F. Hiraga, Y. Kiyanagi, T. Nakamura, H. Nakashima, T. Shibata, T. Hashirano, F. Inoue, K. Sennyu, T. Sugano, T. Ohba, S. Tanaka., *"CONSTRUCTION OF A BNCT FACILITY USING AN 8-MeV HIGH POWER PROTON LINAC IN TOKAI"*, THPPR048, Proc. of IPAC2012(New Orleans)

Low-energy Neutron Spectrometer for Boron Neutron Capture Therapy

Isao Murata and Tsubasa Obata
Division of Electrical, Electronic and Information Engineering, Graduate School of Engineering, Osaka University
Yamada-oka 2-1, Suita, Osaka 565-0871, Japan
Tel: +81-6-6879-7892, Fax: +81-6-6879-7899.
E-mail: murata@eei.eng.osaka-u.ac.jp

Abstract: *Characterization of thermal/epi-thermal neutron spectrum becomes crucial recently especially in medical application, i.e., boron neutron capture therapy (BNCT). In this paper, we described the preliminary result of ongoing study of a new low-energy neutron spectrometer using a commercially available ^{3}He position sensitive proportional counter.*

1. Introduction

Boron neutron capture therapy (BNCT) is a new radiation therapy which kills tumor cells selectively, simultaneously suppressing influence against healthy cells. In BNCT, cases were reported only in nuclear reactors. Recently, accelerator based neutron sources (ABNS) are being developed because they can be implemented in medical facilities such as hospitals. However, at the moment patients should be positioned very close to the accelerator target because the source strength is quite weak. This leads to a problem that the spectrum is distorted and becomes different from the desirable (standard) neutron field. It also means that the spectrum shape varies depending on kind of accelerator. Since for safe therapies the neutron field should be characterized accurately for each accelerator, we are developing a low-energy neutron spectrometer covering epi-thermal neutron energies of 0.5eV to 10 keV.

2. Measuring technique

2.1 Detection principle
No straightforward method exists to measure low-energy neutron spectrum, because epi-thermal neutron energy is so smaller than Q values of nuclear reactions normally used to detect low-energy neutrons. The important point is to find physical quantity to be able to expand small energy difference in the low-energy region. A possible physical quantity is reaction cross section, because some nuclear reactions have very large reaction cross section values in the low-energy region and the values decrease drastically with increase of energy. In addition, there exists clear one-to-one correspondence between energy and the cross section value in such reactions, because they have an inverse velocity cross section curve in the low-energy region.

The reaction cross section difference may create a detection position (depth) difference especially in a gas counter, because low energy neutrons can be captured immediate after entering into the detector, however, higher energy neutrons can transmit to deeper places until captured. With a position sensitive gas proportional counter, we can measure reaction depth distribution, which possesses the neutron energy information. Then, the neutron spectrum could be reproduced from the

measured reaction depth distribution with a suitable response function, that is, the reaction depth distribution for each energy bin.

2.2 Detector
We used a commercially available position sensitive ^{3}He proportional counter shown in Fig. 1. The length and diameter of detector are 40cm and 2.5cm, respectively. The ^{3}He gas pressure is 0.5 MPa. To measure the detection position (depth) distribution of an incident low-energy neutron, the detector is so set that incident neutrons come into the detector from one of two ends, i.e., the neutron beam direction is parallel to the detector axis. Two signals from both ends of the detector are measured by two pairs of pre-amplifier and main-amplifiers and fed to a multi-parameter system (MPS-1600 (Laboratory Equipment Corporation)) to obtain a two dimensional contour which has energy information.

Fig. 1. ^{3}He position sensitive proportional counter.

3. Experimental

Experiments were carried out at OKTAVIAN facility of Osaka University, Japan. To prepare thermal/epithermal neutrons, we first designed and constructed a graphite thermal column with an AmBe source. The ^{3}He proportional counter was so set up that the neutron beam direction became perpendicular to the detector axis, (1) to confirm whether the detection position difference would appears in the measured two-dimensional spectrum and (2) to assign the real detection position to the channel of the measured detection position distribution by using an appropriate neutron-absorber (cadmium) collimator.

4. Results and discussion

4.1 Two-dimensional spectrum
A measured two-dimensional spectrum is shown in Fig. 2. The horizontal axis shows one of the two signals and the vertical axis shows the other signal. In this measurement, no cadmium collimators as neutron absorber were used, meaning that neutrons are entering

the detector from the side surface uniformly. It was confirmed that the detection position information could successfully be extracted.

4.2 Detection position identification

To confirm one-to-one correspondence between the position (coordinates) in the measured two-dimensional spectrum and the real detection position in the detector, the detector was covered with a cadmium collimator to shield thermal neutrons. Neutrons only entering from open windows of 1cm width of the collimator can be detected. The schematic view of the detector set-up is shown in Fig. 3. In this case, center positions of 2 open windows (A and B in the figure) were 9.5cm, 29.5cm from one side edge (X), at which the corresponding spectrum was observed in Fig. 4. We then projected the counts of the two-dimensional spectrum along a line starting from the origin as a function of angle from x-axis. The result is shown in Fig. 5, in which two peaks are observed corresponding to the positions where no cadmium covers exist. By repeating this experiment, we could assign the real detection position from 0 cm to 40 cm in the detector to the angle in Fig. 5.

5. Future work

In the next phase, the incident direction of source neutrons is changed to be parallel to the detector axis in order to check how well the neutron spectrum could be reproduced from the measured detection depth distribution. For this purpose, several neutron sources having different neutron spectra are to be utilized, i.e., mono-energetic thermal neutrons at JRR-3M, JAEA, thermal/epithermal neutrons at OKTAVIAN facility of Osaka University and 8 keV neutrons at FRS facility of JAEA.

6. Conclusion

We carried out the series study concerning thermal/epithermal neutron spectrometer especially for BNCT. In the present study, we tested a commercially available position sensitive ^{3}He proportional counter as the neutron spectrometer combined with a measuring system with a multi parameter MCA and a thermal neutron field designed and constructed for test measurement. From the measurement, the detection position information could successfully be obtained as a two dimensional spectrum. And, the real detection position could be assigned to the position in the measured detection position. In the next phase, we will carry out the real detection depth distribution measurement with incident neutrons being parallel to the detector axis in several neutron facilities available in Japan.

Acknowledgement

References

[1] I. Murata and H. Miyamaru, "Low-Energy Neutron Spectrometer Using Position Sensitive Proportional Counter - Feasibility Study Based on Numerical Analysis - ,", Nucl. Instrum. Meth. in Phys. Res. **A 589**, pp 445-454 (2008).
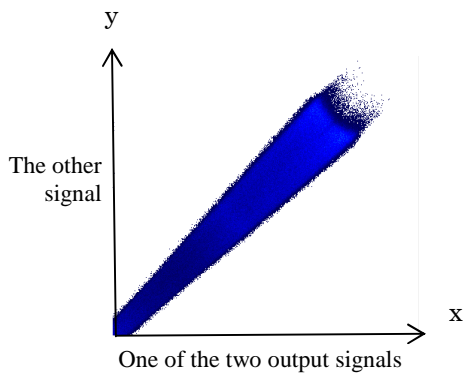

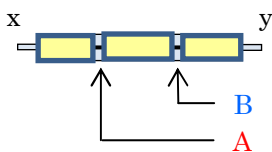Fig. 2. Measured two-dimensional spectrum.

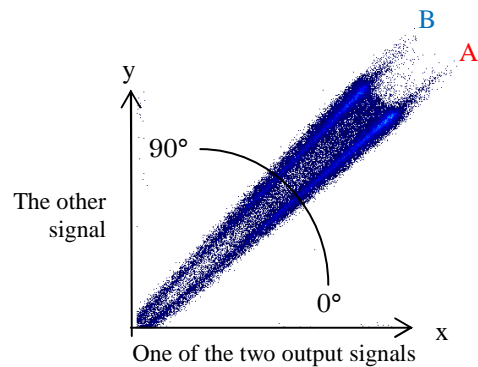Fig. 3. Schematic view of the detector set-up.

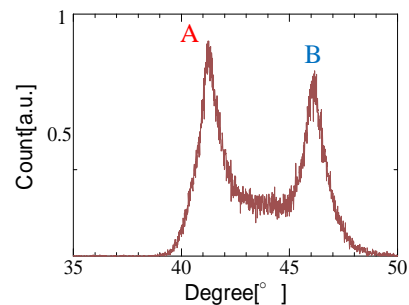Fig. 4. Measured two-dimensional spectrum with the detector set-up in Fig. 3.

Fig. 5. Obtained detection position information from the result in Fig. 4.

A new neutron time-of-flight detector to measure the MeV neutron spectrum at the National Ignition Facility

R. Hatarik[1], J. A. Caggiano[1], V. Glebov[2], J. McNaney[1], C. Stoeckl[2], and D. H. G. Schneider[1]

[1] Lawrence Livermore National Laboratory, 7000 East Avenue, Livermore, CA 94550, USA, +1-925-422-5611, hatarik1@llnl.gov
[2] Laboratory for Laser Energetics, University of Rochester, 250 East River Road, Rochester, NY 14623, USA

Abstract: *A new time-of-flight detector has been developed to measure the neutron spectrum at the National Ignition Facility. This detector allows for a more accurate measurement of the down scattered neutrons as well as the determination of the TT neutron spectrum. First measurements with this detector are being presented.*

1. Introduction

The National Ignition Facility (NIF) uses 192 lasers to deliver up to 1.8MJ of light to a target with the goal to ignite the fuel of a DT capsule. To achieve this, several conditions have to be met which can be observed with target diagnostics. An important target diagnostic is the neutron time-of-flight (nToF), which is used to determine neutron yield, ion temperature and the areal density of the fuel. An accurate measurement of the neutron spectrum following a NIF shot also serves as basis for many basic science studies, including neutron capture measurements relevant to astrophysics or understanding of the break up of the t+t compound system.

With the flight path for NIF nToF diagnostic having a length of ~20 m, primary 14 MeV neutrons and down scattered 12 MeV neutrons get separated by only 30 ns. Therefore a detector with a fast time response is needed in order to separate those.

A new scintillation detector has been designed to improve neutron spectroscopy from 1 MeV to 12 MeV following a NIF shot. This detector uses a new organic crystal, which was found to have an extremely high suppression of delayed light [1], improving the measurement of the ratio of neutrons down scattered into the 10 to 12 MeV region relative to the number of unscattered 14 MeV neutrons. In addition, the detector allows for the simultaneous use of up to four photo multiplier tubes (PMTs) to determine the neutron spectrum from 1 to 5 MeV with higher accuracy.

2. New detector design considerations

The 20 m nToF systems have three primary objectives: measurement of neutron yield, ion temperature and the down scattered ratio of neutrons (DSR). The ion temperature measurement accuracy depends mainly on the intrinsic width of the signal, whereas the DSR signal needs low background in the 10 to 12 MeV region. The DSR measurement accuracy suffers from a significant detector background from the primary peak due to scintillation light decay, response from the rather long cables currently in use and local neutron scattering. The design of the new nToF detector mitigates this background and improves the dynamic range over the old nToF detectors, by using the following improvements: A bibenzyl crystal [2] is being used as scintillator, which has highly-suppressed delayed light [1], while having a higher sensitivity than previously used xylene detectors [3]; reduction in mass of material surrounding the scintillator, which reduces background due to neutron scattering events; an increase in the dynamic range of the detector by using four gated PMTs, which look at the scintillator simultaneously; reduction of scintillator thickness which, with a comparable prompt scintillation light decay leads to higher accuracy in the ion temperature measurement.

To achieve the reduction in mass around the scintillator the rather massive PMTs had to be moved away from the scintillator and placed at backward angles. To maintain light collection, tubes of aluminized mylar foil were used as light guides. Fig. 1 shows the finished detector.

Fig.1. Picture of the new nToF detector installed at NIF.

3. First data from new detectors

The newly designed and constructed detector was tested at OMEGA before its installation at NIF [4]. A total of three of these detectors have been constructed so far. Two of them have been installed as permanent diagnostics at NIF. The third was used for astrophysics measurements on OMEGA and is planned to be used as an upgrade to another NIF nToF detector.

Due to their isotropic nature and their low areal density, exploding pusher shots are being used to calibrate the nToF detector relative to neutron activation diagnostics. By using DD and DT exploding pushers the detector sensitivity can be calibrated for 2.45 MeV and 14.03 MeV neutrons. Fig. 2 shows the spectrum of the detector for a DT exploding pusher on NIF.
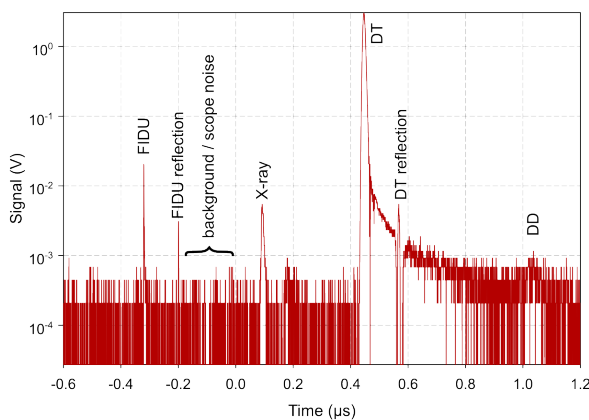
Fig. 2. Time-of-flight spectrum of the new nToF detector from an exploding pusher shot. Several features of the spectrum are visible: Fiducial signals for timing the X-rays from the shot as well as the DT neutron signal with a cable reflection.

4. Data from pure tritium filled capsules

Due to the big difference in the reaction cross section even a small deuterium contamination in a tritium fill will lead to the DT neutrons being the dominant part of the spectrum. To obtain a good measurement of the TT neutron spectrum a fast detector response will significantly reduce the background from the always present DT signal. Fig. 3 shows the neutron spectrum for a NIF TT shot recorded with the new detector. Clearly visible is the peak from the t+t → ^{5}He + n reaction. In addition the new detector was used on two shot days at OMEGA in November 2012. The analysis of this data is currently in progress.

5. Conclusions

A new nToF detector with a bibenzyl crystal as a scintillator was designed and manufactured for the NIF.

First data taken with this detector shows that it has a fast response time and lowers the background from the primary DT signal in the down scattered region significantly. It can measure ion temperature and neutron yield on DD shots at NIF with yields as low as 10^{10} neutrons. TT neutron spectra have been recorded from shots at NIF and OMEGA; the analysis of this data is currently work in progress.
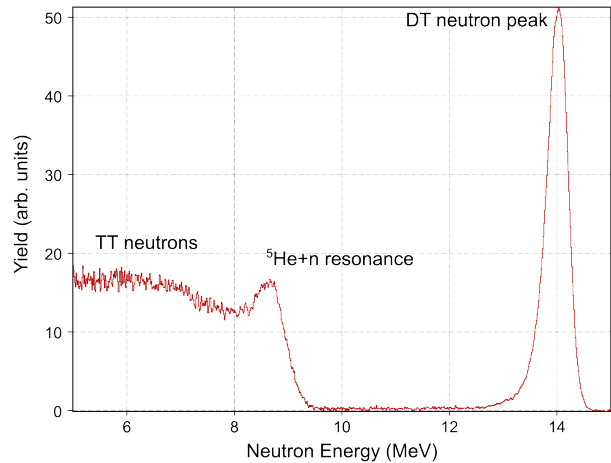

Fig. 3. TT neutron spectrum obtained from new nToF detector.

References

[1] R. Hatarik, L.A. Bernstein, M.L. Carman, D.H.G. Schneider, N.P. Zaitseva, and M. Wiedeking, Rev. Sci. Instrum. **83** 10D911 (2012).

[2] N. Zaitseva, A. Glenn, L. Carman, R. Hatarik, S. Hamel, M. Faust, B. Schabes, N. Cherepy, and S. Payne, IEEE Trans. Nucl. Sci. 58, 3411 (2011).

[3] V. Glebov, T. C. Sangster, C. Stoeckl, J. P. Knauer, W. Theobald, K. L. Marshall, M. J. Shoup III, T. Buczek, M. Cruz, T. Duffy, M. Romanofsky, M. Fox, A. Pruyne, M. J. Moran, R. A. Lerche, J. McNaney, J. D. Kilkenny, M. J. Eckart, D. Schneider, D. Munro, W. Stoeffl, R. Zacharias, J. J. Haslam, T. Clancy, M. Yeoman, D. Warwas, C. J. Horsfield, J.-L. Bourgade, O. Landoas, L. Disdier, G. A. Chandler, and R. J. Leeper. Rev. Sci. Instrum. **81** 10D325 (2010).

[4] V. Glebov, C. Forrest, J. P. Knauer, A. Pruyne, M. Romanofsky, T. C. Sangster, M. J. Shoup III, C. Stoeckl, J. A. Caggiano, M. L. Carman, T. J. Clancy, R. Hatarik, J. McNaney, and N. P. Zaitseva. Rev. Sci. Instrum. **83** 10D309 (2012).

High-performance neutron imaging with microns scale resolution using LiF crystal detector

A. Faenov[1,2], M. Matsubayashi[3], T. Pikuz [1,2], Y. Fukuda[1], M. Kando[1], R. Yasuda[3], H. Iikura[3], T. Nojima[3], T. Sakai[3], M. Shiozawa[4], Y. Kato[5]

[1] Quantum Beam Science Directorate, Japan Atomic Energy Agency, Kyoto 619-0215, Japan
Phone +81-774-71-3354, e-mail: anatolyf@hotmail.com
[2] High Temperatures, Russian Academy of Sciences, Izhorskaja Street 13/19, Moscow, Russia
[3] Quantum Beam Science Directorate, Japan Atomic Energy Agency, Tokai, Ibaraki 319-1195, Japan
[4] Nippon SOKEN, Inc., Iwaya 14, Shimohasumi, Nishio, Aichi 445-0012, Japan
[5] The Graduate School for the Creation of New Photonics Industries, Hamamatsu, Shizuoka 431-1202, Japan

Abstract: *We present the overview of main findings, which clearly demonstrated that the LiF crystal performs efficiently as imaging detector based on optically stimulated luminescence of color centers, generated by neutrons irradiation. It was shown that the obtained neutron images are almost free from granular noises, have spatial resolution of ~5 μm, practically linear response with the dynamic range of at least 10^3 and two holes with less than 2% transmittance differences could be distinguished. We propose to use such detector in areas, where a high spatial resolution with a high image gradation resolution is needed.*

1. Introduction

Typically neutron radiography with high spatial resolution tries to solve two types of tasks: i) to perform self imaging of different large size (Fig.1a) or tiny (Fig.1b) neutron sources and ii) to do imaging of internal structure of matter by neutron absorption (Fig.1c)
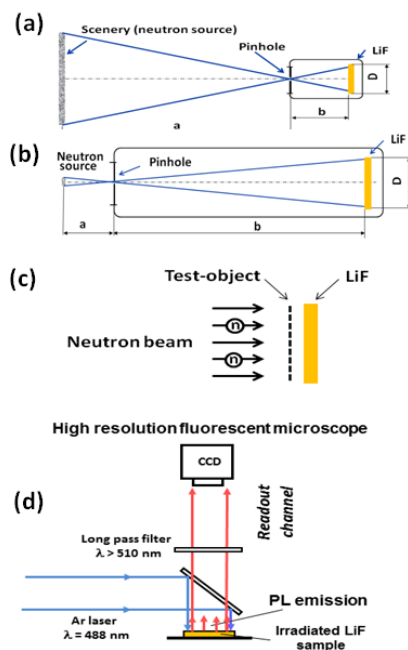

Fig.1 Schematic layouts for neutron radiography by LiF detector. It consists of two stages: neutron irradiation of LiF crystal detector (image recording a,b,c) and image readout (d) Self radiography of large size (a) and tiny (b) neutron sources using pin-hole imaging approach and high-resolution LiF crystal detectors. Neutron radiography of internal structure of objects (c).

For all such different scientific and industrial applications development of neutron detectors with spatial resolution improved up to 1-10 μm and with a high (some %) sensitivity to variation in material thickness and structure are strongly required. Unfortunately the best nowadays neutron detectors allowed to reach spatial resolution around 15-20 μm [1-2]. At the same time it is well-known that point defects or, as they are also called color centers (CCs), are produced sufficiently easily under interaction of particles or photons with LiF crystal. Such CCs could be hosted in LiF at room temperature for a very long time and then under excitation by UV radiation the CCs would emit photoluminescence (PL) in the visible spectral range and allowed to reach submicron spatial resolution. In such case, recently in [3-6] we proposed to use LiF crystals as a high performance neutron imaging detectors. In this presentation we will give an overview of our main results performed for characterization of such detectors and using them for high spatial resolution thermal neutron radiography.

2. Experimental set up and obtained results

The thermal neutron radiography facility (TNRF-2) at the research reactor JRR- 3M (20 MW thermal output) at JAEA has been used for micron scale neutron imaging in our experiments. The beam line for TNRF-2 provides [3] thermal neutrons (peak energy of approximately 30 meV) with the flux of 1.0×10^8 n/cm^2 s and the L/D ratio varied from 100 up to 460, where L is the distance from the reactor to the sample and D the aperture size at the reactor. In the TNRF- 2 station, dose rate of the gamma-rays has been measured to be 2.16 Sv/h. Image recording and acquisition set up for the neutron imaging experiments using LiF crystals is shown in Fig. 1(c,d). The objects were placed in close contact with a LiF single crystal of 20 mm diameter and 3 mm thickness. The procedures of neutron irradiation of different samples and readout process were described in details in [3-6]. In Fig. 2,3 the neutron images of the edge of 100 μm thick Cd plate and the Gd line pair indicator are presented.

Obtained results obviously show that spatial resolution ~ 5 μm was demonstrated.
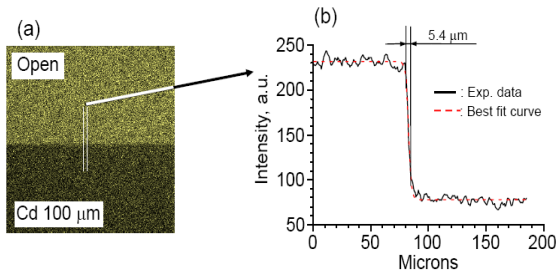

Fig. 2 (a) Neutron image of a 100 μm -thick Cd plate taken with 10 s exposure. (b) Trace of the neutron image across the edge, which is compared with a calculation at a spatial resolution of 5.4 μm.
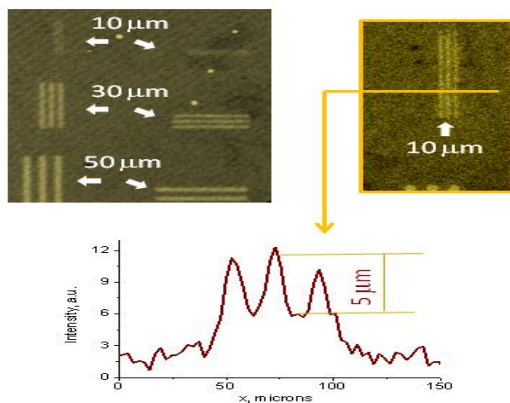

Fig. 3 Line-pair images obtained using the LiF single crystal detector and line profiles of the pairs with widths of 10 μm [5]

High sensitivity of LiF detector allowed clearly recorded (Fig.4) even the thinnest Au wire of 42 μm diameter with the signal-to-noise ratio ~ 50. It is necessary to stress that for such wire neutron attenuation is of only ~ 2.35%.
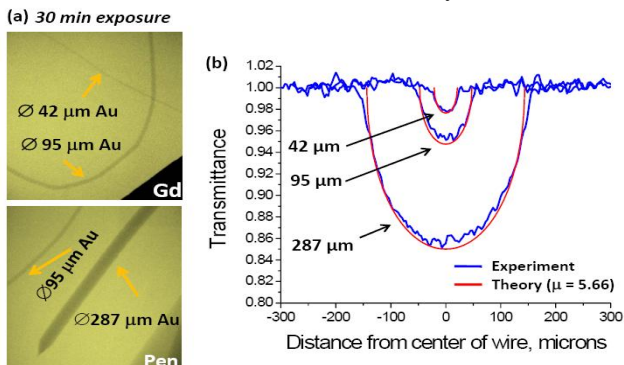
Fig 4. a) Neutron images of the Au wires of 42, 95 and 287 μm diameters recorded with the exposure time 30 min.(b) Comparison of the traces of experimental intensity transmittance of neutrons through the Au wires (solid curves) and their comparison with the theoretical transmittance (dashed curves).

Additional proving of high spatial resolution, high sensitivity and high contrast of neutron radiography by LiF crystal detectors is clearly seen from Fig. 5. Obtained image obviously shows that changes of thickness of hammered Gd plate from approximately 0 μm up to ~ 25 μm could be measured with accuracy

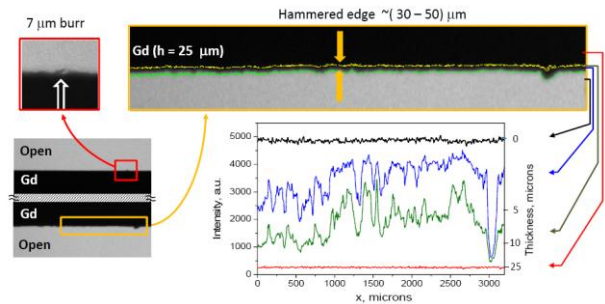Fig. 5 Neutron radiography of a 25-μm thick Gd plate. Defect with the size of ~ 7 μm and the microns scale changes of thickness of hammered Gd plate edge (due to the cutting Gd plate by the scissors) are clearly seen in the magnified images of different parts of sample
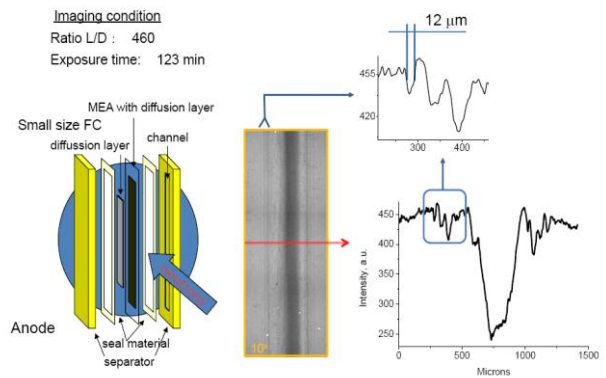

Fig. 6 A schematic drawing of a small type fuel cell and neutron image of it. Tiny details of fuel cell structure and its unhomegentiy along and perpendicular to the anode-cathode directions is clearly resolved

of some microns. Additionally tiny defects on the surface and edge of foil could be clearly distinguished with some microns resolution.

Very important neutron radiography application is high-performance imaging of fuel cells. In Fig.6 the image demonstrated tiny details of cell structure with spatial resolution better than 12 μm along full field of view ~ 1.5 x 4.5 mm^2 is presented.

Our results show that LiF crystal detectors have excellent characteristics and big advantages compared with traditionally used neutron detectors in areas, where a micron scale spatial resolution is needed and we hope will be used not only for neutron imaging by low energy neutrons, but also for diagnostics of different plasma sources.

References

 [1]E.H. Lehmann, P.Boillat, G.Scherrer, G.Frei," NIMA **605,** 123–126 (2009)

[2] T. Caillaud, O. Landoas, M. Briat et al., Rev. Sci. Instrum. **83**, 033502 (2012)

[3] M. Matsubayashi, A. Faenov, T. Pikuz et al., NIMA **622,** 637–641 (2010)

[4] M. Matsubayashi, A. Faenov, T. Pikuz et al., NIMA **651**, 90-94 (2011)

[5] R. Yasuda, M. Matsubayashi, T. Sakai et al., Physics Procedia, (2013) submitted

[6] A. Faenov, M. Matsubayashi, T.Pikuz et al., Physica status solidi C Phys. Status Solidi C **9**, 2231-2234 (2012)

Nuclear Emulsion Technique for Fast Neutron Measurement using Automatic Track Analysis System

Hideki TOMITA[1] Haruna MINATO[1] Yosuke SAKAI[1] Kunihiro MORISHIMA[2] Kohei ISHIHARA[1]
Mitsutaka ISOBE[3] Jun KAWARABAYASHI[1] Tatsuhiro Naka[2] Takashi Asada[2]
Toshiyuki Nakano[2] Mitsuhiro Nakamura[2] Tetsuo IGUCHI[1] Kunihiro OGAWA[3] Kentaro OCHIAI[4]

[1] Graduate School of Engineering, Nagoya University, Furo-cho, Chikusa-ku, Nagoya, 464-8603, Japan
sakai.yosuke@f.mbox.nagoya-u.ac.jp
[2] Graduate School of Science, Nagoya University, Furo-cho, Chikusa-ku, Nagoya, 564-8603, Japan
[3] National Institute for Fusion Science, 322-6 Oroshi-cho, Toki 509-5292, Japan
[4] Fusion Research and Development Directorate, Japan Atomic Energy Agency, Tokai, Naka, Ibaraki 319-1195, Japan

Abstract: *We investigated basic performance of state-of-the-art nuclear emulsion technique using automatic track analysis system for shot-integrated fast neutron measurement. Energy resolution was estimated to be about 20% FWHM at 2.5 MeV by calculated spectrum with a pinhole collimator. 14 MeV neutron pinhole imaging was demonstrated using accelerator based neutron source.*

1. Introduction

Fast neutrons with energies up to several MeV are produced by neutron source such as laser-driven fusion device and accelerator based neutron source. Recoiled proton caused by elastic scattering of incident neutron with hydrogen atom in a detector is used to detect fast neutron. Nuclear emulsion consists of hydrogen-containing emulsion layer put on a base plate is a solid state nuclear track detector. Since recoiled proton track recorded in the emulsion with high position and angular resolution, it is suitable for fast neutron imaging and energy measurement. Here, high-speed and automatic scanning system to accumulate recoiled proton tracks recorded in the emulsion is crucial for applications of the nuclear emulsion. We have developed nuclear emulsion technique for fast neutron measurement using automatic track analysis system [1-5]. In this paper, we calculated a response of the nuclear emulsion to fast neutron based on Monte-Carlo simulation and demonstrated fast neutron imaging using accelerated DT neutron source.

2. Principle of fast neutron imaging and energy measurement

Figure 1 shows the conceptual drawing of fast neutron imaging and energy measurement using a nuclear emulsion detector and a pinhole collimator. The detailed principle was described in our previous paper [1, 4] and is described only briefly here. Fast neutron incident into a emulsion layer passing though a pinhole makes a track of recoiled proton via elastic scattering. Neutron energy E_n is derived from scattering angle θ of recoiled proton and recoiled proton energy E_{rp} as follows:

$$E_n = E_{rp}/\cos^2\theta. \tag{1}$$

Incident direction of neutron is determined as a line extending from a starting point of the track to the pinhole, therefore the scattering angle θ would be derived from a angle between the track and the incident direction. Since the track length depends on the recoiled proton energy, the incident neutron energy can be estimated from the Eq. (1). In addition, neutron emission profile from the neutron source is reconstructed based on pinhole imaging.
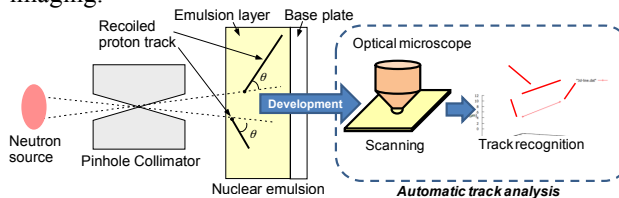

Figure 1 Conceptual drawing of fast neutron measurement using a nuclear emulsion detector and a pinhole collimator.

3. Basic performance for fast neutron measurement

We considered an expected performance of energy measurement for 2.5 MeV neutron based on Monte-Carlo simulation of neutron transportation by Particle and Heavy Ion Transport code System: PHITS. Recoiled proton tracks were calculated by events of elastic scattering of neutron reached to the emulsion layer through the collimator. Figure 2 shows an estimated neutron spectrum derived from calculated recoiled proton tracks and Eq. (1) with a pinhole collimator made of tungsten alloy (50 mm×50 mm×100 mmt with 10° tapered-angle pinhole). Neutron energy was also estimated for each track calculated with the collimator of which the pinholes were filled by the two circular-cone shaped pieces, or a tungsten alloy block. Peak at 2.5 MeV in the spectrum was clearly obtained with the pinhole collimator. Energy resolution was estimated to be about 20% FWHM at 2.5 MeV neutron.
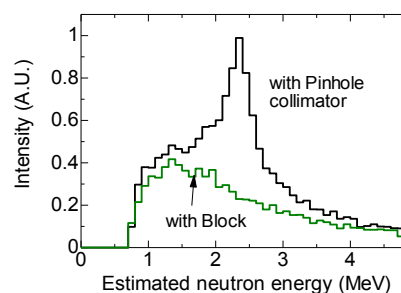

Fig. 2 Estimated neutron spectra with the pinhole collimator and the tungsten alloy block.
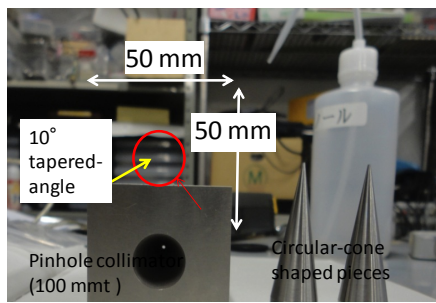
Fig. 3 Photograph of the pinhole collimator and the two circular-cone shaped pieces.

We demonstrated 14 MeV neutron pinhole imaging using accelerator based DT neutron pencil beam at Fusion Neutronics Source (FNS), Japan Atomic Energy Agency. The pinhole collimator set up at 11.9 m far from a exit hole of 14 MeV pencil neutron beam at FNS. Figure 3 shows the photograph of the pinhole collimator. We also used two circular-cone shaped pieces made of tungsten alloy to fill the pinholes (see Fig. 3). We used nuclear emulsion "OPERA film"[6]. After development of nuclear emulsion irradiated by neutron, each starting point of the recoiled proton track was analyzed by the latest automated scanning system called "S-UTS" [7,8]. Figure 4(a) shows profile of recoiled proton tracks on the emulsion obtained with the pinhole collimator. Line profile of recoiled proton tracks is shown in Fig. 4(b). By comparison of profiles of recoiled proton tracks on the emulsion between with the pinhole collimator and the tungsten alloy block, it is found that background counts in the fast neutron pinhole image are caused by transmitted neutrons through the collimator. Net neutron profile can be obtained by difference in counts between those two images.
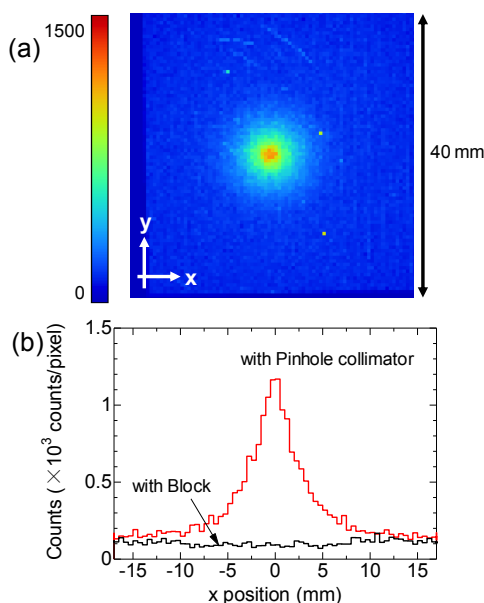

Figure 4 (a) Profile of recoiled proton tracks on the emulsion obtained with the pinhole collimator and (b) line profile of recoiled proton tracks.

4. Conclusions

We investigated basic performance of nuclear emulsion technique using an automatic track analysis system for fast neutron measurement. Energy resolution was estimated to be about 20% FWHM at 2.5 MeV neutron using a combination of a pinhole collimator and a nuclear emulsion detector by Monte-Carlo simulation. In addition, 14 MeV neutron pinhole imaging was demonstrated experimentally using the latest automated scanning system "S-UTS". Recently, we also developed a novel nuclear emulsion including AgBr nano-grains to suppress sensitivity for gamma-ray [9-11]. It enables to measure fast neutron in the presence of high-intensity background gamma-rays. Therefore, state-of-the-art nuclear emulsion technique using automatic track analysis system would be promising for the shot-integrated fast neutron measurement in various fields such as high-resolution fast neutron radiography and laser-based inertial confinement fusion experiment.

References
[1] Y. Nomura *et al*., "Design Consideration on Compact Neutron Pinhole Camera with Nuclear Emulsion for Energetic-ion Profile Diagnostics", Plasma Fusion Res. **6**, 2402148, (2011).
[2] K. Morishima, "Measurement of high energy neutron with nuclear emulsion", Ionizing Radiation, **37**, 173-178 (2011).
[3] M. Isobe *et al*., "Application of Nuclear Emulsion to Neutron Emission Profile Diagnostics in National Spherical Torus Experiment ", submitted in proceedings of ITC22.
[4] H. Minato *et al*., "Development of Fusion Neutron Pinhole Imaging using Nuclear Emulsions for Energetic Ion Diagnostics", submitted in proceedings of ITC22.
[5] K. Morishima *et al*., "Development of 14MeV neutron measurement with nuclear emulsion for D-T burning plasma diagnostics", submitted in proceedings of ITC22.
[6] T. Nakamura *et al*., "The OPERA film: New nuclear emulsion for large-scale, high-precision experiments", Nucl. Instrum. Meth. A, **556**, 80-86, (2006).
[7] K. Morishima and T. Nakano, "Development of a new automatic nuclear emulsion scanning system, S-UTS, with continuous 3D tomographic image read-out", J. Instrumentation, **5**, P04011, (2010).
[8] K. Morishima *et al*., "Development of an automated nuclear emulsion analyzing system", Radiation Measurements, (*accepted*).
[9] J. Kawarabayashi *et al*., "Development of Neutron Measurement in Intense Gamma Field Using New Type of Nuclear Emulsion", Journal of ASTM International, **9**, JAI104007, (2012).
[10] K. Ishihara *et al*.,"Selective Fast Neutron Detection under Intense Gamma-ray Fields with Novel Nuclear Emulsion Technique", Radiation Measurements, (*accepted*).
[11] K. Ishihara *et al*., "Investigation of development condition with NGITA emulsion for neutron measurement under high gamma-ray background", Progress in Nuclear Science and Technology, (*submitted*).

Efficient and stable neutron generation by Coulomb explosion of solid nanoparticles using DPSSL-pumped high-repetition-rate 20-TW laser

Nakahiro SATOH, Takeshi WATARI, Koji MATSUKADO, Takashi SEKINE, Yasuki TAKEUCHI, Yuma HATANO, Ryo YOSHIMURA, Katsunobu NISHIHARA, Masaru TAKAGI, and Toshiyuki KAWASHIMA
Hamamatsu Photonics, K. K. 1820, Kerematsuchou, Nishi-ku, Hamamatsu City, Sizuoka Pref., 431-1202 Japan Phone: +81-53-487-5100 Fax: +81-53-487-3132, Email: naka@crl.hpk.co.jp (Nakahiro SATOH)

Abstract: Efficient and stable neutron generation was obtained by irradiating an intense femtosecond laser pulse of $\sim 4 \times 10^{18}$ W/cm^2 to relatively large deutrated-polystylene nanoparticles of ~250 nm in diameter. A yield of $\sim 10^5$ neutrons per shot was stably observed during continuous 100 shots.

1. Introduction

Recent developments of high-intensity laser enable us to evolve a new type neutron source. A number of experiments [1-5] demonstrated the possibility of laser-driven fusion using pure D_2 or CD_4 clusters. In these works, multi-keV deuterium ions were generated by Coulomb explosion of a few nanometres clusters. Since the cross-section of deuterium-deuterium (DD) reaction reaches its maximum at 1750 keV with center-of-mass system, much higher ion energy is required for efficient neutron generation.

Features of the Coulomb explosion are that ion energy distribution function is proportional to the square root of its energy and the maximum energy is proportional to its radius [6]. Larger particles result in higher ion energy, although an intense laser irradiation is required for expelling electrons from the larger particles. We fabricated the solid density deuterated-polystyrene (CD) nanoparicles of 250 nm in diameter to obtain high ion energy of ~1 MeV. Stable neutron generation was demonstrated by irradiating 20-TW diode-pumped-solid-state-laser (DPSSL) to these solid nanoparticles.

2. Experimental setup

2.1 Laser system

In our laboratory, we have developed a DPSSL-pumped high-repetition-rate 20-TW laser (MATSU-1) which consists of a Ti:sapphire chirped pulse amplification system and a pump laser KURE-1, a laser-diode-pumped Nd:glass laser system [7]. MATSU-1 generated 1.2 J ($\lambda = 800$ nm) with a pulse width 60 fs at 10 Hz. DPSSL is extremely stable at a longer life compared with conventional flash-lamp-pumped laser. In the focus spot of the MATSU-1 laser, 40 percent of the energy was focused into 8 μm diameter spot. Considering the laser transmission efficiency, the laser intensity on the target was $\sim 4 \times 10^{18}$ W/cm^2. The repetition rate was 0.1-1 Hz due to the limitation of data acquisition.

2.2 Target and injection system

We developed CD nanoparticles used as a target instead of gas clusters [8]. Figure 1(a) shows the SEM image of the nanoparticles which average size was 250 nm. The average size can be controlled with high precision

between 150-700 nm. We, therefore, expect to give a certain amount of selectivity to the ion energy obtained by Coulomb explosion of these nanoparticles. Figure 1(b) shows the schematic view of the nanoparticle injection system. MATSU-1 enters from the direction perpendicular to the paper. Injection timing and number density of the nanoparticles were measured by the Mie scattering light intensity using He-Ne laser probe. The nanoparticles are injected to the MATSU-1 focus point at the center of interaction chamber. In this experiment, typical number density of injected nanoparticles was $\sim 10^9$ cm^{-3}.
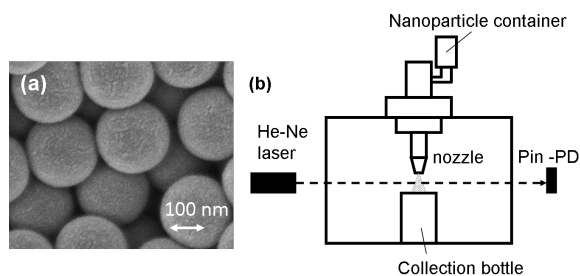

Figure 1. (a) SEM image of CD nanoparticles which average size was 250 nm. (b) Schematic view of the nanoparticle injection system.

2.3 Measurement equipments

We have developed a Multichannel Time-of-flight system with Kinetic energy Analyzing Device (MT-KAD) to observe the ions of multispecies generated from relativistic laser plasma [9]. In this experiment, we used MT-KAD system to observe the ions generated from Coulomb explosion of CD nanoparticles. This system is composed of a ten-channel scintillation detector array and a permanent magnet that generates a magnetic field of ~0.09 T. The magnetic field and time-of-flight (TOF) information enables us to distinguish protons, deuterons, and stripped carbons. The layout of our detectors is shown in Fig. 2. The MT-KAD system constructed in the detector chamber and observed ions accelerated forward. Neutron detector, consisting of a plastic scintillator (BC420, 180 mm diameter, 100 mm long) coupled to a photomultiplier tube (H2431-50,

Hamamatsu Photonics K.K.) was located outside the interaction chamber at distance of 140 cm from the laser focus point.
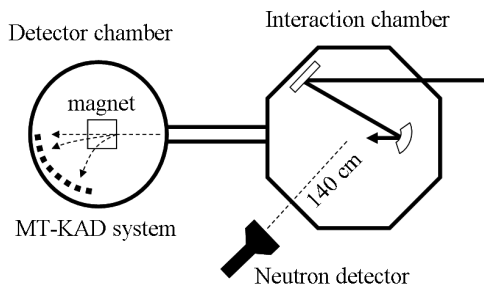

Figure 2. The layout of the detectors

3. Experimental results

At first, we measured the deuterium ions generated by Coulomb explosion. Figure 3 shows the typical ion TOF signal of a single shot with CD nanoparticles. These signals were obtained by three of ten-channel detectors in detector chamber. Generation of high energy deuterium ions with energy up to 700 keV by Coulomb explosion of the nanoparticle was demonstrated. It should be mentioned there were no strong signals for CH nanoparticles, instead.
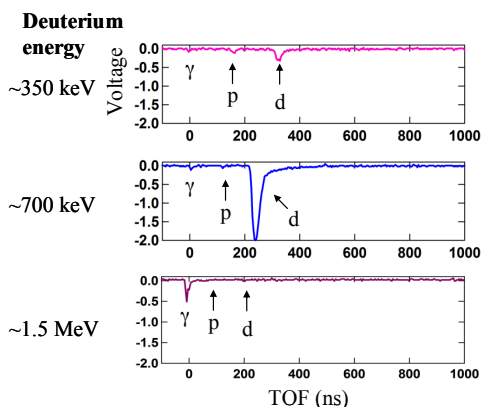
Figure 3. Single shot ion TOF signal from TOF system in the detector chamber

In the neutron generation experiment, we used a cylindrical CD plane, called "neutron booster", in the interaction chamber. It was arranged around a nanoparticle injection nozzle to enhance the fusion reactions (See Fig.4(a)). High energy deuterium ions generated by Coulomb explosion might hit the plane and increase DD fusion reactions.

A typical signal of a neutron detector in the neutron generation experiment is shown in Fig.4(b). The signals due to the γ-ray and neutron bursts are easily resolvable. The relative delay with > 60 ns corresponds to the sum of the traveling time of 700-keV deuterium inside the booster and the TOF of 2.45-MeV neutron to the detector. Assuming the neutron isotropic emission, the

neutron yield was $\sim 10^5$ per shot. Such an efficient neutron generation was stably observed during continuous 100 shots (See Fig. 4(c)).
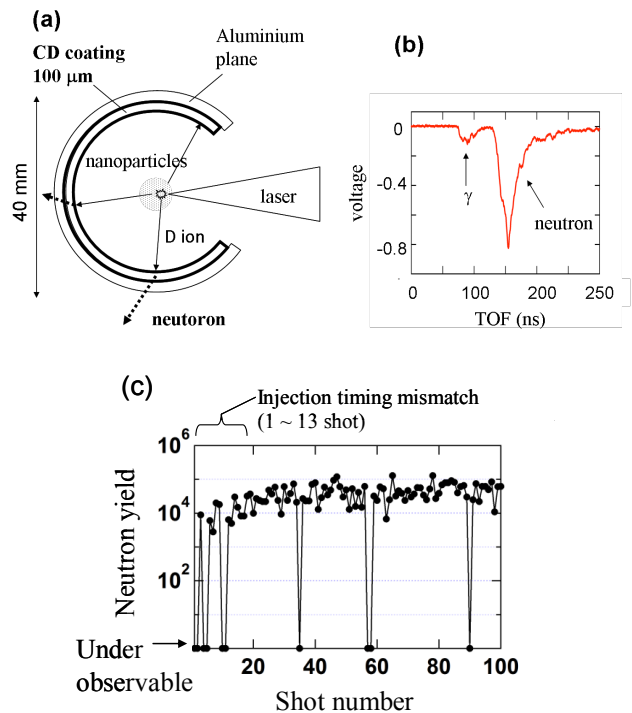

Figure 4. (a) Schematic view of the "neutron booster". (b) Single shot neutron TOF signal. (c) The history of neutron generation during continuous 100 shots.

4. Conclusions

Neutron generation experiment with 20-TW LD-pumped laser and CD nanoparticle was demonstrated. Energetic deuterium ions with energy up to 700 keV were observed. A yield of $\sim 10^5$ neutrons per shot was stably observed during 100 shots of 0.1-1 Hz continuous operation. This indicates that it may be possible to further enhance the neutron generation with an increase in laser energy.

This demonstration will be expected to bring the progress of novel neutron source, which is characterized by a pulsed emission and point source, for many applications.

References

[1] T. Ditmire et al., Nature **398**, 489 (1999)
[2] T. Ditmire et al., Phys. Plasmas **7**, 1993 (2000)
[3] K. W. Madison et al., J. Opt. Soc. Am. B **20**, 113 (2003)
[4] K. W. Madison et al., Phys. Rev. A **70**, 053201 (2004)
[5] R. Hartke et al., Nucl. Instrum. Methods Phys. Res. A **540**, 464 (2005)
[6] K. Nishihara et al., Nucl. Instrum. Methods Phys. Res. A **464**, 98 (2001)
[7] R. Yasuhara et al., Opt. Lett. **33**, 1711 (2008)
[8] A. Tsukigase, H. Nakamura, Kobunshi Ronbunshu, **63**, 266 (2006)
[9] K. Matsukado et al., Rev. Sci. Instrum. **81**, 023304 (2010)

High Yield Neutron Production via Laser Accelerated Deuteron Ion Beam

F.Aymond[1], D. Kelley[1], J.T. Morrison[1], M. Storm[1], M. McMahon[1], K.U. Akli[1],, E. Chowdhury[1],
R.L. Daskalova[1], D. Schumacher[1],R. R. Freeman[1]
[1] The Ohio State University – SCARLET Laser Facility, 191 W Woodruff Ave Columbus OH 43202
Ph: 214-729-6707 Fax:614-292-7557 aymond.1@osu.edu

Abstract: *Using a pitcher-catcher target design combined with a novel strategy of deuterated target design which has demonstrated sharp increase in deuteron production while suppressing proton generation, we are able to take advantage of higher ion capture cross sections in Lithium and expect neutrons yields of up to 10^{12} neutrons/second.*

1. Introduction

Neutron generation has a variety of applications, including national security, and laser neutron generation offers many advantages to conventional neutron generation methods. We present a method using laser acceleration that will allow for ultra-high quasi-beam like neutron production. We expect to generate neutron yields in excess of 10^{11} neutrons/shot using the 1J, 30 fs SCARLET laser system at The Ohio State University. With only moderate advances in laser technology we expect yields of up to 10^{12} neutrons/second will be available from relatively inexpensive (~$10M USD) laser systems, which will allow for a new generation in portable neutron detection applications.

2. Ion beam generation

2.1 Pitcher-Target Approach to Neutron Production

Intense short laser pulses, when incident on a target deposit a large fraction of laser energy into hot electrons and cause rapid and complete target ionization. Approximately ~.1% of the electrons escape the target's back surface creating a large positive potential with typical field strengths on the order of MV/ μm. This field rapidly accelerates the back surface ions in a process known as Target Normal Sheath Acceleration (TNSA). [1] As shown in figure 1, it is possible to put a secondary ('catcher') target with high ion capture cross section, e.g. lithium, behind the primary TNSA ('pitcher') target which result in neutron generation.
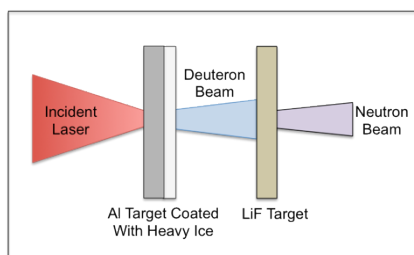

Fig. 1. Pitcher-Catcher Target geometry.

2.2 Advantages of the d-Li reaction

TNSA preferentially accelerates ions with the highest charge to mass ratio. This results in acceleration of protons from the hydrocarbon and water contaminant layer present on the back of all targets. However the d+^{7}Li$\rightarrow$ n+^{8}Be reaction has a much higher ion cross section then the similar p-Li reaction, as shown in figure 2. This broad capture spectrum is key in creating a high yield neutron source. Additionally, the d-Li reaction has a high Q value (15 MeV) thus even low to moderate energy deuterons are capable of producing high-energy neutrons. Deuterons also have a further advantage over protons in they can further produce neutrons through proton stripping of the deuteron ion. Since the deuteron ion is weakly bound (E_b~2.8 MeV) the proton can be removed from a collision with a background nucleus and the freed neutron will have continue with roughly half the energy of the deuteron.
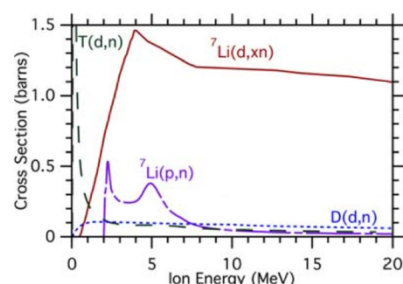

Fig. 2. Various nuclear capture cross sections in lithium. Figure adapted from Higginson *et al* [2]

2.3 Deuteron production

Simply using a deuterated catcher target is not a viable method of deuteron production as a hydrocarbon contaminant layer will remain and the protons from this layer will dominate the ion acceleration process. By spraying heavy water into the target chamber we were able to evenly deposit a layer of heavy ice onto the rear surface of the target. Using this technique we have successfully shown suppression of proton acceleration (figure 3a) and enhancement deuteron acceleration (figure 3b) when compared to targets with a layer of deuterated plastic on the back surface. Using this technique we were able to successfully accelerate an ion beam with a deuteron peak three orders of magnitude greater then the proton peak. The deuterium ions in this work originated from a layer of heavy ice that was deposited on to the rear surface of a 500nm thick membrane of Si_3N_4 and Al from the .5 J GHOST laser at The University of Texas. The maximum recorded
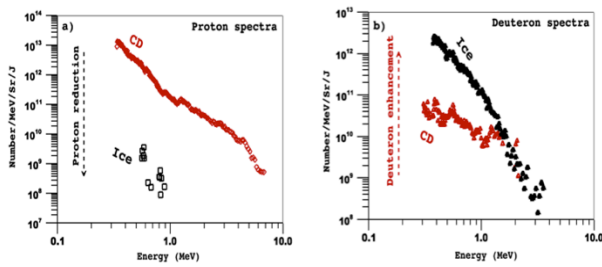
Fig. 3. Confirmation of (a) proton suppression and (b) deuteron enhancement in targets coated with heavy ice as opposed to a simple CD back layer.

deuterium ion energy was 3.5 MeV, with a yield of 1.2×10^{12} sr^{-1}.

Using ponderomotive scaling for fast electrons excited by a 10^{20} W/cm^2 laser pulse and assuming a Maxwellian distribution for both electron and proton energy distributions we expect our ion to have a slope temperature of 4 MeV, which well matches our experimental data. We are currently investigating this process using the PIC code LSP[3] via injection of electrons into a full scale target based on a model of the laser plasma interaction[4] and via full, self-consistent treatment of the laser interaction. Collisions, radiation loss, and photoionization are treated. An equation-of-state is included.

3. Neutron yield calculation

We are able to calculate the total expected neutron yield using a continuously slowing deuteron approximation in which as deuterons propagate through our catcher target they move to progressively lower energy bins. Given an initial deuteron energy the neutron production calculated from the ^{7}Li(d,n) → ^{8}Be at each energy stage where the stopping power for each energy bin is obtained from software package SRIM. As shown in figure 4, we find a peak in neutron production corresponding to a yield of 2.6×10^{-2} neutrons/deuteron corresponding deuteron energy of 20 MeV. The neutron yield remains greater then 1.5×10^{-2} neutrons/deuteron up to deuteron energies of 70 MeV. In order to figure the total neutron yield per shot we assume 12% laser to ion efficiency conversion as measured by Snavely et al [5], which gives neutron yield into the full 4π spatial directions of 1.5×10^{11} neutrons/shot. The size of neutron source depends on spatial dimension and angle of incidence of our ion beam as well as the target geometry but we estimate beam widths of ~1 mm.

4. Future applications

With a one shot/minute repetition rate on SCARLET and the expected improvements in laser focusing we should be able to quickly optimize deuteron and neutron production to theoretical levels. A currently cutting edge but commercially available laser with >100 J, <300 fs laser system [6] would also be expected deliver the >10^{11} neutrons/shot. However if such a laser system were able

to fire at 10 Hz we could expect neutron generation on the order of 10^{12} neutrons/second which is the necessary threshold to make portable neutron detection feasible. While such a rapidly firing laser is just out of current technological reach, promising work as been done on improving cooling of Nd:glass which could allow such a system to be possible in five years time. [7]
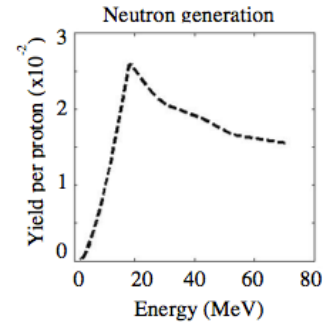

Figure 4: Expected neutron yield with respect to incident deuteron energy

5. Conclusions

We have successfully demonstrated a technique that selectively accelerates deuterons via TNSA. Using this technique we expect to demonstrate high neutron yield (>10^{11} neutrons/shot) on the recently completed SCARLET laser facility. With only moderate advances in laser technology we expect this to be the first step on the road to a compact, affordable high-yield neutron source.

References

[1]S.P. Hatchett, et al. "Electron, photon and ion beams from the relativistic interation of Petawatt laser pulses with solid targets", Phys Plasmas. **7** 2076-2082 (2000).
[2] D.P. Higgenson, et al. "Production of neutrons up to 18 MeV in high-intensity, short-pulse laser matter interactions", Phys Plasmas **18** 100703-1-4 (2011).
[3] D. R. Welch, D. V. Rose, R. E. Clark, T. C. Genoni, and T. P. Hughes, "Implementation of an non-iterative implicit electromagnetic field solver for dense plasma simulation" Comput. Phys. Commun. **164**, 183-188 (2004).
[4] A. Link, R. R. Freeman, D. Schumacher and L. Van Woerkom, "Effects of target charging and ion emission on the energy spectrum of emitted electrons" Phys. of Plas. **18**, 053107-1-8 (2011).
[5] R.A. Snavely, M.H. Key, S.P. Hatchett et al. "Intense high-energy proton beams from petawatt-laser irradiation of solids" Phys. Rev. Lett. **85** 2945-2948 (2000).
[6] National Energetics Inc. http://www.nationalenergetics.com/
[7] J.H. Campbell, J.S. Hayden and A. Marker. "High-Power Solid-State Lasers: a Laser Glass Perspective" Int. J. of App. Glass Sci. **2** 3-29 (2011).

Monte-Carlo simulations for neutron production of laser driven D(d,n) and ^{7}Li(d,xn) reactions using MCUNED

J. Alvarez[1], P.Sauvan[2], J. Perlado[1], J. Sanz[2]

[1] Instituto de Fusión Nuclear, Universidad Politécnica de Madrid, José Gutierrez Abascal, 2. 28006, Madrid, Spain
+34913363108, +34913363002, jalvarezruiz@gmail.com
[2]Departamento de Ingeniería Energética, Universidad de Educación a Distancia, Juan del Rosal 12, 28040, Madrid, Spain

Abstract: *Ultra intense lasers can be a promising and cost-effective neutron source. MCUNED Monte-Carlo code is applied to the simulation of neutron production by laser driven D-D and D-Li^7 nuclear reactions. Results are compared with other computational codes and experiments, showing the good performance and high flexibility of the code.*

1. Introduction

Ultra intense lasers can be a promising and cost-effective neutron source. At present, the most efficient nuclear reactions to produce neutrons with laser systems are based on the acceleration of Deuterium ions. Those ions, typically generated by the Target Normal Sheath Acceleration mechanism, show a broad energy spectrum ranging from hundreds of keV to tens of MeV with an exponentially decreasing distribution. In the Pitcher-Catcher configuration, the accelerated D ions impinge on a second target in which the production of neutrons takes place. The most common targets to induce the nuclear reactions are deuterated plastics and Li based materials (eg. LiF) which give place to D(d,n) and 7Li(Li,xn) reactions. At present, maximum neutron fluences of around 10^{10}/Sr for large laser facilities and 10^6/Sr for "table-top" ones are achieved. These neutron yields can be improved optimizing the composition and geometry of the reaction target and computational simulations on the transport and nuclear reactions can be of a great help.

2. Simulation Monte Carlo codes

To our knowledge, there are no general-purpose Monte Carlo codes prepared to adequately simulate the D nuclear reactions in the range of the mentioned energies. Thus, general transport codes such as MCNPX or GEANT4 use the Cascade Model to implement D nuclear reactions which, at energies below 1 MeV, give very poor results. Other codes as FLUKA do not even implement D nuclear reactions in the range of a few MeV. Case-specific Monte Carlo codes [1, 2] are more suitable for this purpose but they necessarily have to give up some of the potentialities of broader developed codes.

This contribution presents simulations on the neutron production of laser driven D-D and D-Li nuclear reactions, making use of the MCUNED code[3], a modified version of the MCNPX code, which among other capabilities, allows the possibility of using external nuclear data libraries adequate for this problem. Since it is based on MCNPX, MCUNED is very flexible to simulate any kind of geometry and source. It can perform a fully 3D simulation for both ion and neutron transport taking into account subsequent nuclear reaction induced by transported particles. Nuclear data for deuteron induced nuclear reaction relies on the ENDF/B.VII.1 library which has been recently released and for this reaction contains data from 0.1 keV up to 10 MeV.

3. Results with MCUNED and comparisons with other codes and experiments

Several simulations of laser driven D-D and D-Li reactions carried out with the MCUNED code will be compared with results attained with other codes [2,4,5] as well as comparisons with experimental results [5,6]. A detailed error analysis and an evaluation of the main differences among codes will be provided.

4. Conclusions

The main causes of the observed difference between the results obtained with the MCUNED code and other available codes will be identified, stressing the potentialities of this multi-purpose code. It is concluded that MCUNED offers more flexibility and accuracy in the simulation of the production of neutrons by laser driven D reactions than present available codes.

Acknowledgement

References

[1]H. Habara,R. Kodama,Y. Sentoku,N. Izumi,Y. Kitagawa,K. A. Tanaka, K. Mima, and T. Yamanaka. "Fast ion acceleration in ultraintense laser interactions with an overdense plasma". Phys. Rev. E **69,** 036407 (2004)

[2] J. Davis and G.M. Petrov "Angular distribution of neutrons from high-intensity laser–target interactions" Plasma Phys. Control. Fusion **50** 065016 (2008)

[3] P.Sauvan, J.Sanz, F.Ogando, "New capabilities for Monte Carlo simulation of deuteron transport and secondary products generation", Nucl. Instr. Meth. in Phys. Res. A **614,** 323 (2010)

[4] C. L. Ellison and J. Fuchs. "Optimizing laser-accelerated ion beams for a collimated neutron source" Phys. Plasmas **17,** 113105 (2010)

[5] L. Willingale, G. M. Petrov, A. Maksimchuk, J. Davis, R. R. Freeman et al."Comparison of bulk and pitcher-catcher targets for laser-driven neutron production" Phys. Plasmas **18**, 083106 (2011)

[6] D. P. Higginson, J. M. McNaney, D. C. Swift, G. M. Petrov, J. Davis3, J. A. Frenje, L. C. Jarrott, R. Kodama, K. L. Lancaster, A. J. Mackinnon, H. Nakamura, P. K. Patel, G. Tynan, and F. N. Beg. "Production of neutrons up to 18 MeV in high-intensity, short-pulse laser matter interactions." Phys. Plasmas **18**, 100703 (2011)

Poster presentations

The development of the neutron detector for the fast ignition experiment by using LFEX and Gekko XII facility

Takahiro NAGAI[1], Mitsuo NAKAI[1], Yasunobu ARIKAWA[1], Yuki ABE[1], Sadaoki KOJIMA[1], Shohei SAKATA[1], Hiroaki INOUE[1], Shinsuke FUJIOKA[1], Hiroyuki SHIRAGA[1], Nobuhiko SARUKURA[1], Takayoshi NORIMATSU[1], and Hiroshi AZECHI[1]

1) Institute of Laser Engineering, Osaka University, 2-6 Yamada-oka Suita Osaka Japan,
TEL:06-6879-8775 and FAX:06-6879-8776, EMAIL: nagai-t@ile.osaka-u.ac.jp

Abstract: Neutron detection after intense γ ray flash in the fast ignition experiment is exceedingly challenging. The γ-ray background noises are γ ray coming to detector directly from target, γ ray scattered from target bay wall and photo-nuclear neutron generated from constructions such as the target chamber. Using the low-afterglow liquid scintillator, the photo multiplier tube gating and locating the radiation shield made it possible the diagnostics of the nuclear fusion neutron in the fast ignition experiment.

1. Introduction

Fast ignition experiment using LFEX and Gekko XII facility has been conducted since 2009. [1] Diagnostics in the fast ignition is extremely difficult due to intense γ ray generated from ultra-intense laser. [2] The γ ray coming to detector, the γ ray scattered from target bay wall, the photo-nuclear neutron ((γ, n) neutron) generated from the construction such as the target chamber interfere fusion deutron-deutron (DD) neutron detection. In the scintillation neutron measurement, it is a critical issue that the DD neutron is masked by the γ-ray background noises as shown in Fig. 1. The γ-ray background noises are the scintillation slow component (afterglow), the signal saturation and the afterpulse of photo multiplier tube (PMT) generated from the γ ray, and the radiation background noise such as the scattered g ray and the (γ, n) neutron. [2]

In this work, the DD neutron was successfully diagnosed by reducing the γ-ray background noises in the 2012 fast ignition experiment.
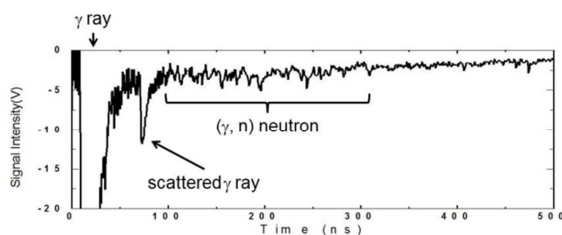

Fig. 1. Signal measured by the conventional detector in fast ignition experiment. LFEX laser energy is 540 J.

2. Designing works

2.1 Low-afterglow liquid scintillator[3]

The scintillation afterglow masks the small signal of DD neutron. Xylene-based 4,4'''-Bis[(2-butyloctyl)oxy]-1,1':4',1":4",1'''-quarterphenyl (BBQ) liquid scintillator enriched oxygen was developed. [3] Figure 2 shows the comparison of the scintillation afterglow and the first decay component of the BBQ scintillator and the conventional plastic scintillator (BC-422Q). The scintillation afterglow of the BBQ scintillator is ~1/50

that of the plastic scintillator at 100 ns. First decay time of the BBQ scintillator (0.76 ns) is as fast as that of the plastic scintillator (0.65 ns).

2.2 Photo Multiplier Tube

The scintillation of the intense γ ray causes the PMT saturation due to charge drain from the capacitor. For avoiding charge drain, gated PMT (Hamamatsu R2256-02, C1392) was used. Figure 3 shows the PMT gating avoid the PMT saturation. The gated signals show the scintillation decay curves though non-gating signal shows weak signal after the γ ray flash. Applied voltage of the PMT was adjusted because of changing electron transit time in the PMT in order to distinguish the DD neutron signal from the PMT afterpulse signal.
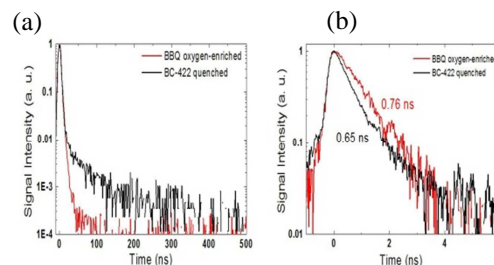

Fig. 2. The comparison of the Scintillation decay between the oxygen-enriched BBQ scintillator and the conventional plastic scintillator. (a) the afterglow comparison, (b) the first decay time comparison.
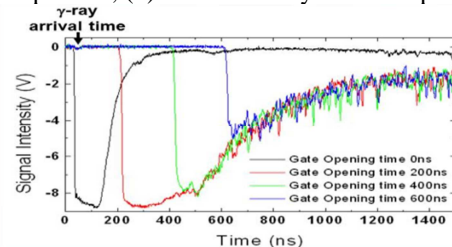

Fig. 3. The PMT gating avoiding the PMT saturation due to the intense γ ray shot by using the linear electron accelerator.

2.3 Detector design

2 kinds of the detection systems were developed for the fast ignition experiment as shown in Fig. 4. One of the systems is a detector located in the flight path behind the concrete wall at 13.35 m from the center of the target chamber. 180 mmφ ×100 mm thick volume of the BBQ liquid scintillator attached to the acrylic light guide and the PMT was designed by calculating the neutron detection efficiency and the scintillation collection efficiency. The multistep polyacetal neutron collimators are equipped for reducing the γ-ray background noises. In the comparison of with-or-without the multistep collimators, the reduction rate of the (γ, n) neutron by the collimators at the DD neutron arrival time was estimated 95 % by using MCNP simulation code as shown in Fig. 5 (a).

  Another system is multi-channel detector located in the concrete wall at 8 m. 7-channel 180 mmφ×20 mm thick volume of the BBQ liquid scintillator are designed. Output of each scintillator were adjusted by using the neutral density filter and Benzophenone (1 wt%) for obtaining high dynamic range. The polyacetal and water neutron collimator are equipped in order to reduce the background noise. The reduction rate of the (g, n) neutron by the collimators at the DD neutron arrival time is estimated 98 % by MCNP simulation code as shown in Fig. 5 (b).
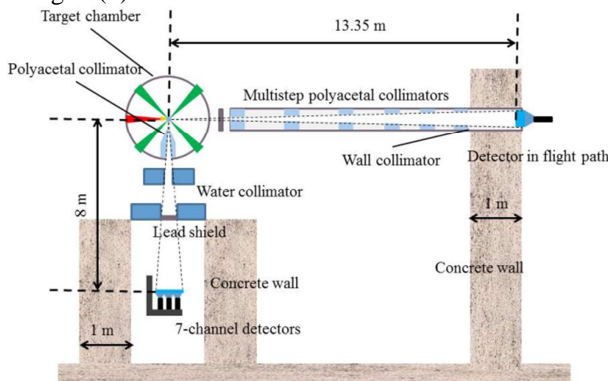

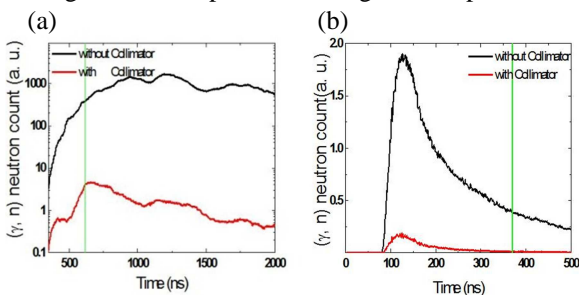Fig. 4. The setup for the fast ignition experiment

Fig. 5. The comparison of the (γ, n) neutron count with-or-without the collimator by MCNP simulation code. (a) (γ, n) neutron count detected at 13.35m in the flight path. (b) (γ, n) neutron count detected at 8 m under the chamber.

3   Neutron diagnostics in the fast ignition experiment

Neutron detection in the fast ignition experiment was succeeded by reducing the γ-ray background noises. Figure 6 shows the signal measured by the newly-developed detection system. The DD neutron signal measured by the detector in the flight path was clearly measured by the multistep neutron collimators and the concrete wall as shown in Fig. 6 (a). The γ-ray background noises are reduced by the PMT gating and distinguished from the PMT afterpulse in the signals measured by the multi-channel detector as shown in Fig. 6 (b) Unfortunately, a background can be still seen in the signals after the gate turns off. This background noise is caused by the scintillation afterglow because this detector is located closer to the target chamber than the detector in the flight path.
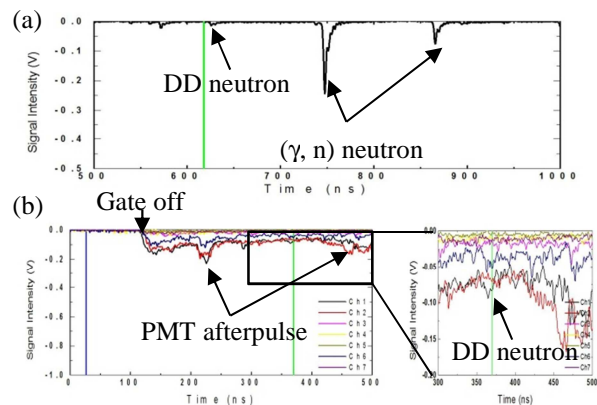

Fig. 6. Data acquired in the fast ignition experiment. LFEX energy is 670 J. (a)The signal measured by the detector in the flight path, (b)The signals measured by the 7-channel detector. Blue and green line are g-ray and DD neutron arrival time relatively.

4   Conclusions

In the fast ignition experiment, the neutron measurement in the intense g-ray background noises is extremely challenging. By using the oxygen-enriched BBQ liquid scintillator, the PMT gaiting, and the collimators for the γ-ray background noises, the DD neutron signal was detected clearly.

References
[1] H. Shiraga, *et al.*, Plasma Phys. Control Fusion, **53**, 124029 (2011)
[2] Y. Arikawa, *et al.*, Rev. Sci. Instrum., **83**, 10D909 (2012)
[3] T. Nagai, *et al.*, J. J. Appl. Phys. **50**, 080208 (2011)

Development of multichannel TOF neutron spectrometer
for The Fast Ignition Experiment

Yuki Abe, Hirokazu Hosoda, Yasunobu Arikawa, Takahiro Nagai, Sadaoki Kojima, Shohei Sakata, Hiroaki Inoue,
Yuki Iwasa, Keisuke Iwano, Mitsuo Nakai, Takayoshi Norimatsu, and Hiroshi Azechi
Institute of Laser Engineering, Osaka University, 2-6 Yamada-oka Suita Osaka Japan,
Tel: +81-6-6879-8775, Email: abe-y@ile.osaka-u.ac.jp

Abstract: In the fast-ignition experiment, the neutron diagnostics have a critical issue of the harsh background caused by hard X-rays and photonuclear neutrons generated by the fast heating laser. The multichannel time-of-flight neutron spectrometer named MANDALA was improved in suppressing the background by the installation of downsized scintillators and a neutron collimator in Institute of Laser Engineering, Osaka University. The neutron diagnostics of low yield shots with the upgraded MANDALA was successfully demonstrated in the Fast Ignition Experimental Campaign 2012.

1. Introduction

Inertial confinement fusion (ICF) which is apploaching the final goal of ignition producing energy at National Ignition Facility. At the same time, the fast ignition scheme urged in Institute of Laser Engineering has been expected to be ten times efficient mode. The neutron diagnostics which can directly measure the fusion plasma parameter is essential. However, the neutron diagnostics have a critical issue of the harsh background caused by hard X-rays and photo-nuclear neutrons (hereinafter referred to as γ-rays and γ-n neutrons) generated by the fast heating laser. In this regard, γ-shields and γ-n shields are indispensable for the neutron detectors. A huge neutron collimator successfully demonstrated the attenuation of γ-n neutrons, and neutron diagnosis was conducted with the upgraded MANDALA (Multi-angle Neutron Detector at Large Area). Here we present the design of the neutron collimator and the experimental results in 2012.

2. Upgrades of MANDALA

MANDALA is a neutron spectrometer with an array of 600 individual scintillation detectors located at 13.5 m from the center of the main experiment chamber of the GEKKO-XII and LFEX laser. This detectors array is designed to perform spectroscopy of low yield neutrons down to 8×10^4 with 66 keV energy resolution by time-of-flight (TOF). The count-mode data acquisition system with a leading edge discriminator and 500-ps Time-to-digital Converter (TDC) is adopted, and the ion temperature can be obtained from the arrival time distribution of neutrons that interacted in the detectors array [1]. Additional lead γ-shields have been installed and 5×10^{-4} attenuation of γ-rays was achieved in our previous work [2], and, more 2×10^{-1} attenuation was demonstrated by downsizing scintillators. In addition, a huge polyethylene neutron collimator was installed for γ-n shield. Figure.1 shows the geometry of the collimator. Figure.2 (a) shows γ-ray and γ-n neutron flux map simulated by Monte Carlo simulation with MCNP5 and (b) shows the geometry of the simulation. In this
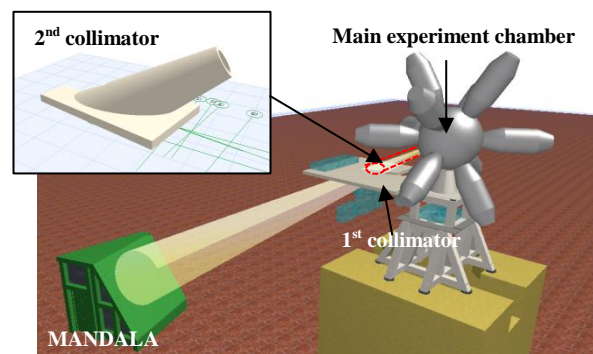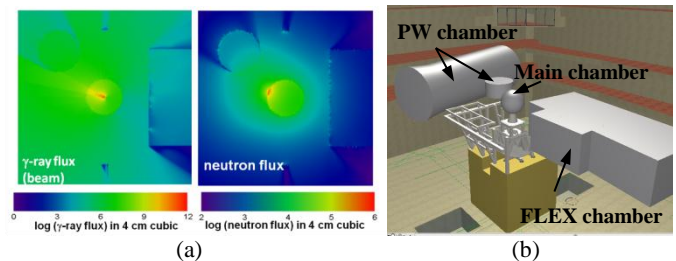

Fig.1 The geometry of the collimator

Fig.2 (a) The calculated γ-ray and γ-n neutron flux map around the main experiment chamber for beamed γ-ray sources (b) The geometry of the simulation

simulation, we assumed the γ-ray spectrum with a 5 MeV slope temperature [3] and the angular distribution of the γ-ray beam with a $(\cos^5(0.5\theta))$ function [4]. Figure.2 (a) clearly shows that the main chamber is the dominant γ-n neutron source among the any components in the simulation. The neutron collimator was designed to suppress the γ-n neutrons from the main chamber. The collimator consists of two parts. 1st collimator is a polyethylene-board with 2.4×10^4 cm^2 and 10-cm thickness, and the 2nd collimator is a polyethylene "cannon" with a 20-cm diameter, 1.7-m length and 10-cm thickness. This collimator shields γ-n neutron from the main chamber
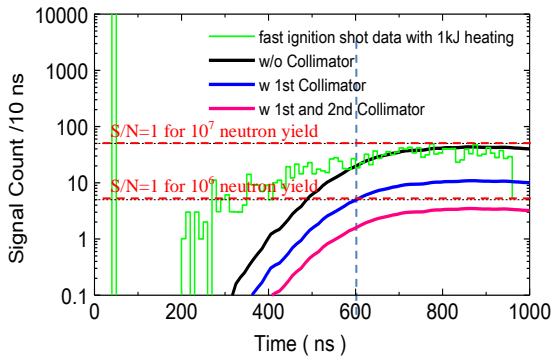
Fig.3 The calculated γ-n signal with or without collimators. The two horizontal dotted lines show the peak DD-pulse count considered the system response. DD-neutrons is detected at 630 ns. γ-n profile must be lower than this line. The black line is simulated line which was scaled experimentally.

Table.1 The calculated attenuation of the collimator

Object	Total γ-n neutrons (%)	γ-n neutrons in 600-700ns (%)
w/o Collimator	100	18
w 1st Collimator	19	3
w 1st + 2nd Collimator	7	0.7

and while fusion originated neutrons can go through. Figure.3 shows the simulated profile of γ-n neutrons. The two horizontal dotted lines show the peak DD-pulse count considered the system response. DD-neutrons is detected at 630 ns. γ-n profile must be lower than this line. The black line is simulated line which was scaled experimentally. 1st collimator is enough for the diagnosis of deuteron-deuteron (DD) neutrons in the 10^6 yield shots with 1kJ heating, while 2nd collimator will improve 4 times as shown in the Table.1. 1st collimator was installed in 2012 and the diagnosis of DD-neutron was successfully demonstrated. Whole collimator will be completed in a few months.

3. Experimental result

The neutron diagnosis with the upgraded MANDALA was successfully demonstrated in the fast ignition experiment in 2012. Fig.4 (a) shows an example of the signal before upgrade in the 576 J heating shot in 2010, and (b) shows an example after upgrade in the 953 J heating shot in 2012. DD-neutron signals are clearly seen at 650 ns in 2012, although it was masked in the background caused by γ-n signals in 2010. This background can be subtracted because the energy spectrum is broad. The calculated time profile of γ-n signals was fitted with the background of (b) and then subtracted. At the result, The DD-neutron yield of was confirmed to be $(5.9 \pm 0.9) \times 10^6$ in this shot.
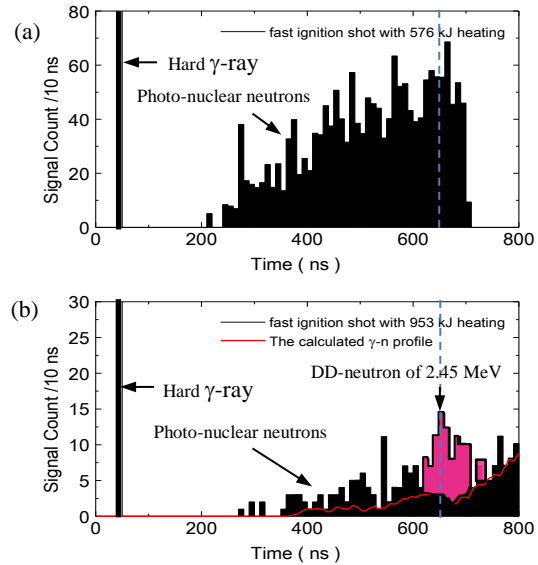

Fig.4 The example of signal (a) shows the example of the signal before upgrade in the shot with 6 J heating in 2010, and (b) shows an example after upgrade in the 953 J heating shot in 2012

4. Conclusions

Neutron diagnosis with upgraded MANDALA system was demonstrated in the fast ignition experiment. γ-ray and γ-n signals were successfully suppressed by the installation of downsized scintillators and a neutron collimator. The whole collimator is under construction and will be completed in late 2013.

References

[1] N. Izumi et al., Rev. Sci. Instrum. **70**, 1221 (1999)
[2] H. Hosoda et al., JPCS. **112**, 032079 (2008)
[3] T. Tanimoto et al., Phys. Plasmas. **16**, 062703 (2009)
[4] Y. Arikawa et al., Rev. Sci. Instrum. **83**, 10D909 (2012)

The neutron imaging diagnostics and unfolding technique for fast ignition experiment

H. Inoue[1], Y.Arikawa, S. Nozaki[2], S. Fujioka[1], T.Nagai[1], S. Kojima[1], Y. Abe[1], S.Sakata[1], M. Nakai[1], H. Shiraga[1], and H.Azechi,[1]

[1] Institute of Laser Engineering, Osaka University, 2-6, Yamadaoka Suita, Osaka Japan, 565-0871,
phone +81-6-6879-8775, and inoue-h@ile.osaka-u.ac.jp,
[2] Okinawa National College of Technology,

Abstract: *In the fast ignition experiment the imaging diagnostics of the fusion neutron has been desired. In this study the neutron or high energy x-ray imaging detector by using multi-penumbral array was developed. The unfolding technique by using Heuristic method was successfully demonstrated in the fast ignition experiment.*

1. Introduction

In the fast ignition experiment, imploded plasma core is heated by fast electrons induced by an ultra-intense laser. In this experiment diagnosing of the special distribution of the temperature is strongly important, thus imaging diagnostics of the fusion neutron of high energy x-ray have been expected to be promising method. The penumbral aperture is well known method for imaging neutrons or high energy x-ray, and the unfolding process is essential in the penumbral imaging [1]. In recent studies a novel technique in the unfolding by using Simulated Annealing Heutistic method was proposed for reconstructing clear images. In this study the neutron and high energy x-ray imaging detector by using a custom designed multi penumbral aperture array was developed, and the unfolding technique by using Heutistic method was developed. The performance of the imaging diagnostics was demonstrated with high energy x-ray in the fast ignition experiment.

2. Designing work of the Penumbra appertures

The fusion neutron or x-ray having high energy needs very thick apertures due to its high transmission characteristics. The penumbral aperture made of lead with the thickness of 10 cm with which it has 1/10 of attenuation length was developed in our previous work [2]. The shape of the inner surface was designed to be toroidal in order to obtain uniform point spread function for large angle. Figure 1 shows schematic of the comparison of the point spread function of between cylindrical and toroidal penumbral aperture. The point
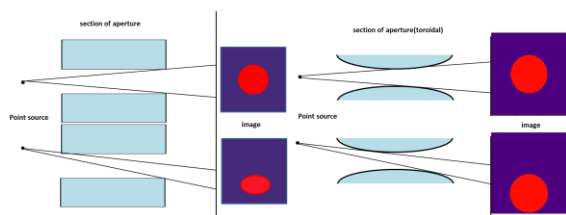

Figure 1 The schmatic of the cylindolical and toloidal shaped penumbral apperture and point spread function.
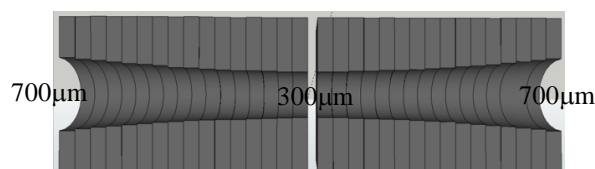

Figure 2 The schematic view of the penumbral aperture developed.

spread function (PSF) of the cylindolical aperture at the large angle is distorted, on the other hand toroidal one shows small distortion in any angle. The 10-cm thick 32 penumbral apertures array was developed the constructed 100 separate 1-mm thick lead plates as shown in Fig.2. The diameter of the entrance, centor, and exit were designed to be 700μm, 300 μm, 700 μm, respectively.

3. Unfolding technique by using Heuristic method

A novel technique for unfolding the penumbral image was developed in our previous work [3,4]. In this method the reconstructed image is iteratively inferred. In this study the high energy x-ray (less than 200 keV) generated in the fast ignition experiment was used to demonstrate the detector and the unfolding technique. The pointspread functions from every source point were calculated separately by using the analytic calculation and the Monte-Carlo simulation code MCNP5. The figure 3 shows the example of the PSF from the variour point source. The small distortion was seen in the PSF from the source far from the central position. The size of image we intend to observe is comparable with the aperture diameter, thus the space-variant PSF should be treated in the unfolding process. The similar work was reported in the paper [5], however in this method non space variant PSF is used, thus image quality is affected from misalignment of the penumbra.The Heutristic method can be easily applied with the space-variant PSF, and furthermore this method has been known as a very robust for noises.
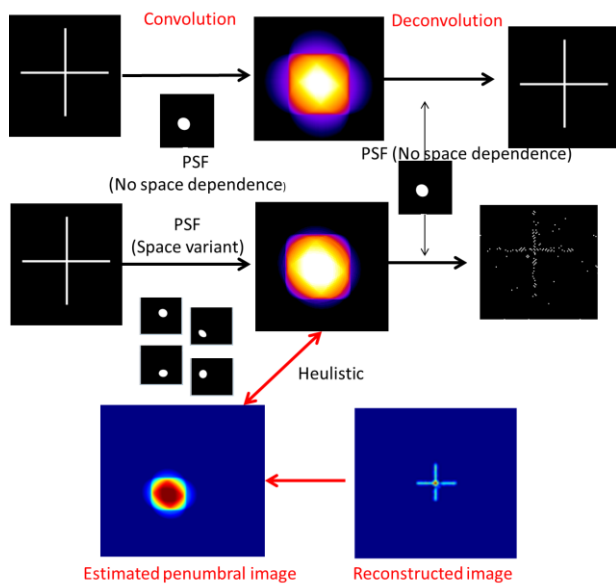
Figure 4 the comparisons of the tested images by using artificially made cross shape image shown on the left side was convoluted with non-space variant PSF which is PSF of the center source or space variant PSF.

Before the fast ignition originated x-ray was examined, we tested our unfolding technique by using artificially made samples. Figure 4. Shows the comparisons of the tested images by using artificially made cross shape image shown on the left side was convoluted with non-space variant PSF which is PSF of the center source or space variant PSF. The small difference was observed in the convoluted image at the outer region. Theses images were deconvoluted with the non-space variant PSF and compared in the right hand. The deconvoluted image with non-space variant PSF significantly distorted and affected from the numerical noise. This is essential problem in the deconbolution process. On the other hand reconstructed images by using our Heuristic method shows excellent performance.

4. Experimental results

The fast ignition experiment was conducted in the GEKKO XII and LFEX laser facility in Institute of Laser engineering, Osaka University. The penumbral detector was implemented in the experiment and the x-ray image from the typical fast-heating shot was clearly observed. The figure 5 (a) shows observed image and (b) is zoomed image on the central aperture image. We applied our Heuristic method to reconstruct the image. Figure 5 (c) shows the tentative image obtained image via our process. At this image numerical noise is still too strong so that image was not able to reconstructed well enough. This can be improved by improving the PSF matrix.
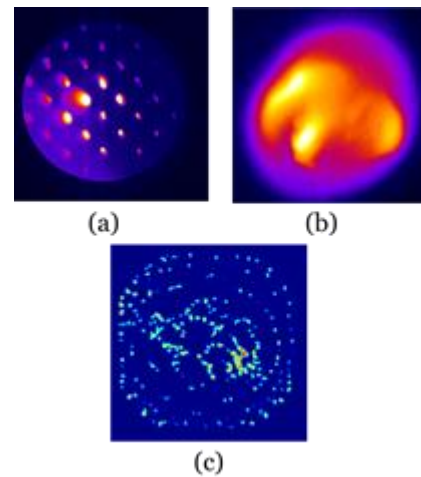

Figure 5 (a) shows observed image and (b) is zoomed image on the central aperture image. We applied our Heuristic method to reconstruct the image. Figure 5 (c) shows the tentative image obtained image via our process.

5. Conclusions and future prospects

The neutron of high energy x-ray imaging detector by using multi channel penumbral aperture array was developed for fast ignition laser fusion experiment. The unfolding method by implementing Heuristic algorism was developed and successfully applied in the experiment. The performance of the Heuristics method was tested by using pattern sample image, and the excellent quality was demonstrated. The high energy x-ray image was firstly reconstructed in the fast ignition experiment.

Acknowledgement

References

[1] D. Ress, et. al., Science, **24**,1 956
[2].T Ueda Master thesis Osaka University,2010
[3] S.Nozaki, et. al., REVIEW OF SCIENTIFIC INSTRUMENTS,**75,**10,PartII, 2004
[4] S.Nozaki et .al., REVIEW OF SCIENTIFIC INSTRUMENTS ,**74**,3 ,2003
[5] E.N.Loomis,et.al., REVIEW OF SCIENTIFIC INSTRUMENTS,**81**,1010D311,2010

Generation of Directed Energetic Neutron Beams Using Short Pulse Lasers

G. M. Petrov[1], D. P. Higginson[2], J. Davis[1], Tz. B. Petrova[1], C. McGuffey[2], B. Qiao[2] and F. N. Beg[2]

[1] Naval Research Laboratory, Plasma Physics Division 4555 Overlook Ave. SW, Washington, DC 20375, USA

[2] Mechanical and Aerospace Engineering, University of California-San Diego, La Jolla, CA 92093, USA

Abstract: *A roadmap is proposed for the production of directed high-energy (>15 MeV) neutron beam using short pulse lasers. Three nuclear reactions, $d(d,n)^3He$, $^7Li(d,n)^8Be$, and $^7Li(p,n)^7Be$, are studied using 2D particle-in-cell and 3D Monte Carlo simulations. Experiments performed with the Titan laser provided experimental verification of the concept.*

1. Introduction

Neutron beams are extensively used in science and technology in fields ranging from fundamental physics to medical research. They are traditionally produced using particle accelerators, but short pulse lasers have emerged as a viable alternative. Besides being more compact compared to particle accelerators, lasers can generate neutron beams with exceptional properties: high temporal resolution (<< 1 ns), "point source" (<< 1 mm^3), directionality (<1 sr) and high fluence (10^9–10^{10} n/sr). The lower price of the driver (short pulse laser) makes them widely available to a large research community such as universities and research centers.
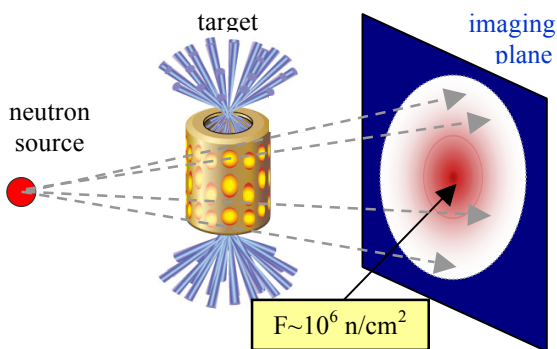

Fig. 1. Concept for neutron radiography. This scheme exploits the small size of the source and directionality of the neutron beam.

Generation of neutron beams with isotropic distribution and neutrons with energy ~2.5 (d-d) and ~14 MeV (d-t) is straightforward. Therefore, the challenge is to produce neutron beams that are directional with spectra extending beyond 14 MeV. Numerical simulations and recent experiments on the Titan laser at LLNL confirmed the feasibility of developing such a compact neutron source using short-pulse laser-matter interactions [1,2]. In the next section we discuss the most important neutron beam characteristics: yield, fluence, directionality and spectrum, and the methods of their generation using short pulse lasers.

2. Neutron beam properties

2.1 Neutron yield and fluence

Three nuclear reactions, $d(d,n)^3He$, $^7Li(d,n)^8Be$, and $^7Li(p,n)^7Be$, have been selected as the most likely candidates for laser-produced neutron beams. The d-d

reaction is the simplest, most studied and easiest for simulations. The d-Li reaction is attractive as the cross section for neutron production is very large (~1 barn). The p-Li reaction is important since protons can be accelerated to kinetic energy of up to 100 MeV. Figure 2 (left) plots the neutron yield per incident ion versus ion energy. The d-Li reaction is the most efficient, but does not always yield the largest number of neutrons because in actual experiments protons are generated in number and energy that far exceed that of deuterons. For this reason the p-Li reaction is the dominant one [1]. When using lasers, the calculation of the neutron fluence and spectra is rather complex because the neutron production is a two-stage process. Therefore, the neutron beam parameters are quantified using both measurements and simulations. Since lasers have vastly different parameters, we adopted the normalized neutron yield (number of neutrons per joule laser energy) as a convenient measure of neutron production efficiency. Simulations indicate that for the d-d, p-Li and d-Li reactions it is ~10^6, ~10^7 and >10^7 neutrons/Joule, respectively [3]. A 100 J class laser such as the Titan laser can produce ~10^9–10^{10} neutrons [1,2].
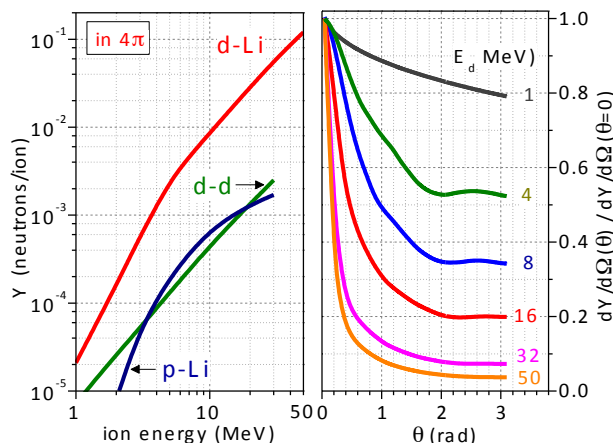

Fig. 2. Neutron yield per incident ion from d-d, d-Li and p-Li nuclear reactions (left) and normalized neutron fluence from d-Li reactions (right).

2.2 Directed neutron beams

Directed (pencil-like) neutron beams are highly desirable to improve the neutron fluence on target. Laser-produced neutron beams can be directional, which is demonstrated using the $^7Li(d,n)^8Be$ reaction [4,5]. The most striking feature of the neutron beam from this reaction is the

production of a very narrow cone of neutrons. The onset of directionality commences at incident deuteron energy E_d of 5–10 MeV and gradually improves with deuteron energy increasing as $\bar{\theta} \cong \sqrt{\varepsilon_d / E_d}$, where ε_d=2.24 MeV is the binding energy of the deuteron. At E_d>10 MeV the emitted neutrons have a strongly peaked forward angular dependence as shown in Fig. 2 (right). Other reactions such as d-Be exhibit similar properties and are equally suited for production of directed neutron beams.

2.3. High-energy neutron beams
Another remarkable feature of deuteron-driven reactions (d-Li, d-Be, etc.) is the neutron energy distribution. The neutron spectra exhibit a broad peak at ~E_d/2 and a secondary peak with energy E_d+Q (Q is the Q-value of the reaction) [4]. The latter can be used to 'tune' the neutron beam energy to a desired range. Thus d–Li or d–Be nuclear fusion reactions can be used to generate high-energy collimated neutron beams.

3. Numerical simulations of laser-produced neutrons
Numerical simulations are performed to calculate the neutron spectra in a pitcher-catcher setup, in which the pitcher (ion source) is a thin CD foil and the converter is a thick (1–2 mm) slab of Li. A two dimensional, relativistic, electromagnetic PIC code is used to model the laser-foil interaction and generation of the deuteron beam. The output is fed into a 3D Monte Carlo code, which transports the deuterons through a converter and computes the neutron spectra at various directions of observation. Simulation results, shown in Fig. 3, demonstrate that high-energy directional neutron beams can be generated in laser-target interactions.
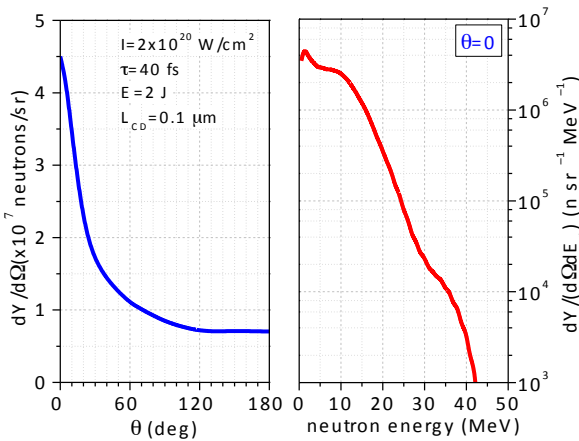

Fig. 3. Simulated neutron fluence in the forward direction from a laser pitcher-catcher setup. Laser parameters: peak intensity 2×10^{20} W/cm^2, pulse duration 40 fs, spot size 5 μm, wavelength 1 μm, energy 2 J. Foil parameters: L_{CD}=0.1 μm. Converter: Li.

4. Experimental verification of the concept
The first experimental demonstration of high-energy neutron production using short-pulse, high-intensity lasers was performed at the Jupiter Laser Facility at the Lawrence Livermore National Laboratory (LLNL) using the Titan laser [2]. Laser pulses with energy 360 J, duration 9 ps and intensity 2×10^{19} W/cm^2 incident on a 25 μm CD$_2$ foil accelerated deuterons from the foil rear

surface. These ions were then incident on a 1.8 mm LiF slab placed 1 mm away from the foil, where they generated neutrons through nuclear reactions in the LiF converter. nTOF detectors placed roughly 5 m from the foil were used to measure the neutron spectrum, and CR-39 to measure the neutron fluence. We measured a fluence 8×10^8 [n/sr] in the forward direction.
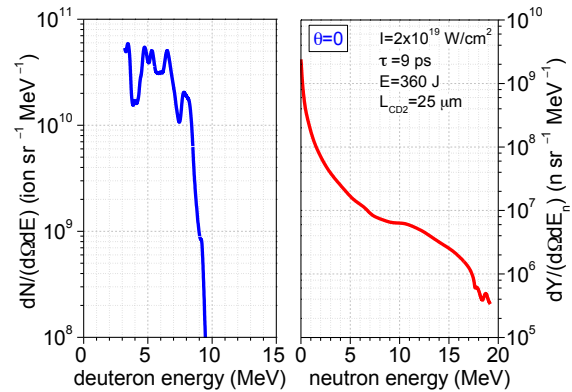

Fig. 4. Deuteron (left) and neutron spectrum from d-Li reactions (right) driven by the LLNL Titan laser.

5. Conclusions
Generation of high-energy directed neutron beams using short pulse lasers is discussed. Numerical simulations and experimental data demonstrated the feasibility of the concept.

References
[1] D. P. Higginson, J. M. McNaney, D. C. Swift, T. Bartal, D. S. Hey, R. Kodama, S. Le Pape, A. Mackinnon, D. Mariscal, H. Nakamura, N. Nakanii, K. A. Tanaka, and F. N. Beg, "Laser generated neutron source for neutron resonance spectroscopy", Phys. Plasmas **17**, 100701 (2010)
[2] D. P. Higginson, J. M. McNaney, D. C. Swift, G. M. Petrov, J. Davis, J. A. Frenje, L. C. Jarrott, R. Kodama, K. L. Lancaster, A. J. Mackinnon, H. Nakamura, P. K. Patel, G. Tynan, and F. N. Beg, "Production of neutrons up to 18 MeV in high-intensity, short-pulse laser matter interactions", Phys. Plasmas **18**, 100703 (2011)
[3] J Davis, G M Petrov "Neutron production from ultrashort pulse lasers using linear and circular polarization", Phys. Plasmas **18**, 073109 (2011)
[4] J. Davis, G. M. Petrov, Tz. Petrova, L Willingale, A. Maksimchuk and K. Krushelnick, "Neutron production from ^{7}Li(d,xn) nuclear fusion reactions driven by high-intensity laser–target interactions", Plasma Phys. Control. Fusion **52**, 045015 (2010)
[5] G. M. Petrov, D. P. Higginson, J. Davis, Tz. B. Petrova, J. M. McNaney, C. McGuffey, B. Qiao, and F. N. Beg, "Generation of high-energy (>15 MeV) neutrons using short pulse high intensity lasers", Phys. Plasmas **19**, 093106 (2012)

Conference on Laser and Accelerator Neutron Sources and Applications(LANSA'13), Yokohama, Japan, Apr. 23 - Apr. 25, 2013

Simplified neutron detector for angular distribution measurement of p-Li neutron source

Makoto Sakai, Shingo Tamaki, Isao Murata
Graduate School of Engineering, Osaka University

Abstract: *Boron Neutron Capture Therapy (BNCT) is one of the most promising cancer therapies and p-Li accelerator is expected for the neutron source. However to use p-Li neutron source for BNCT, measurement of the angular distribution is important. We have developed a simplified neutron detector and measured the angular distribution.*

1. Introduction

Boron Neutron Capture Therapy (BNCT) is less invasive cancer therapy using $^{10}B(n, \alpha)^7Li$ nuclear reaction[1]. Because nuclear reactor is currently used for BNCT, the therapy is much restricted. Many kinds of accelerator neutron sources for BNCT are being developed worldwide and p-Li accelerator is expected because the energy is comparatively low and no gamma-ray is produced from p-Li reaction. To use a p-Li accelerator for BNCT, measurement of the angular distribution is important. The energy of p-Li neutron depends on the neutron emission angle with respect to the proton beam. So a neutron detector, the efficiency of which is not dependent on energy is needed. Though Long Counter is known to be available for that purpose, long counter is complicated and expensive. Thus we have developed a neutron detector with constant efficiency for 100-700 keV neutron, which is the energy of neutrons produced from p-Li reaction, and measured the angular distribution from the p-Li neutron source.

2. Design of the detector

Figure 1 shows a conceptual arrangement before the design calculations. To make a constant-efficiency neutron detector, we employed a He-3 proportional counter covered with polyethylene moderator. And cadmium was used to shield thermal neutron scattered from the wall of experimental room.
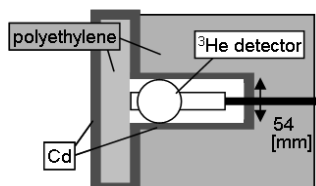

Fig. 1. Conceptual arrangement before the design calculations. p-Li neutrons are moderated in the front polyethylene. And the scattering neutrons from wall are shielded with side and back polyethylene and cadmium.

Simulation calculations were performed to investigate the optimum amounts of moderator and shielding materials to shield scattered neutrons and to estimate the detector efficiency for 100-700 keV source neutron using MCNP-5 (A General Monte Carlo N-Particle Transport Code). JEDLE 4.0 was used as a neutron cross section library.

3. Calculation and design results

Calculated relative increase due to scattered neutrons in the wall is shown in Figure 2 as a function of surrounding polyethylene thickness. The increase effect of scattered neutrons decreases with the thickness of polyethylene. Because the effect becomes saturated for thickness more than 7 cm, 7.3 cm thick polyethylene shield was adopted. Relative detector efficiencies for various thicknesses of front polyethylene moderator are shown in Figure 3 as a function of the source neutron energy of 100-700 keV. The calculation indicates 3.4 cm thickness of polyethylene is the best and the difference of efficiency is suppressed to be within 9%. Thus we made a neutron detector with 3.4 cm thick front polyethylene moderator and 7.3 cm thick shielding polyethylene (Figure 4).
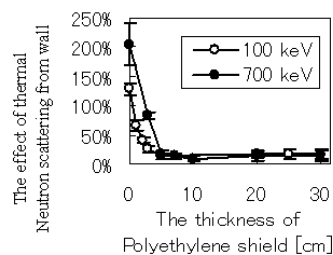

Fig. 2. Calculated relative increase due to thermal neutrons scattered in the wall as a function of the thickness of the shielding polyethylene. The symbol indicates the source neutron energy: ●; 100 keV and ○; 700 keV.

4. Comparison between test measurements and simulation calculations

To compare the simulation calculation with the experimental result using the developed detector, D-T and Am-Be neutron sources were used together with stainless steel moderator. The D-T neutron experiment was carried out at the Intense 14 MeV Neutron Source Facility, OKTAVIAN, of Osaka University. The Am-Be neutron source generates ~10^6 n/s and the neutrons were moderated by 50 cm thickness of stainless steel. The count rates of He-3 detector were compared with the calculation value in Figure 5. The measured count rates were in good agreement with the calculation results (the ratio between simulations and irradiation experiments were 0.97 and 1.01 for Am-Be and D-T sources, respectively)
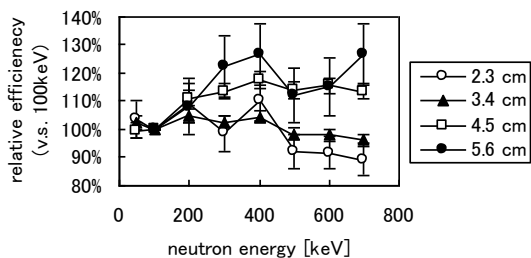
Fig. 3. Relative efficiency as a function of source neutron energy. The symbol indicates the front polyethylene thickness: ○; 2.3 cm, ▲; 3.4 cm, □; 4.5 cm and ●; 5.6 cm.
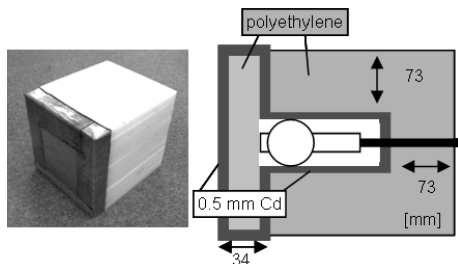

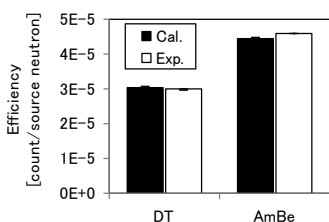Fig. 4. Photo of produced detector (left) and the design details (right).

Fig. 5. Comparison between measurement and calculation. Efficiency was expressed and the black bars indicate the calculation and the white bars indicate the experimental result.

5. Measurement of p-Li angular distribution

We measured the angular distribution of p-Li neutron source with the developed detector using a Dynamitron accelerator in Tohoku University. The proton energy was 2.5 MeV and the beam current was 1μA. The number of generated neutrons was relatively monitored by a BF_3 counter fixed near the Li target. Figure 6 shows the angular distribution normalized by the BF_3 counter as a function of cosine of the emission angle (= μ). The obtained distribution increases with μ.

6. Discussion

The measurement of neutron angular distribution was affected by the Li target assembly. Thus we corrected for the influence of the target assembly using MCNP-5 (Figure 7). We compared the corrected results with analytical calculation by DROSG-2000[2]. As a result, the distribution is in good agreement with the analytical calculation except around μ = 0.2. Around μ = 0.2, the flux intensity was strongly depending on the precise position of p-Li reaction, consequently leading to the substantial difference in the comparison in Fig. 7, because the Li target assembly has a quite complicated structure. The value estimated varies from 87% to 153% if changing the position of the p-Li reaction. Since it is

difficult to determine the position, estimation of the precise correction value around μ = 0.2 is a new challenge in the future.
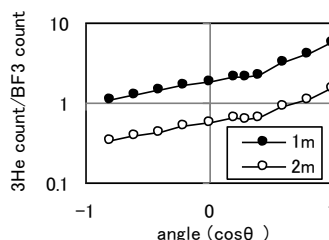

Fig. 6. Angular distribution from Li target assembly corrected by BF_3 counter. The distance from target to the detector: ●; 1 m and ○; 2 cm..
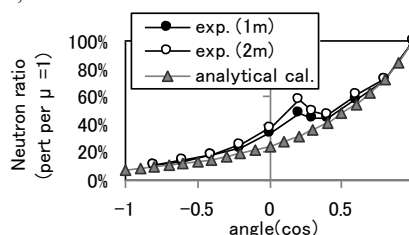

Fig. 7. Comparison with analytical calculation and experimental result corrected by MCNP. The effect of scattering with Li assembly was corrected by MCNP calculation. The value normalized by μ = 1 is expressed as a function of angle (μ). Circle symbols indicate experimental values followed by the distance from target to the detector in parentheses: ●; 1 m and ○; 2 cm. Triangle symbol shows the analytical calculation.

7. Conclusion

p-Li accelerator is expected as a neutron source for BNCT. To use p-Li neutrons, measurement of angular distribution is important. We designed and made a simplified neutron detector having constant efficiency in energy range of 100-700 keV and measured the angular distribution with a Dynamitron accelerator. The result was in good agreement with analytical calculation by DROSG-2000 except around μ = 0.2. It was difficult to measure the value accurately because of scattering in the Li target assembly. To estimate the precise value around μ = 0.2 further studies will be performed to explain this discrepancy.

References
[1] RF Barth , et al., "Current status of boron neutron capture therapy of high grade gliomas and recurrent head and neck cancer," Radiat Oncol, 7:146, (2012).
[2] M. Drosg, "DROSG-2000: neutron source reactions data files with computer codes for 57 monoenergetic neutron source reactions v 1.01.," Report IAEA-NDS-87 Rev. 5 (Vienna: IAEA) (2000).

Development of Compton X-ray spectrometer for the fast ignition experiment

S. Kojima[1)], Y. Arikawa[1)], T. Nagai[1)], Y. Abe[1)], S. Sakata[1)], H. Inoue[1)], T. Namimoto[1)], M. Nakai[1)], H. Shiraga[1)], H. Azechi[1)]
M. Asakawa[2)], T. Ozaki[3)], R. Kato[4)]

[1)]Institute of Laser Engineering, Osaka University, 2-6 Yamadaoka, Suita, Osaka, Japan, Tel: +81-6-6879-8775
[2)]Kansai University
[3)]National Institute for Fusion Science
[4)]The Institute of Science and Industrial Research, Osaka University

Abstract: *In the fast ignition experiment, the fast electron temperature is key parameter for determining the coupling efficiency from the heating laser to the fast electron. The bremsstrahlung X-ray is an attractive alternative diagnostics for this aim. In this study, the single-shot high-energy X-ray spectrometer with the sensitivity up to 4 MeV by using Compton scattering has been developed, and tested by using ^{60}Co.*

1. Introduction

In the fast ignition experiment, the compressed fuel is heated by the fast electron. The deposition efficiency strongly depends on the fast electron energy. Thus, measuring and controlling the fast electron energy is important.[1] However, it is difficult to measure initial fast electron temperature from the outside of plasma because of the strong sheath potential around the target. The bremsstrahlung X-ray is an attractive alternative diagnostics for this aim.[2][3] In this study, the single-shot high-energy X-ray spectrometer with the sensitivity up to 4 MeV by using Compton scattering has been developed, and tested by using ^{60}Co.

2. The principles of measurement

The photons around 1MeV mainly interact by Compton scattering in which the energy of incident x-rays is determined by the energy and the angle of recoil electrons. The structure of Compton x-ray spectrometer is shown as Fig1. Firstly, the high energy X-rays from target are collimated by the lead collimator. Then, the collimated x-ray recoils electrons via Compton scattering in the converter. The electrons passed through the aluminum slit set in front of the converter are measured their energy by electron spectrometer (ESM) with Image Plate (IP). The energy of the energy is measured by the signal position on the IPs.
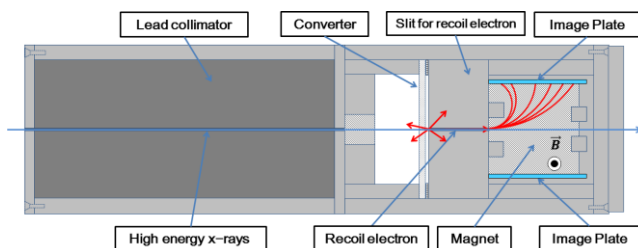

Fig.1 The structure of developed detector

3. Designing works

3.1. Designing of the slit

The detector is designed to satisfy requirement needed in the experiment. Firstly, we chose the slit which determines energy resolution. Fig.2 shows calculated trajectory of electron having various energies and initial positions. In this work the width of the slit was set 0.9mm and the length of the slit was set 2cm. Maximum of magnetic field is 0.4T. In this condition, energy resolution becomes 9% for 1MeV x-rays. Besides energy resolution, length of slit satisfies requirement to need to collimate electrons up to 10MeV.
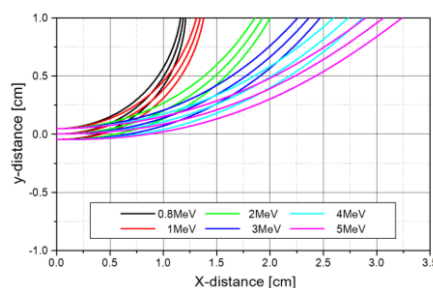

Fig.2 Electron trajectory in ESM

3.2. Converter

The sensitivity can be estimated from cross section, transmittance of electron and scattering effect. Cross section and transmittance of electron can be approximated as

$$\sigma_{compton} \propto NZ(h\nu)^{-1} \tag{1}$$

$$-\frac{dE}{dx} \propto NZ \tag{2}$$

where N is the number of the atom per cm3, Z is the atomic number and $h\nu$ is the incident photon energy. Both factors are directly proportional to the number of the electron per cm3. Thus, we can achieve similar performance about the thin converter made of low-Z material and the thick converter made

of high-Z material. On the other hand, we consider the scattering of electron in the converter. Differential cross section of coulomb scattering can be approximated as

$$\frac{d\sigma_{scatter}}{d\Omega} \propto \frac{Z^2}{(h\nu)^2} \tag{3}$$

In high-Z material, efficiency of the back scattering is higher than low-Z material due to strong coulomb potential around the protons. Fig.3 shows Monte Carlo simulated results. The red lines show backscattering, the black lines show forward scattering. From results, efficiency of backscattering increases in the high-Z material.
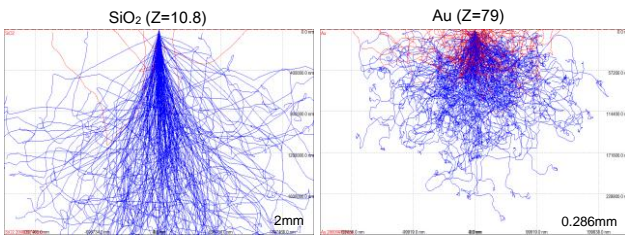

Fig.3 Scattering of electrons in the converter

As discussed above, optimum property of the converter is determined the thick converter made of low-Z material. In the experiment, we need to align the detector by using alignment visible laser. In conclusion, we chose SiO_2 which is low-Z and transparent material.

3.3. Back ground

In the experiment, the several causes of the noise signal are considered to be, the x-rays directly entering IPs, the electrons injecting from outside of the detector and electrons generated by the collimator. The detector is covered with the shielding box made of lead and equipped two magnets in front of the lead collimator and in front of the aluminum slit, respectively.

We subtract the B.G signal from the raw signal by using another IP set at opposite side. We set IP for B.G. at the opposite side of the IP for recoil electrons
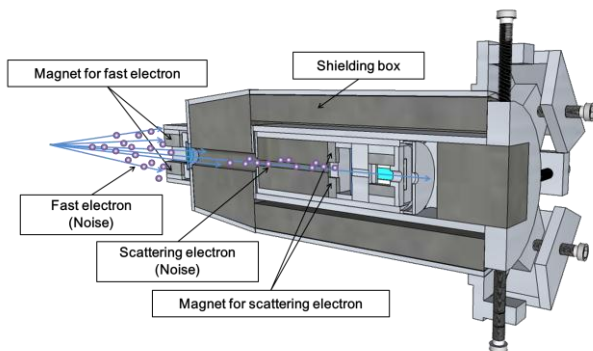

Fig.4 Shielding box and two magnets

4. Calibration experiments by using ^{60}Co

Cobalt60 has two ways of nuclear decay and emits two kinds of energy γ-rays (1.1732MeV, 1.3325MeV). We test the new detector by using ^{60}Co. Au foil (50μm) is chosen as the converter. The converter is thin enough. Thus, energy loss of the recoil electrons in the converter can be ignored. Fig.5 is recoil electron spectrum from ^{60}Co. The red dots show experimental data, the black line shows the Monte Carlo simulated result. Fig.5 shows that the detector can discriminate two lines γ-rays with the energy resolution as designed. Energy resolution is estimated by fitting peak with Gaussian function. Energy resolution is estimated to be 6.4% (when 1.1732MeV), to be 11.2% (when 1.3325MeV), respectively.
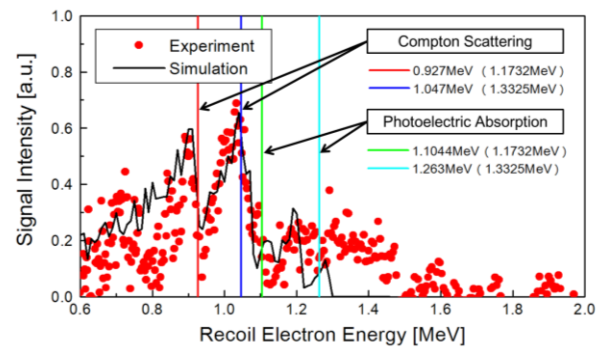

Fig.5 Recoil electron spectrum from ^{60}Co

5. Conclusions

In this study, the single-shot high-energy X-ray spectrometer with the sensitivity up to 4 MeV by using Compton scattering has been developed, and tested by using ^{60}Co. From data, Energy resolution of detector is estimated 6.4% (when 1.1732MeV), 11.2% (when 1.3325MeV).

References

[1] T. Iwawaki, H. Habara, T. Tanimoto, N. Nakanii
    K. Shimada, T. Yabuuchi, K. Kondo and K. A. Tanaka(2010)
    Development of multi-channel electron spectrometer
    REVIEW OF SCIENTIFIC INSTRUMENTS **81**, 10E535

[2] B. Westover, C. D. Chen, P. K. Patel, M. H. Key
    H. McLean, R. Stephens, and F. N. Beg (2011)
    Fast electron temperature and conversion efficiency
    measurements in laser-irradiated foil targets using a
    bremsstrahlung x-ray detector
    PHYSICS OF PLASMAS 18, 063101

[3] M.M.Günther, K.Sonnabend, E.Brambrink, K.Vogt,
    V.Bangnoud, K.Harres, and M.Roth (2011)
    A novel nuclear pyrometry for the characterization of high-
    energy bremsstrahlung and electrons produced in relativistic
    laser-plasma interactions
    PHYSICS OF PLASMAS 18, 08310

Development of the high energy bremsstrahlung
X-ray spectrometer by using (γ,n)reaction

S.Sakata[1], Y.Arikawa[1], S.Kojima[1], Y.Abe[1], T.Nagai[1], H.Inoue[1], R.Kato[2], M.Nakai[1], H.Siraga[1], H.Azechi[1]

[1] Institute of Laser Engineering, Osaka University, 2-6 Yamadaoka, Suita, Osaka, Japan 565-0871 Tel: +81-6-6879-8775

E-mail: sakata-s@ile.osaka-u.ac.jp

[2] Institute of Science and Industrial Research, Osaka University

Abstract: *In the fast ignition experiment, the implosion core plasma of heat is affected by the fast electron. As an alternative diagnostic of fast electron, the bremsstrahlung X-ray spectrometer which can measure the X-ray with the energy range from 4MeV to 30MeV by using (γ,n)reaction was developed , and evaluated by using LINAC facility.*

1. Introduction

In the fast-ignition laser fusion, high density fuel produced by the implosion is heated by using the fast electron generated by ultra intense laser.The measurement of the bremsstrahlung X-ray generated by the fast electron is attractive alternative-diagnostic of the fast electron. Related works has been presented describing, bremsstrahlung X-ray spectrometry by using nuclear activation-based method. [1] This method is focused on γ-ray generated from activation target and it can measure bremsstrahlung X-ray in the energy above 7MeV. In this study, We focused on neutron generated by (γ,n)reaction (photo-nuclear neutron) and developed bremsstrahlung X-ray spectrometer by (γ,n)reaction.

2. Princeple of measurement

Bremsstrahlung X-ray spectrum exceeds threshold of photo-nuclear can be measured via photo-nuclear reaction. Photo-nuclear neutron reflects the X-ray spectrum near the resonance energy. Fig.1 shows schematic view of the principle of measurement and, Fig.2 shows (γ,n)reaction cross-section.
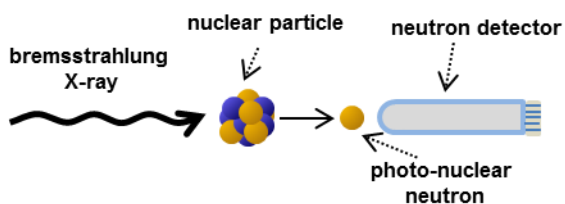

Fig.1 schematic view of the principle of measurement

X-ray spectrum near the resonance energy can be measured by counting photo-nuclear neutron. For example, neutron generated from lead is originated from the X-ray spectrum around (γ,n)reaction resonance peak with the energy of 13 MeV. Wide range of the X-ray spectrum can be measured by using a wide variety of material.

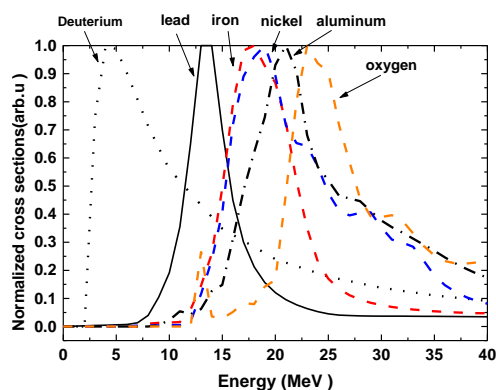Fig. 2 (γ,n)reaction cross-sections from JENDLE photo-nuclear data 2004.

3. Designing works

We use deuterium water, lead, iron, nickel, aluminium, and hydrogen water as converter. They have a variety of the energy (γ,n)reaction resonance peak from 4MeV to 22MeV. The thickness of converter was determined to be 5mm, with which can generate enough photo-nuclear neutron for bubble detector.

Bubble detector [2] was chosen as a neutron detector. When neutrons enters bubble detector, small visible bubbles appear instantly and that shows neutron flux. The bubble detector was experimentally confirmed to have no sensitivity. The bubble detector was irradiated by 1MeV γ-ray from Co^{60} (8 Tbq) at Institute of Science and Industrial Research, Osaka University, and no bubble was observed.

In order to shield bubble detector from back-ground neutrons, the paraffin block was chosen as the neutron shield. Back-ground neutron includes photo-nuclear neutron from the circumjacent structure, Deuterium-Deuterium neutron (D-D fusion neutron) and photo-nuclear neutron from the target. D-D fusion neutron accounts for a large number of back-ground neutrons. They can be shielded by the neutron shield with thickness of 20cm which is quintuple mean free pathes of D-D fusion neutrons with the energy of 2.45MeV. A

bubble detector without converter is also equipped in the center of the spectrometer for measurement of cross-talk from converters. The structural drawing of the spectrometer is shown in Fig.3.
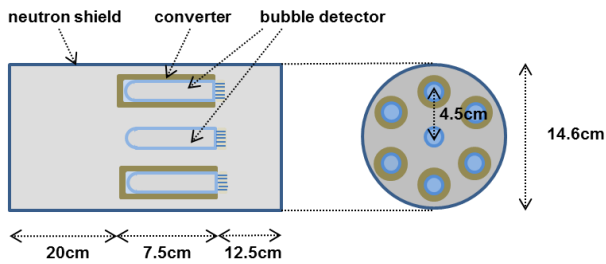

Fig.3 The structural drawing of the spectrometer. (0.8cm-diameter bubble detector in the 1.3-cm diameter cylindrical converter are set up in a concentric.)

4. Experiment for diagnosing princeple

The high energy X-ray spectrum was demonstrated by using LINAC facility at Osaka University. The experimental configuration is shown in Fig4.The bremsstrahlung X-ray with the number of 1.1×10^{12} generated by irradiating linear electrons into the lead-target with the energy of 26MeV. The dimension of the lead-target was $0.5cm \times 5cm \times 5cm$. The X-ray spectrometer was set up in front of lead-target from distance of 139cm and with the angle 15 degrees.
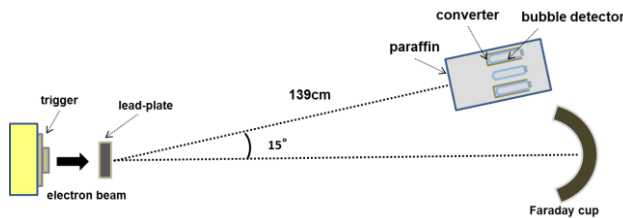

Fig.4 The experimental configuration

The number of bubbles in the experiment and simulation is shown in Fig.5. The bubble count simulated by using Monte Carlo code (MCNP5).
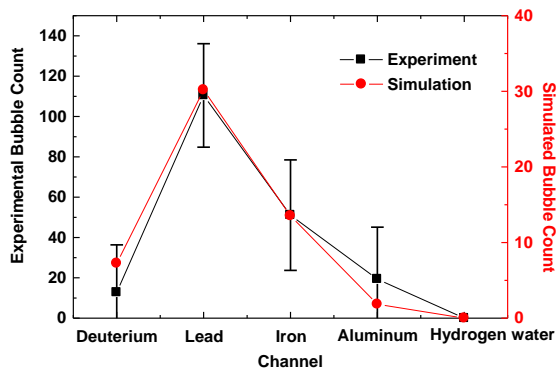
Fig.5 The result of the exceriment and simulation. The left side is experimental bubble counts with count errors. The right side is simulated bubble counts.

The spectrum observed in the experiment agree with the simulation. On the other hand, the experimental bubble counts is about four times higher than simulated bubble counts in every channel. This discrepancy is considered to be the imperfective in the simulation method. This will be improving our future works.

6. Conclusions

In this study, We developed the high energy bremsstrahlung X-ray spectrometer. The performance of spectrometer was confirmed by X-ray irradiation experiment at LINAC facility.

Acknowledgement

References

[1] M. M. Gu¨nther et al. "A novel nuclear pyrometry for the characterization of high-energy bremsstrahlung and electrons produced in relativistic laser-plasma interactions", Physics of Plasmas 18, 083102 (2011)
[2] H. Ing, R.A. Noulty and T. D. Mclean "BUBBLE DETECTORS-A MATURING TECHNOLOGY" Radiation Measurements, Vol.27, No.1, pp. 1-11, 1997

Study on Nuclear Transmutation of Nuclear Waste by 14MeV Neutrons

Takanori Kitada[1], Astuki Umemura[1], Kohei Takahashi[1]

1)   Osaka University, Graduate School of Engineering, Division of Sustainable Energy and Environmental Engineering,
Yamada-oka 2-1, Suita, Osaka, 565-0871, Japan, Tel:+81-6-6879-7901, Fax:+81-6-6879-7903,
E-mail:kitada@see.eng.osaka-u.ac.jp, a-umemura@ne.see.eng.osaka-u.ac.jp, k-takahashi@ne.see.eng.osaka-u.ac.jp

Abstract: The object of this study is to clarify the possibility of 14MeV neutrons to decrease the radioactivity of nuclear waste, especially fission products. Simulations were performed for several fission products by Monte-Carlo code. The results show that 14MeV neutron of especially high flux is effective to decrease the radioactivity.

1. Introduction

Nuclear waste disposal is a big problem not only in Japan but also all over the countries using nuclear power plants. Nuclear wastes are categorized into two materials : fission products (FPs) and minor actinides (MAs). There are some choices how to dispose them, and nuclear transmutation by neutrons with reprocessing has been investigated to minimize the burden for geological disposal. Our considering scenario consists of the followings; MAs, such as Np and Am, are transmuted in Fast Reactor (FR) and/or Accelerator Driven Subcritical Reactor (ADS) as fissionable materials. FPs are vitrified after several decades storage so as to decrease their radioactivity during the period. The main isotopes of FPs radioactivity after cooling period are ^{90}Sr, ^{137}Cs and their daughters, and thus we selected these isotopes as main targets to annihilate in this study. In addition, Tc and I are also selected as the target because these are possible to separate from other elements, and have relatively long half-lives over 10^5 years. The transmutation rate of these isotopes by neutron irradiation depends on several neutronic parameters described below, and the possibility of 14MeV neutrons for the transmutation is investigated in detail in this study.

2. Neutronic parameter

2.1 Burnup chain

Figure 1 shows an example of burnup chain related to ^{90}Sr. Burnup chain shows the relation among many isotopes; ^{90}Sr is transmuted to ^{91}Sr by neutron capture, ^{90}Sr is transmuted to ^{89}Sr by (n,2n) reactions, ^{90}Sr decays into ^{90}Y in 29 years half-life with beta-ray emission, etc.
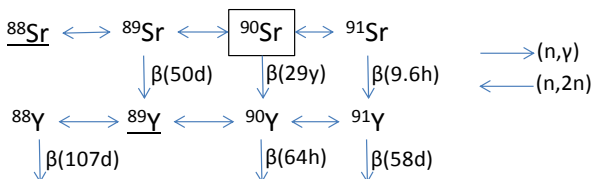

Figure 1 Burnup chain related to ^{90}Sr

The produced isotopes from ^{90}Sr have relatively short half-lives, and this tendency is almost the same for ^{137}Cs.

2.2 Cross section

Each isotope has its own reaction cross section for neutrons as shown in Fig. 2. Figure 2 shows the cross sections of ^{90}Sr and ^{137}Cs for capture and (n,2n) reactions. Most of all isotopes have the same tendency for capture reaction cross section which is larger in lower energy of irradiating neutron, and for (n,2n) reaction cross section which has the threshold around 10MeV. This shows that (n,2n) reaction is remarkable if 14MeV neutron is used for the irradiation, and this point is the characteristics of this study from the former investigations.
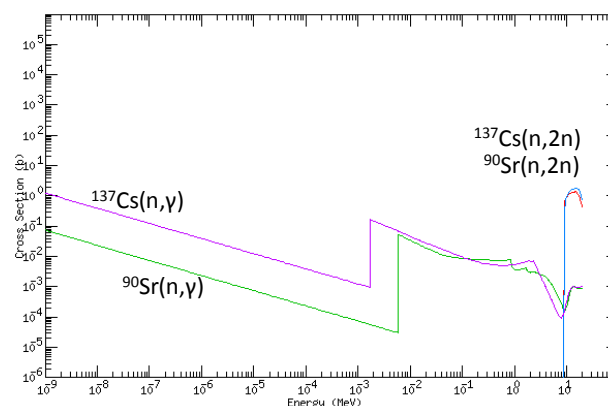
Figure 2, Cross section of ^{90}Sr and ^{137}Cs

3. Calculation conditions

The magnitude of neutron flux affects the transmutation, as easily expected. In this study, the magnitude was changed as 5×10^{14}, 5×10^{15} and 5×10^{16}[/cm^2/sec] to consider the necessary magnitude for the effective transmutation.

Irradiation period was set up to 1000 days, and the following cooling period was set up to 3500 days to consider rapid decreasing of short-lived radioactivity produced during the irradiation. Non-irradiated case was also simulated for the comparison.

The target elements are Cs, Sr, Tc, and I without considering isotope separation, and the mass composition of the target material is (Cs : Sr : Tc : I) = (9.36 : 3.00 : 2.87 : 0.71) as shown in Table 1. The mass

ratio of 4 elements in nuclear waste is trivial but the reactivity of them is remarkable. The target materials are stored at wall region (40cm-thickness) of D-T fusion reactor and 14MeV neutrons are irradiated to the wall.

Table 1, Composition of the target

	mass ratio		radioactivity ratio
	Nuclear waste	FP	
U,Pu	97.04%		21.6%
Np, Am, Cm	0.10%		0.5%
Cs (Ba)	0.27%	9.36%	**38.8%**
Sr (Y)	0.09%	3.00%	**27.2%**
Tc	0.08%	2.87%	0.0%
I	0.02%	0.71%	0.0%
others	2.41%	84.06%	11.9%

Calculations were done by using continuous energy Monte Carlo code named MVP-II [1] to evaluate reaction rates of each isotope, and burnup simulation code named ORIGEN2 [2] to evaluate the change of the target composition during the irradiation and/or cooling period. The cross section library used in this study is JENDL-4.0 [3].

4. Results and discussions

The radioactivity of the target materials are summarized in Table 2. The values are normalized as 100% for the total radioactivity of target material before irradiation. The magnitude of neutron flux more than 5×10^{15}[/cm^2/sec] is necessary to reduce the radioactivity of the target compared to the cooling only case.

Table 2, Radioactivity during irradiation and cooling

	before irradiation	1000 days			cooling only
		5E+14	5E+15	5E+16	
Cs−134	5%	3%	17%	63%	2%
Cs−135	0%	0%	0%	0%	0%
Cs−137	28%	26%	24%	13%	26%
Ba−137m	27%	25%	23%	12%	25%
Sr−90	21%	19%	18%	10%	19%
Y−90	19%	19%	18%	13%	19%
others	0%	12%	110%	525%	0%
Total	100%	105%	210%	635%	92%
		4500 days			cooling only
		5E+14	5E+15	5E+16	
Cs−134		0%	1%	2%	0%
Cs−135		0%	0%	0%	0%
Cs−137		21%	19%	10%	21%
Ba−137m		20%	18%	10%	20%
Sr−90		15%	14%	8%	15%
Y−90		15%	14%	8%	15%
others		0%	0%	3%	0%
Total		71%	67%	40%	72%

The residual radioactivity at 4500days shows that 5×10^{14} case is meaningless to irradiate while 5×10^{16} case shows remarkable reduction of the radioactivity of the target materials. At 1000 days, the radioactivity is remarkably large especially for 5×10^{16} case because many short-lived isotopes are produced during irradiation, and all of those isotopes decay into stable isotopes in a short period. Table 3 shows the radioactivity ratio at 4500days normalized to the original (0 days) for each isotope. The 5×10^{16} case shows desirable transmutation of FPs not only Cs and Sr but also Tc and I, and those radioactivity are reduced to about 40%. The transmutation by 14MeV neutron is NOT effective if the magnitude of the neutron flux is less than 5×10^{15} with 1000 days irradiation period.

Table 3, Radioactivity ratio to the original

	4500 days			cooling only
	5E+14	5E+15	5E+16	
Cs−134	3%	13%	48%	1%
Cs−135	99%	92%	50%	100%
Cs−137	74%	69%	36%	74%
Ba−137m	74%	69%	36%	74%
Sr−90	73%	68%	38%	74%
Y−90	73%	69%	38%	74%
Tc−99	99%	92%	44%	100%
I−129	99%	91%	41%	100%

5. Conclusions

The application of 14 MeV neutrons for nuclear waste transmutation was investigated to be clear the effectiveness in order to reduce the radioactivity of fission products. Although the 14MeV neutron is useful for the nuclear transmutation by (n,2n) reaction, it was found that higher flux more than 5×10^{15}[/cm^2/sec] is necessary for effective reduction of the radioactivity.

References

[1] Y. Nagaya, K. Okumura, T. Mori and M. Nakagawa, "MVP/GMVP II : General Purpose Monte Carlo Codes for Neutron and Photon Transport Calculations based on Continuous Energy and Multigroup Methods," JAERI 1348 (2005).

[2] A. G. Croff, "ORIGEN2 – A Revised and Updated Version of the Oak Ridge Isotope Generation and Depletion Code," ORNL-5621 (1980).

[3] K. Shibata, O. Iwamoto, T. nakagawa, N. Iwamoto, A. Ichihara, S. Kunieda, S. Chiba, K. Furukata, N. Otuka, T. Ohsawa, T. Murata, H. Matsunobu, A. Zukeran, S. Kamada and J. Katakura, "JENDL-4.0 : A New Library for Nuclear Science and Engineering," J. Nucl. Sci. Technol., 48(1), 1-30 (2011).

Method of Beam Steering with FWM in ICF
-Compensation of PC Beam Direction and Generation with Scattered Beam from a Foam Target-

Nobukazu Kameyama[1)], Hiroki Yoshida[2)]

[1)] Gifu University, 1-1 Yanagido, Gifu-shi, Gifu 501-1193, Japan, +81-58-293-4545, q3814101@edu.gifu-u.ac.jp
[2)] Gifu University

Abstract: *The method for compensating the direction of the PC beam with FWM is shown. It is possible to tilt one pump beam at a small angle from the counter-propagating alignment. The generation of the PC beam with the scattering beam from the moving foam target is confirmed.*

1. Introduction

High power lasers are irradiated a target which is injected at ~100 m/s and 10 Hz in Inertial Confinement Fusion (ICF). The system to steer the beams is required to irradiate the target within the margin of error of ten micrometers so that the target has a displacement from the focal point of final optics. One of the methods of beam steering is to use phase conjugate (PC) mirrors. It's not need mechanical devices like active mirrors. Probe beams, which is week enough not to damage the target, are irradiated to obtain the scattered beams in the all direction as shown in Fig. 1. The probe beams have enough diameters to cover the area that the targets can be injected. A part of the scattered beams are collimated with final optics, amplified, and focused into PC mirrors, which generate a PC beam that has a conjugate phase and propagates an opposite direction of an incident beam. For the property, the PC beams retrace the same paths of the scattered beams and irradiate the point that the probe beams are scattered by the target. Since the probe beams are irradiated in the area covering the displacements of the target, the PC beams are irradiated it all of the shots. However, the target has moved about one hundred micrometers when the PC beams come back so that it injected at around 100 m/s and the beams travel a round trip of several hundred meters. Therefore the directions of PC beams have to be compensated [1].

In this paper, the method of compensating the direction of the PC beam with four wave mixing (FWM) and the generation of the PC beam originated from the scattered beam from the moving foam target are shown.

2. Compensation with FWM

In FWM, two pump beams counter-propagate through a nonlinear material and a seed beam is irradiated into the interaction region, then the PC beam is generated. When two pump beams propagate in direct opposition to each other, the PC beam propagates in opposite direction of the seed beam. If one pump beam tilts at a small angle from the counter-propagating condition, the PC beam has the same angle from the seed beam [2]. Setting the adequate angle between two pumps, it is possible to compensate the direction of the PC beam so as to accurately irradiate the target with laser beams.
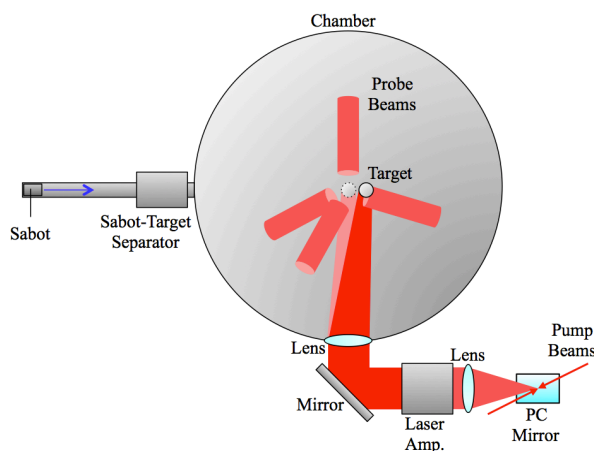

Fig. 1 Schematic diagram of ICF with FWM.

We consider the system constructed with lens, amplifiers, spatial filters, and beam expanders. Figure 2 shows the compensation of a PC beam with FWM in the system. The compensated angle $d\theta$ is calculated by

$$\delta \pm d\delta = (-1)^n \frac{f_{2n+1}}{f_0} \cdot (d \pm dz) d\theta \prod_{k=1}^{n} \frac{f_{2k-1}}{f_{2k}} \quad (1)$$

where δ is the target moving distance, $d\delta$ is the acceptable error of the laser radiations, d is the displacement from the focal point of the lens L(0), dz is the error margin of the target injection in the z-direction (the target is injected from bottom to top in Fig. 2), and f_i
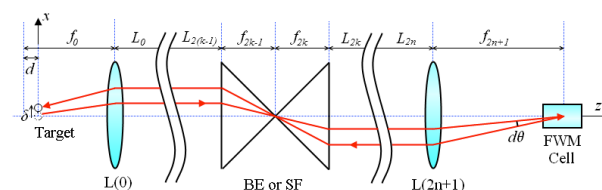

Fig. 2 Compensation of a PC beam: L(i), lenses; f_i, focal length of the ith lenses; L_i, optical path length between lenses; d, displacement from focal point of L(0); δ, target moving distance; $d\theta$, compensated angle.

is the focal length of the ith lens. It is not related with optical path length. When $\delta = 100$ μm, $d\delta = 10$ μm, $f_0 = 1000$ mm, $f_{2n+1} = 5000$ mm, $d = 12$ mm, and $\Pi(f_{2k-1}/f_{2k}) = 10$, the compensated angle is given by $d\theta = 4.2$ mm. In the condition, dz is 1.2 mm.

3. Generating the PC beam with a foam target

Figure 3 shows the experimental equipment of irradiating a target with PC beam originated from the seed beam scattered from a moving foam target. YAG laser ($E = \sim40$mJ, $\lambda = 1064$ nm, $\tau = 5\sim7$ ns) is used as the sources of two pump beams and a probe beam. The first pump beam propagates forward to the cell containing FC-72 as the material for FWM. The calorimeter CM1 measures the energy of it. The second pump beam is given by reflecting the first one with the mirror. The probe beam is given by reflecting the beam with the beam splitter and irradiated the foam target that is rotating at around 40 m/s. The amplified energy is measured with CM2 The scattered beam is collimated by the lens that focal length is 64 mm, amplified, and focused into the cell. The PC beam is amplified and measured by CM4. The energies of the first pump beam, the seed beam, and the PC beam are 17 mJ, 3 μJ and 80 nJ, respectively.

4. Conclusions

The PC beam can be compensated by setting the angle between the pump beams. In the case that the laser system has lenses included in spatial filters or beam expanders, the compensated angle is given by the focal lengths, the target moving distance, and the target
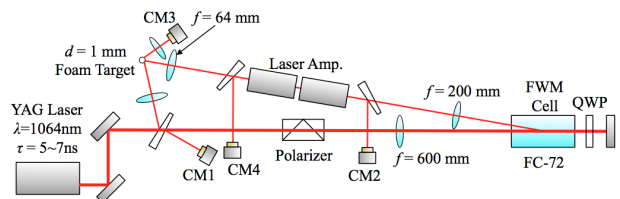

Fig. 3 Experimental equipment: CM1-CM4, calorimeter; QWP, quarter-wave plate.

displacement from the focal length of the final optics. The angle is independence of the optical path length.

We confirmed the generation of the PC beam originated from the moving foam target.

Acknowledgement

References

[1] M. Kalal, H. J. Kong, O. Slezak, E. R. Koresheva, S. Park and S. A. Startsev, "Recent Progress Made in the SBS PCM Approach to Self-navigation of Lasers on Direct Drive IFE Targets", J. Fusion Energy, 527-531 (2010).

[2] N. Kameyama and H. Yoshida, "Compensating for Target Motion Between Seed Pulse and Phase Conjugate Beam Arrival Times at the Target ", Fus. Sci. Technol. to be published.

Generation of monoenergetic deuterons by tailored intense laser pulses for high fluence energetic neutron production

S. M. Weng [1)], M. Murakami [1)], J. W. Wang [1,4)], M. Chen [2)], Z. M. Sheng [2)], N. Tasoko [1)], P. Mulser [3)], W. Yu [4)]

[1)] Institute of Laser Engineering, Osaka University, Osaka 565-0871, Japan
[2)] Key Laboratory for Laser Plasmas and Department of Physics, Shanghai Jiaotong University, Shanghai 200240, China,
[3)] Theoretical Quantum Electronics (TQE), Technische Universität Darmstadt, D-64289 Darmstadt, Germany
[4)] Shanghai Institute of Optics and Fine Mechanics, Chinese Academy of Sciences, Shanghai 201800, China

Abstract: *A novel scheme has been suggested for the efficient generation of monoenergetic deuterons from thick overdense targets by tailored intense laser pulses. Particle-in-Cell (PIC) simulations show that the accelerated deuterons by this scheme have a good quality of being monoenergetic (energy spread ~10%) at energy of several tens MeV, and a conversion efficiency as high as 20% can be achieved. Furthermore, these good qualities can be well maintained in the whole duration of interaction with a long laser pulse. Therefore, it is capable of generating a high fluence of monoenergetic deuterons using tailored intense laser pulses. Consequently, such a high fluence of monoenergetic deuterons are particularly suitable for the production of high-energy neutron beams at a high fluence enough for practical applications.*

1. Introduction

Due to its unique properties, neutron source has a very brilliant prospect of applications in medicine, security, industry, and fundamental physics [1], such as neutron radiography, detection of special material in cargo containers, and transmutation of nuclear waste. The interaction of an intense laser pulse with deuterated target can generate deuterons, which may subsequently drive nuclear fusion reactions. Thus it is expected to be an alternative approach to produce neutrons by the laser-driven deuterons with a relatively low cost in contrast to the traditional reactor-driven neutron sources [2,3].

Experiments demonstrate that neutrons with energies in excess of 10 MeV can be produced by the laser-driven energetic deuterons [4,5]. In such a laser-driven high-energy neutron source, the efficient generation of a high fluence of monoenergetic deuterons is critical for the production of neutrons with a high fluence enough for applications or even just above the detection limit [4]. Moreover, the energy spectrum of produced neutrons are closely related to the quality of fast deuteron beam. Therefore, many ion acceleration schemes have been designed and refined for the efficient generation of high-energy neutrons by intense short laser pulses [5-7]. In this paper, we propose a hole-boring ion acceleration scheme using the temporally tailored pulse, which is capable of generating monoenergetic deuterons with a high fluence for efficient neutron production.

2. Theory of hole boring by tailored laser pulses

According to the hole-boring theory of a circularly polarized (CP) pulse in a uniform plasma [8,9], the laser front propagation velocity and the mean accelerated ion energy are given by

$$v_b = c\Pi / (1 + \Pi), \qquad (1)$$

$$\varepsilon_i = m_i c^2 \, 2\Pi^2 / (1 + 2\Pi), \qquad (2)$$

where the characteristic parameter Π is defined as

$$\Pi = a(Zm_e n_c / 2Am_p n_e)^{1/2}, \qquad (3)$$

with the critical density $n_c = m_e \varepsilon_0 \omega^2 / e^2$, the dimensionless laser amplitude $a = (I\lambda^2/1.37\times10^{18} \text{ Wcm}^{-2}\mu\text{m}^2)^{1/2}$, the ion mass in units of the proton mass $A = m_i/m_p$, the ionic charge state Z, the electron mass m_e and density n_e, and the laser wavelength λ and frequency ω.

Now we consider the hole boring of a laser pulse in an inhomogeneous plasma, we assume that the semi-infinite plasma has a density profile $n(x)$ in the space $x \geq 0$ and the pulse with a temporal profile $a(t)$ irradiates from the left side. Equations (1) and (2) suggest that a time-independent Π_0, *i.e.* a stable hole-boring velocity v_b, is essential for monoenergetic ion generation during the laser propagation in an inhomogeneous plasma. With a constant $v_b = c\Pi_0/(1 + \Pi_0)$, the time t_s when the slice at the t' interval of the pulse catches up with the plasma can be calculated from $ct_s = ct' + v_b t_s$ [9]. Thus the instantaneous interface position can be calculated as

$$x' = v_b t_s = c\Pi_0 t'. \qquad (4)$$

Combining Eqs. (3) and (4) gives the temporal intensity profile to generate monoenergetic ions with $n(x)$ as

$$a(t) = (2Am_p / Zm_e)^{1/2} \Pi_0 n_e^{1/2}(c\Pi_0 t). \quad (5)$$

Particularly, an exponential density profile $n_0\exp(x/L)$ is widely present in the pre-plasma during the laser-plasma interaction [10] or the pre-compressed fuel target for inertial confinement fusion [11]. Correspondingly, the temporally tailored laser profile in this case is

$$a(t) = a_0 \exp(t / 2T_0), \qquad (6)$$

where $a_0 = \Pi_0(2Am_p n_0/Zm_e n_c)^{1/2}$, $T_0 = L/c\Pi_0$, and n_0 is the electron number density at the left boundary. From the acceleration region $0 \leq x \leq x_{max}$, a total energy fluence of monoenergetic ions

$$F_i = \varepsilon_{i,0}\int_0^{x_{max}} n(x)dx = \varepsilon_{i,0}L(n_{max} - n_0), \quad (7)$$

can be generated by a tailored pulse rising from a_0 to $a_{max} = a_0\exp(x_{max}/2L)$ within a duration of $x_{max}/c\Pi_0$, where $n_{max} = n_0\exp(x_{max}/L)$ and $\varepsilon_{i,0} = m_i c^2 2\Pi_0^2/(1+2\Pi_0)$.
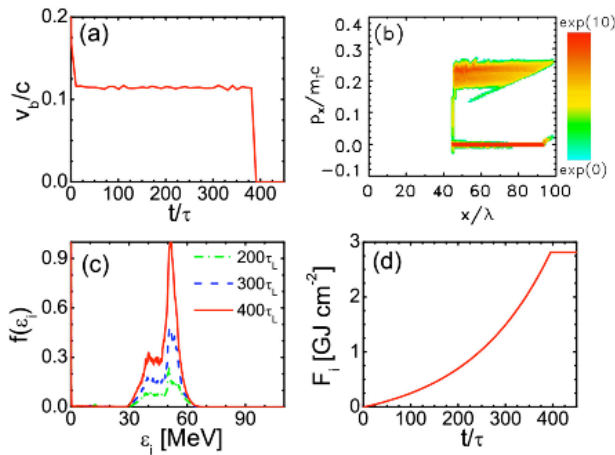
3. Simulation results

Fig. 1. (a) Laser front propagation velocity, (b) deuteron momentum distribution, (c) energetic deuteron spectra at different times, and (d) energy fluence of deuterons produced by a temporally tailored pulse from PIC simulations. Simulation parameters are given in the text.

The efficient generation of monoenergetic deuterons by hole boring of a tailored pulse has been verified by PIC simulations. The code employed is similar to that used in previous investigations [8]. In the simulation, it is assumed that the laser pulse is circularly polarized with a wavelength λ=1.06μm, thus n_c=9.9217×10^{20} cm^{-3}. The plasma has a profile of $20n_c$exp($x/20\lambda$) rising from 20 up to $200n_c$ over a distance of 46λ and then remain uniform, and ions are deuterons. Eq. (6) suggests that a tailored pulse with a_0=49.63 and T_0=154.44λ/c can result in a stable hole-boring velocity v_b=0.1147c (i.e. Π_0=0.1295) and generate monoenergetic deuterons at a mean energy of 50 MeV. Simulation results of such a tailored pulse with a duration of 350 laser cycles have been shown in Fig. 1. An almost constant laser front propagation velocity of 0.115c has been identified during the whole duration of interaction as shown in Fig. 1(a). Therefore, deuterons can be accelerated to momenta with a time-independent mean p_x=0.23$m_i c$ as illustrated in Fig. 1(b). Moreover, these deuterons have a good quality of being monoenergetic, and such a good monoenergetic quality can be well maintained in the whole duration of the interaction. The energy spreads are always about 11.3% as indicated by the energetic deuteron spectra at different times in Fig. 1(c). Finally, Fig. 1(d) shows that a total deuteron energy fluence of 2.82 GJ cm^{-2} can be achieved by such a tailored pulse with a laser energy fluence of 13.94 GJ cm^{-2}. In other words, the conversion efficiency of this deuteron acceleration scheme is about 20.23%, which is in a good quantitative agreement with the theoretical estimate 20.57%. This efficient generation of a high fluence of monoenergetic deuterons provides a promising approach to produce the high fluence high-energy neutron sources [4,5] as well as to trigger the fast ion ignition of inertial confinement fusion [12].

4. Conclusions

In conclusion, we have formulated the temporal profile of a laser pulse to drive hole boring at a constant velocity in an inhomogeneous plasma for the efficient generation of monoenergetic ion beams with a high fluence. For a deuterated target with an exponential density profile, simulation results indicate that monoenergetic deuterons can be efficiently generated by the hole-boring ion acceleration using a temporally tailored intense CP pulse. In particular, the high conversion efficiency and the good monoenergetic quality of accelerated deuterons can be well maintained in the whole duration of interaction. Therefore, it is capable of generating a high fluence of monoenergetic deuterons efficiently using the temporally tailored pulse, which is particularly suitable for the efficient high fluence high-energy neutron production for practical applications.

References
[1] T. E. Mason, "Pulsed Neutron Scattering for the 21st Century," Phys. Today **59**, 44-49 (2006).
[2] P. A. Norreys et al., "Neutron production from picosecond laser irradiation of deuterated targets at intensities of 10^{19} W cm^{-2}," Plasma Phys. Control. Fusion **40**, 175-182 (1998).
[3] K. W. D. Ledingham, P. Mckenna, and R. P. Singhal, "Applications for Nuclear Phenomena Generated by Ultra-Intense Lasers," Science **300**, 1107-1111 (2003).
[4] G. M. Petrov et al., "Generation of high-energy (>15 MeV) neutrons using short pulse high intensity lasers," Phys. Plasmas **19**, 093106 (2012).
[5] M. Roth et al., "Bright Laser-Driven Neutron Source Based on the Relativistic Transparency of Solids," Phys. Rev. Lett. **110**, 044802 (2013).
[6] G. Grillon et al., "Deuterium-Deuterium Fusion Dynamics in Low-Density Molecular-Cluster Jets Irradiated by Intense Ultrafast Laser Pulses," Phys. Rev. Lett. **89**, 065005 (2002).
[7] M. Murakami, and K. Mima, "Efficient generation of quasimonoengetic ions by Coulomb explosions of optimized nanostructured clusters," Phys. Plasmas **16**, 103108 (2009).
[8] S. M. Weng et al., "Ultra-intense laser pulse propagation in plasmas: from classic hole-boring to incomplete hole-boring with relativistic transparency," New J. Phys. **14**, 063026 (2012).
[9] A. P. L. Robinson et al., "Relativistically correct hole-boring and ion acceleration by circularly polarized laser pulses," Plasma Phys. Control. Fusion **51**, 024004 (2009).
[10] J. Davis, and G. M. Petrov, "Influence of prepulse plasma formation on neutron production from the laser-target interaction," Phys. Plasmas **15**, 083107 (2008).
[11] X. Ribeyre et al., "Compression phase study of the HiPER baseline target," Plasma Phys. Control. Fusion **50**, 025007 (2008).
[12] S. M. Weng et al., "Efficient generation of ultrahigh monoenergetic ion fluence for hole-boring fast ignition using tailored intense laser pulses," to be appeared.

The ESS-BILBAO Project

F. Sordo, The ESS-BILBAO Team
Edificio Cosimet
Paseo Landabarri nº 2, 1ª Planta. 48940 Leioa (España)

The ESS-BILBAO Consortium in its current configuration was set up early 2011 by means of a bilateral agreement between the Basque Government (Spain) and the Spanish Ministry of Science and Innovation. It was conceived as a way to channel the Spanish participation within the ESS project, as well as to develop in-house capabilities in accelerator science and technology. Within the latter, the main goal of this Consortium is to develop a research center in the Bilbao area that could contribute to the design, manufacturing and testing of components for projects such ESS where Spain has a significant participation.

Memo